NASW-4435

IN-37-CR
141623

P- 194

FRONTIER TRANSPORTATION SYSTEMS

FINAL DESIGN REPORT
FOR THE
SIMPSONS PROJECT:

AN INTEGRATED MARS TRANSPORTATION
SYSTEM

FRONTIER TRANSPORTATION SYSTEMS

Systems Integration for Mars Planetary Operations Networks

SIMPSONS Team

Matthew Kaplan - Project Manager

Eric Carlson - Chief Engineer

Sherie Bradfute - Chief Administrator

Kent Allen

François Duvergne

Bert Hernandez

David Le

Quan Nguyen

Brett Thornhill

Acknowledgments

The employees of Frontier Transportation Systems are greatly indebted to many people in private industry and academia, without whom this project would not have been possible.

Among the individuals we wish to thank are George Acker of SWRI, San Antonio, TX, who helped with the internal combustion engines and related design problems, V. Lloyd Howard of Rockwell Space Operations Company for his help with our thermal control systems, and our contacts in Houston: Chau Pham of NASA, and Keith Henderson of USRA.

Numerous people from the Jet Propulsion Laboratory , such as Don Gibson (navigation sensors, communication satellite acquisition and navigation, interface power and data couples, attitude determination), Brian Wilcox (rover wheels, loopwheels), Don Bickler (mobility systems and computer modeling), and John Day (antenna materials), were instrumental in the development of our transportation system.

Naturally, the engineering and science departments of The University of Texas at Austin provided a wealth of information. The people ar U.T. we would like to thank include Dr. Daniel P. Miranker and Dr. Benjamin J. Kuipers, Dept. of Computer Sciences, for their guidance in the computational needs of Artificial Intelligence for autonomous rovers, Dr. Raymond Davis of the Dept. of Natural Sciences for his aid in chemistry, Dr. Ron Matthews and Hank Kleespies of the Mechanical Engineering department, and just about the entire Dept. of Aerospace Engineering and Engineering Mechanics: Dr. John Porter (thermal radiators), Dr. Philip Varghese (thermodynamics of internal combustion engines), Dr. Kenneth Liechti (thermal properties of composites), Dr. Lundberg (orbit determination), Dr. Wallace Fowler, Dr. John Kallinderis, Dr. Jeffrey Bennighof, Phillip Tran (visualization of vehicle designs), and Russel Carpenter (navigation, sensors, and AI on rovers).

Finally, we would like to express our gratitude toward Dr. George Botbyl and Tony Economopoulos for their help in finding reference material and reference people, their encouragement, and their patience.

Executive Overview

Frontier Transportation Systems (FTS) has designed an integrated transportation network to support an advanced Martian base. The following paper represents the completion of the SIMPSONS project (Systems Integration for Mars Planetary Surface Operations Networks).

Our project focuses solely on the surface-to-surface transportation at an advanced Martian base. Several elements, such as interplanetary transfer vehicles, orbiting nodes, and ascent/descent vehicles will be necessary for the sustenance of such a base. Any one of these components would be a significant project in itself; thus, they do not fall within the scope of our project.

Assumptions and Goals

FTS defined the SIMPSONS project with the following assumptions.

- Advanced Martian base exists
- Transportation node in low Mars orbit exists
- Supply route between LEO and LMO is available
- Water is present on Mars

In order to precisely determine the exact goals of our transportation system, the supported base needed a clear definition. To this end, FTS researched the most likely arrangements and locations of an advanced Martian base and selected a specific configuration. The base after which we modeled our system will be located at Utopia Planitia (30°N,240°W). Its favorable proximity to possible mining locations will facilitate the transport of raw materials to the base. Also, this latitude aids the ascent/descent vehicles by minimizing the plane change required to reach the orbiting transportation node which is at an inclination of 25°. Furthermore, this region is the largest flat area on Mars, which makes spacecraft landings, long distance travel, and communications easier. Finally, radiation shielding provided by the Martian atmosphere is increased at this location due to its low altitude (-1 km).

The following operations will be required of this type of advanced base.

- Mining of regolith for H_2O and O_2 to provide life support and fuel
- Scientific exploration and research
- Expansion of the base

The base will accommodate a crew of 12 to 18 persons with the possibility of expansion. The main components of the base shown in Figure 2.1 include the centrally located habitat area, a manufacturing facility, two nuclear power plants, two landing pads, and a garage/maintenance facility.

Surface transportation is needed for travel between some of the more distant elements of the base, as well as for mobility of crew and payload from one area of the base to another. Scientific expeditions require the use of both manned and unmanned transportation systems to reach distant sites of interest. Likewise, outposts such as scientific stations or mining sites need maintenance and replenishment of supplies. This can be accomplished by surface rovers or rocket hoppers. Closer to the base, raw materials must be delivered to the manufacturing facility for the production of necessities, such as oxygen and fuel, for base sustenance and maintainability. All of this requires a flexible transportation system, capable of transferring heavy cargo on a regular basis, and of transporting cargo over distances farther than the confines of the base.

Ultimately, the transportation system selected for the Mars base should be compatible with all payloads and should be adaptable to meet many tasks, including those unforeseen. Along with vehicles for the transfer of non-pressurized cargo, pressurized vehicles will also be needed for long range excursions. A transportation system composed of a set of modular vehicles which fulfills the needs of an advanced Martian base is presented in the following report. These vehicles include an aerial tram, a heavy lifter, a rocket hopper, Martian aircraft, and several different rover designs. This executive summary outlines the purpose and design of each vehicle, as well as recommendations for future analyses.

Aerial Tram

To support the mining operations of this base, it will be necessary to refine 216 MT of regolith per day. Upon analyzing the important aspects of a fixed route transportation system, FTS selected an aerial tram as the most efficient and economical mode of cargo delivery. The aerial tram is easy to construct, as it merely involves the setting up of two stations and intermediate trestles for support. In addition, the tram is easily automated, inexpensive to build and operate, and it requires little maintenance. The other fixed route types of

transportation that were evaluated included trains, elevated rails, and magnetically levitated trains.

The aerial tram requires little mass to construct. The carriers are a simple automated design made of light-weight aluminum. The main mass to be concerned with, other than the payload chambers, is the weight of the hauling/carrying rope which will be made of a zinc-coated steel. The trestle mass should not be of concern, as the use of in-situ materials to form Martian concrete from which to construct these structures will eliminate the need to deliver the heaviest materials from Earth.

The tram we have designed will transport 36 MT per hour for the duration of only a quarter of a day. This will increase the lifetime of the system because it reduces the likelihood of fatigue and the opportunity for failure in general.

This system was a good choice from the perspectives of both the present and the future. From the present point of view, it can be constructed with the technology of today, and has proven to be a safe and reliable system on Earth. From a futuristic point of view, the aerial tram is an advantageous choice with regards to its expandability. First, the tram was designed to be strong enough to carry four times the amount it will actually be carrying. Thus it will be possible to increase its transport capacity in the future to support a larger crew. Secondly, the expansion of the base can be facilitated by first expanding the tram itself since it is possible to construct an additional route that is powered from the same driving station of an existing route. Finally, the tram may be used to efficiently transport humans in either pressurized or non-pressurized passenger cabins on future routes.

Heavy Lifting Vehicle

The lifter is designed to perform the loading and unloading processes within the base vicinity. This vehicle has to operate off of many platforms, ranging from the descent vehicle and the rover flatbed to the Martian surface. FTS will require that there be at least three lifting vehicles. One would be located at the landing pad, one at the base, and one extra should be present at any given time in case of mechanical failure. A crane design was chosen after evaluating forklifts and other lifting vehicles.

The crane must meet the following requirements.

- maximum lifting capacity of 30 MT
- capacity for cargo up to 6m wide and 10m long
- total range of 10 km
- fully telerobotic
- flexible
- durable
- low maintenance
- simplicity of design

In our evaluations, we looked for the least massive crane which still satisfied the original requirements. Therefore, FTS selected trusses as the main lifting component to reduce weight. The selected crane, shown in Figure 4.1, is a composite of many Earth lifting vehicles. As shown, the crane has a horizontal truss and a vertical truss structure similar to the tower configuration of lifting cranes. The horizontal truss moves along the vertical truss in a forklift type movement. In the back of the crane is a large container which is filled with indigenous material to act as a counterweight. The horizontal truss has a maximum extension of about 10 m which provides flexibility in reaching the payload, and the vertical truss has a height of about 13 m. The grasping mechanism which hooks onto the payload can vary in position along the horizontal truss.

The crane is supported by a tracked wheel, which enables the crane to carry the cargo from one place to another. The empty weight of the crane was computed to be no more than 30 MT. By adding regolith as a counterweight, the total weight could go up to as much as 100 MT. The trusses and the grasping mechanism will be made mainly of aluminum alloy materials, which provide lightweight and high strength characteristics.

The grasping mechanism has three degrees of freedom that can accommodate a maximum cargo width of 6 m. The lifter will get its power from a closed-cycle, internal combustion engine, using CH_4 and LOX for fuel and oxidizer, respectively. The lifter needs about 422 kW of power to travel 2 km/hr with a mass of 100 MT. The hoisting of the cargo using the grasping mechanism needs about 40 kW for a hoist rate of about 0.4 m/s. Also, the power required to translate the horizontal truss at a rate of 0.3 m/s along the vertical truss with 30 MT attached is about 50 kW. The crane will be controlled telerobotically by an operator from a command module located

either in the habitation module or near the landing pad, where the majority of the loading and unloading processes will occur. To aide in telerobotics, the crane will need various sensors to accomplish the following tasks.

- avoid obstacles
- detect tilting of the vehicle due to uneven distribution of cargo mass
- detect the range to the obstacle during loading and unloading processes
- provide warnings of undue strains in support members

Ballistic Martian Hopper

A ballistic rocket hopper provides a shorter transit time and a greater operating range. With a given payload of 6.5 MT, this vehicle can complete two missions: 1) carrying one autonomous rover with various scientific payloads, or 2) carrying a rover and a crew of two, with supplies for seven days. Our hopper can transport either payload to a site up to 1000 km from the base, where the small rover would then enable exploration within a 10 km radius around the landing site. Due to the fuel selection for our overall system (methane/oxygen), on-site refueling away from the base would not be feasible; the hopper is, thus, limited to one hop from and one hop to the base.

As can be seen in Figure 5.1.1, the cargo bay was placed at the vehicle's center. The hover engines were then balanced around the bay in two equal, self-contained, and coordinated sets. This arrangement provides stability in firing and reduces shifting of the center of mass as fuel is consumed.

The trajectory of our craft was modeled by three phases – launch, ascent, and touchdown. The launch is basically a hovering maneuver until the reaction control system (RCS) jets are fired to attain the proper attitude for the ascent phase. The main engines located at the rear of the vehicle are then fired for the ascent phase, sending the vehicle into a ballistic trajectory. When the hopper descends to 100 m altitude, a parachute is deployed.

The end result of our analysis consists of a partial load-bearing, functionally gradient material (FGM) skin supported by a graphite/magnesium interior structure. The skin is limited in its ability to bear loads by two main considerations. First, the engines of the undercarriage are recessed, and the ascent and descent thrust cannot be carried by the exterior skin. Also, there are several panels in the skin (clamshell doors,

payload door) which would have to be carefully supported so as not to provide weak points in the structure.

Since the hopper requires the ability to operate autonomously and possibly telerobotically, its command and data handling system will have to be provided with information such as attitude, altitude, velocity and position, and surface mapping. The hopper will require an IMU capable of measuring the changes in attitude and position in three axes to fully define the state of the vehicle.

Unmanned Martian Aircraft

With the low martian gravity and despite the thin atmosphere, studies performed at the Jet Propulsion Laboratory in the late 1970's underlined that there were no technical difficulties involved in designing and operating a remotely piloted Mars airplane. It also appeared that such a vehicle could be most useful in increasing the capability of a Mars surface crew by providing for long range exploration and mapping.

The Mars airplane is well suited for long range scientific exploration, especially over rough terrain, and it can fulfill a wide range of missions such as surface imaging, atmospheric sounding, high altitude meteorology, and radio science. In addition, an unmanned Mars airplane can perform other useful functions such as deployment of remote observing stations , servicing of manned outposts, and search and rescue missions.

In order to enlarge the scope of operation, FTS evaluated both a large and a small aircraft. Because of the thin atmosphere and the need to keep aircraft dimensions and power requirements reasonable, the payloads of the aircraft need to be restricted. The large and small aircraft are restricted to 300 and 100 kg, respectively. The large aircraft has a range of over 12,000 km, and the small one has a range of 8000 km.

For both aircraft, a classical configuration was adopted since this configuration allows high lift-to-drag ratios and high stability. Moreover, the high tail volume can tolerate large shifts in the center of gravity resulting from payload deployment. Other features include an inverted V-tail to reduce mass as well as drag , high aspect ratio wings (22) in order to minimize the induced drag and large propellers for efficient high altitude flight in the thin martian atmosphere.

Because of the composition of the martian atmosphere (95% CO_2), only non air-breathing engines combined with propellers can be used. Because of its high power/mass ratio, a closed loop, internal combustion engine (CH_4/O_2) was chosen. In order to cut the total weight, an all composite structure was chosen, composed of high strength Thoronel 300 carbon-fiber and epoxy composites. This allows for a structural weight fraction between 15 and 20 %.

In order to minimize the take-off distance and thus the runway length, both aircraft are supposed to use a short-take-off device such as a catapult. The landing distance will also be shortened by using slow-down devices, such as nets. The landing gear for both aircraft will be a simple skid very similar to those used on gliders.

Like the rocket hopper, the small aircraft must have the capability to select a suitable site to land and to perform the landing autonomously. Nevertheless, the capacity to be remotely piloted should be available as an emergency back-up or for complex maneuvers. The computer will navigate mainly by a terrain-following procedure, using medium and high resolution images provided by previous or current remote-sensing satellites. The very high resolution images needed for high-precision procedures (vertical landings, for example) would have to be provided by previous aircraft missions. The command and data handling system could also rely on ground-based beacons for navigation. In addition, the avionics also need aircraft attitude, attitude rates, position, and position rates for navigation.

Rovers

The seven rover configurations which were designed for the SIMPSONS Project are: 1) fuel transport vehicle (FTV), 2) manned, short-range vehicle (MSRV), 3) materials transport vehicle (MTV), 4) Mars autonomous rover for ground exploration (MARGE), 5) human-operated Mars exploration rover (HOMER), 6) light cargo vehicle (LCV), and 7) heavy cargo vehicle (HCV). The following table shows the range and payloads for each vehicle.

Table of Ranges and Payload Masses for FTS Rovers

Vehicle	Range (km)	Payload (MT)
FTV	10	7.0
MSRV	30	2.2
MTV	30	7.0
MARGE	200	2.5
HOMER	200	10.0
LCV	200	2.5
HCV	20	10.0

The FTV will refuel the lifters, aircraft, and rovers, and serve as a backup to the pipelines that provide fuel for the hopper at the launch pad. The MSRV can be used for transportation in the base area, or it can serve as a short range exploration vehicle when included as payload on the hopper. The MTV is designed as a backup system to the tram. Since the transport of mined materials to the refining facilities is essential to life support, it is very important that we do not allow this operation to have a single point failure. MARGE will conduct autonomous long range unmanned exploration. HOMER will serve as a mobile lab for long range manned missions. The light cargo vehicle is an autonomous/telerobotic rover whose main purpose is the transportation of light cargo around the base area. The HCV, which will be operated telerobotically, will transport payloads of up to 10 MT within 20 km of the base to aid in such operations as base expansion by moving habitation modules from the descent vehicle to the base.

All of the components of the rovers should be modular. The advantages of this concept are that the modular blocks can be used as spare parts on almost any vehicle, and that new configurations can be made in-situ to meet unforeseen needs of the base. The astronauts will be able to construct (with robotic aid) any new vehicle configurations within the maintenance facility.

The modular components were designed to fit on both a large and a small basic chassis design.

FTS selected hemispherical wheels as the mobility system for both the large and small chassis. The chassis was designed to be constructed of two-celled monocoque aluminum alloy beams. We selected a cell thickness of 5.0 mm for Al 2014-T6 beams after performing a static analysis of several different thicknesses and materials using NASTRAN.

For the purpose of commonality, the main power system for all vehicles with the exception of the rocket hopper and the tram were designed to run on a methane/oxygen internal combustion engines. This commonality in power source will facilitate maintenance of the vehicles and will also simplify the production of fuel since a common fuel is utilized. In addition, a modular concept (coined "legobility") designed for the rovers which employs the interfacing of various subsystem modules (blackboxes) to configure a task-oriented rover (i.e. an unmanned autonomous rover or a manned mobile habitation module) is presented. This concept facilitates maintenance and also introduces redundancy into the system since spare parts are more readily available when needed. All these vehicles, when working together, will provide the support required for the sustenance of the advanced Martian base and indirectly, will lead the way to the settlement of Mars.

Recommendations

Due to the time frame and scope for which this project was undertaken, further analyses of each vehicle and its subsystems should be performed. Although this project gives an overall design for each of the vehicles which will be included in the integrated Martian transportation system, future studies will be required to develop these vehicles beyond the preliminary design stage. For further design of the tram, we recommend an analysis for reliability, and we recommend further research into the feasibility of using indigenous materials for the construction of the trestles. For future studies of a Martian lifting vehicle, we recommend a more detailed structural analysis of the grasping mechanism and the analysis of truss stability. For the hopper, the following areas must be studied further in order to achieve a complete vehicle.

- Vehicle lift-to-drag ratios
- Materials research/analysis
- Aerobraking
- Thermostructures
- IMU calibration

The Martian aircraft needs further analysis in its thermal system, state estimation, takeoff and landing and artificial intelligence for surface terrain following. A dynamic analysis is required for further studies of the rover, as well as a more in depth analysis of the engine performance characteristics.

Table of Contents

List of Tables and Figures

List of Acronyms

AI	Artificial Intelligence
BART	Base Area Regolith Transport
C&DH	Command and Data Handling
CFD	Computational Fluid Dynamics
CG	Center of Gravity
CPU	Central Processing Units
ECLSS	Environmental Control and Life Support Systems
EM	Environmental Model
FGM	Functional Gradient Materials
FRTS	Fixed Route Transport System
FTS	Frontier Transportation Systems
FTV	Fuel Transportation Vehicle
GNC	Guidance, Navigation, and Control
HCV	Heavy Cargo Vehicle
HOMER	Human Operated Mars Exploration Rover
IMU	Inertial Measurement Unit
JPL	Jet Propulsion Laboratory
L/D	Lift to Drag ratio
LCV	Light Cargo Vehicle
LEO	Low Earth Orbit
LMO	Low Mars Orbit
LOS	Line Of Sight
MARGE	Mars Autonomous Rover for Ground Exploration
MSRV	Manned Short-Range Vehicle
MTV	Materials Transport Vehicle
NASA	National Aeronautic and Space Administration
RCS	Reaction Control System
REM	Roentgen Equivalent Man
RPV	Remotely Piloted Vehicle
RTG	Radio-isotope thermoelectric generator
SAR	Search and Rescue
SIMPSONS	System Integration for Mars Planetary Surface Operation Networks
SPE	Solar Particle Event

1.0 Project Overview

This report is in response to the Request for Proposal (RFP) for an integrated transportation system network for an advanced Martian base. In this paper, Frontier Transportation Systems (FTS) presents the results of the SIMPSONS project (Systems Integration for Mars Planetary Surface Operations Networks), which is designed to address the needs for the advanced Martian base. Included in this report are the following six topics.

- the project background
- vehicle designs
- future work
- conclusions
- management status
- cost breakdown

1.1 Introduction

Nearly twenty-three years have passed since the *Eagle* first touched down on the Moon. Since that time, man began to focus his attention on Mars. NASA has planned several missions to the red planet, including the Mars Observer mission, scheduled to launch in 1992. Within the next decade, other precursor missions to Mars will lead the way to man's next great challenge--the settlement of Mars.

Initial manned expeditions will last less than 100 days on the surface of Mars, eventually building up to 600 days. As travel to Mars becomes more frequent, an initial permanent Martian base will be established by the year 2020. Ideally, the base will continue to expand, evolving until the year 2040, when an advanced Martian base will be realized.

1.2 Project Scope and Limitations

Our project focuses solely on the surface transportation support of an advanced Martian base. At this stage of development several elements will be required, including heavy-lift launch vehicles, interplanetary transfer vehicles, orbiting nodes, and ascent/descent vehicles. Any one of these would be a significant project in itself; thus, they do not fall within the scope of this project. However, requirements for ascent/descent vehicles will be

discussed because of their importance to the supply of the Mars inhabitants. A more detailed description of the approach FTS did take toward ascent/descent vehicles appears in Appendix A.

1.3 Assumptions

The transportation system proposed to support the advanced Martian base will assume the following factors.

- Advanced Martian base exists
- Transportation node in low Mars orbit exists
- Supply route between LEO and LMO available
- H_2O present on Mars

1.4 Report Overview

The next section will present the project background which lays the basis for the Martian integrated transportation system. Following the discussion of vehicles, detailed analysis of the common subsystems will be presented, including propulsion/thermal, communications, life support, and command and data handling. Finally, the FTS management structure and the SIMPSONS project cost analysis will be given.

2.0 Project Background

In order to precisely determine the goals of our transportation system, the advanced base needs to be clearly defined. To this end, FTS researched the most likely arrangements and locations of an advanced Martian base and selected a specific configuration. While this represents our expected base site, we have endeavored to make our transportation system adaptable to many locations.

2.1 Base Location

The advanced Martian base will be located in the region of *Utopia Planitia*, approximately 30° North latitude and 240°-280° West longitude. One reason for this selection is its favorable proximity to possible mining locations, which will facilitate the transport of raw materials to the base. Also, this latitude aids the ascent/descent vehicles by minimizing the plane change required to reach the orbiting transportation node. In addition, this region is the largest flat area on Mars, which makes spacecraft landings, long distance travel, and communications easier. Finally, radiation shielding provided by the Martian atmosphere is increased at this location due to its low altitude (-1 km). Other possible base locations are discussed in Appendix B.

2.2 Base Mission Operations

With minimal support from Earth, the Martian base is expected to use indigenous resources to sustain life and maintain base operations . To accomplish this, oxygen and water will have to be extracted from the raw materials which are mined from the surface.

After this, the most important mission of the base is to undertake scientific exploration and research. Included in this category are studies of Martian geology, history, meteorology, and Martian satellites. In addition, such a base will provide a great deal of information about extended duration human operations in low gravity, and can also serve as a way-station for missions to the asteroids and outer planets.

2.3 Base Components and Personnel

The base will accommodate a crew of 12 to 18 persons with the possibility of expansion. The main components of the base include the centrally located habitat area, a manufacturing facility, two nuclear power plants, two landing

3

pads, and a garage/maintenance facility. A more detailed description is given in Appendix B, and the general base layout is shown in Figure 2.1 below.
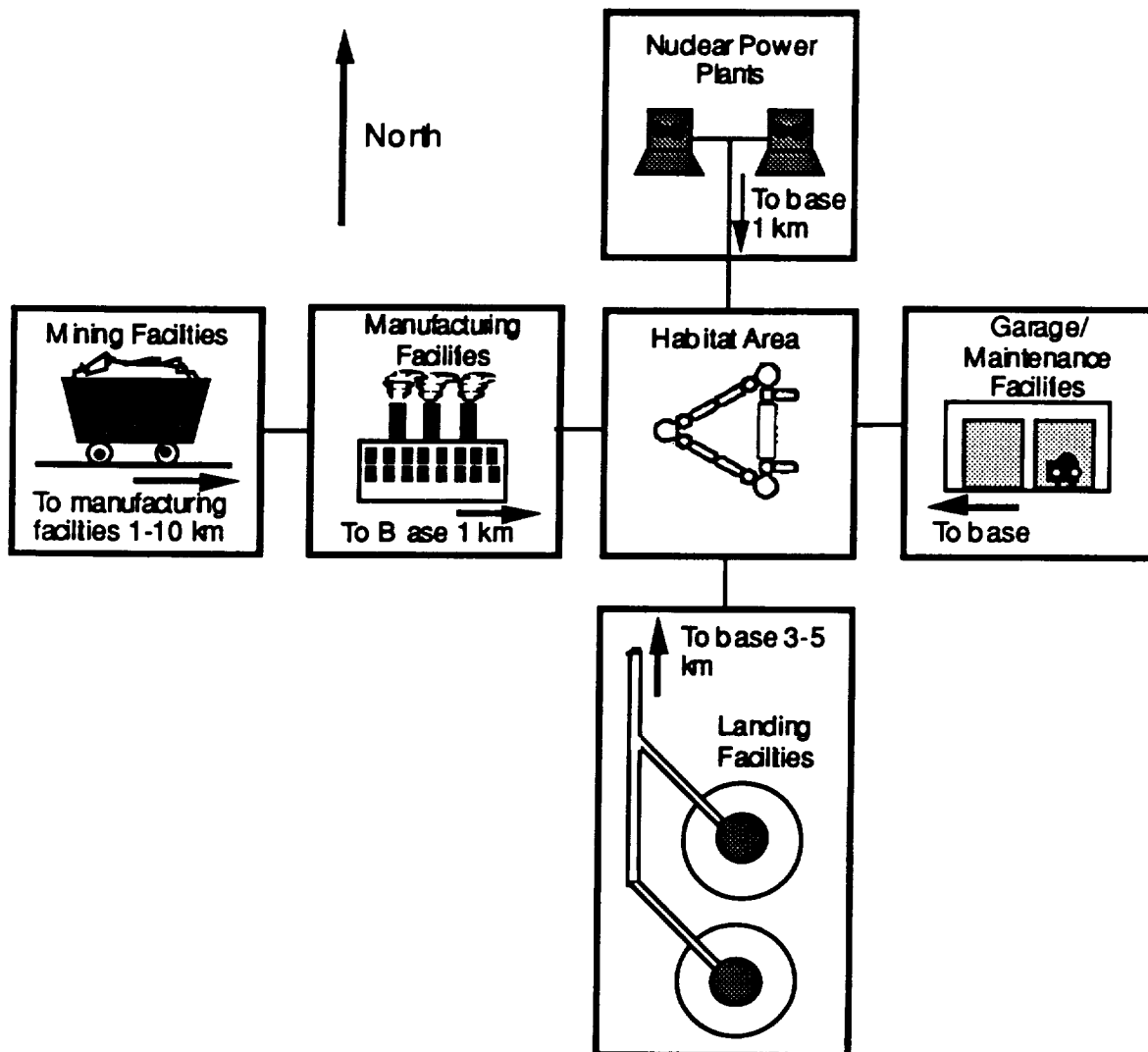
Figure 2.1 General layout of the advanced Martian base

2.4 Transportation Needs

Surface transportation is needed for travel between some of the more distant elements of the base, as well as for mobility of crew and payload from one area of the base to another. Scientific expeditions require the use of both manned and unmanned transportation systems to reach distant sites of interest. Likewise, outposts such as scientific stations or mining sites need maintenance and replenishment of supplies, and this can be accomplished by surface rover transports or rocket hoppers. Closer to home, raw materials must be delivered to the manufacturing facility for the production of

necessities, such as oxygen and fuel, for base sustenance and maintainability. All of this requires a flexible transportation system capable of transferring heavy cargo on a regular basis over distances farther than the confines of the base.

2.5 Overview of Transportation System

Ultimately, the transportation system selected for the Mars base should be compatible with all payloads and should be adaptable to meet many tasks, including those unforeseen. Along with vehicles for the transfer of non-pressurized cargo, pressurized vehicles will also be needed for long term manned travels. In addition, an organized road system between major elements of the base may also lead to more efficient transportation of cargo and crew. A transportation system composed of a set of modular vehicles which fulfills the needs of an advanced Martian base is presented in the following sections. These vehicles include an aerial tram, a lifter, a rocket hopper, Martian aircraft, and several rover designs. In addition, several subsystems will be addressed separately in our report due to their system-wide commonality, including power and propulsion, safety, communications, and command and data handling.

3.0 Fixed Route Transport Systems (FRTS)

The main FRTS requirements, which cater to the mining goals, are as follows.

- 15 km range
- Transport capacity of 216 metric tons of raw material/day
- Modular design of payload chambers

The four candidates which FTS evaluated for a fixed route transport system were an aerial tram, a railway, an elevated rail, and a MAGLEV. Since all vehicles being considered were capable of meeting the required payload capacity and delivery rate, these factors were not included in the FRTS decision matrix shown in Figure 3.0.1. Instead, ease of construction and structural weight, being closely related, were the most important considerations.

The aerial tram is easy to construct, as it merely involves the setting up of two stations and intermediate trestles for support. In addition, the tram is easily automated, inexpensive to build and operate, and it requires little maintenance. The railway is more complicated to construct because a path must be cleared, larger terrain features must be avoided, and frequent maintenance would be required. Both the elevated rail and the MAGLEV require large, heavy structures to support the rail above the ground. The MAGLEV, which is a very complex structure, offers the advantage of incredible speed and less wear on the rails; however, these factors were not as important issues as the others in our selection criteria. Thus, one can see in Figure 3.0.1 that the aerial tram is by far the most favored fixed route transport system.

	Aerial Tram	Railway	Elevated Rail	MAGLEV
Ease of Construction (x 10)	8 / 80	6 / 60	3 / 30	3 / 30
Weight (x 10)	9 / 90	6 / 60	4 / 40	8 / 10
Maintenance (x 6)	10 / 60	4 / 24	4 / 24	5 / 10
Simplicity (x 4)	10 / 40	7 / 28	5 / 20	1 / 10
Total	270	172	134	60

Figure 3.0.1. Fixed Route Transport System Decision Matrix

3.1 Characteristics of an Aerial Tram

In an aerial tram, a motor located at one station pulls the supporting and/or driving cable(s) between the two stations. FTS evaluated the performance of monocable and bicable trams with continuous, or to-and-fro, circulation.

For a monocable system, such as the one illustrated in Figure 3.1.1, a single cable is used as both the supporting and hauling rope. Figure 3.1.1 illustrates the use of to-and-fro movement in which the carrier travels from Station A to Station B, and then retraces its track back to Station A. In this design, a maximum of two carriers (one on each side) can be utilized at once. This is the simplest design possible.
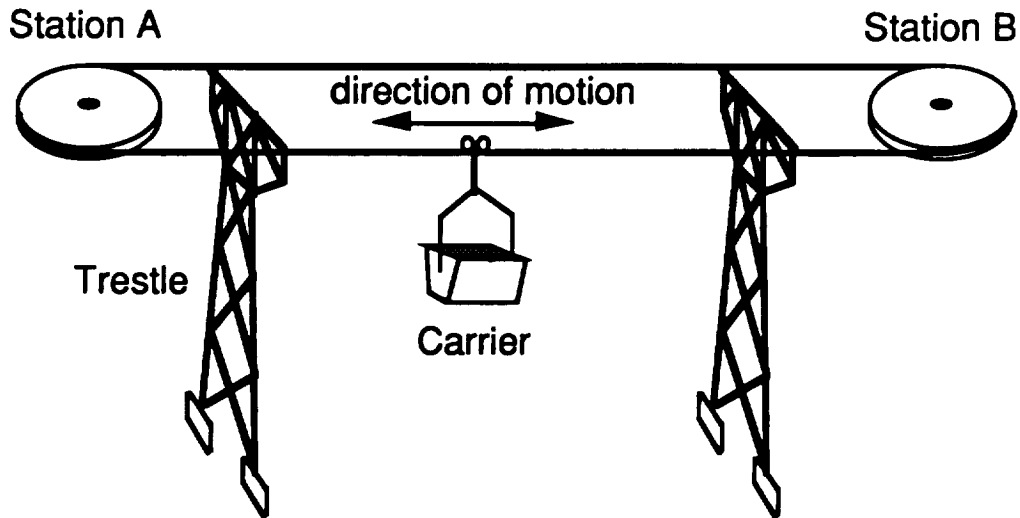
Figure 3.1.1. A basic conceptual monocable, to-and-fro aerial tramway design

A continuous, circulating movement design is shown in Figure 3.1.2. Unlike the to-and-fro movement, the continuous movement allows the carriers to travel in a loop; thus many carriers can be placed on the line at one time. However, the number of carriers is restricted by the load capacity and the transporting distance. Also, in this type of movement, the need for the direction change required in the to-and-fro movement is eliminated.
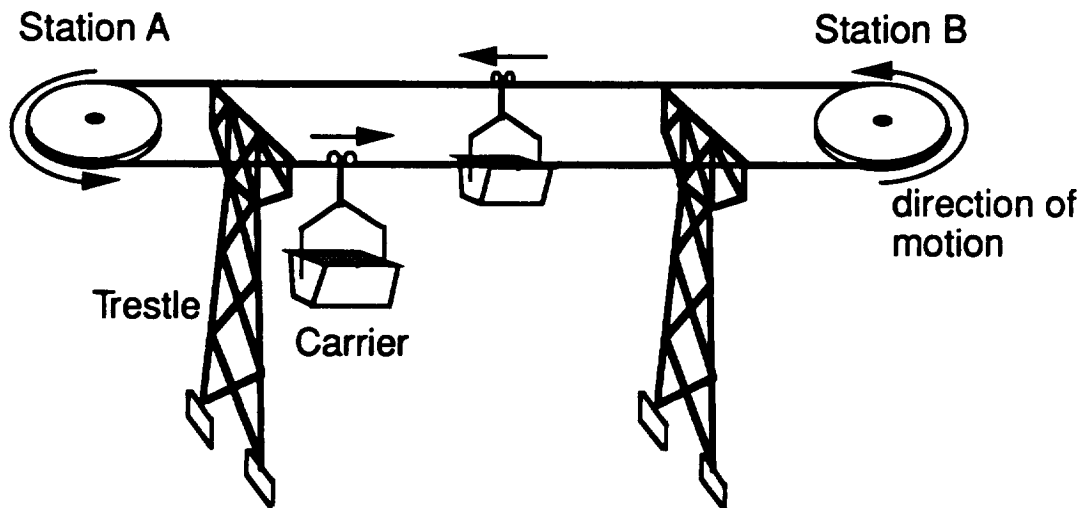
Figure 3.1.2. A Basic Monocable, Continuous Circulating Aerial Tramway

Another, more complex system considered was the bicable system shown in Figure 3.1.3. In this system, two separate cables are used for hauling and carrying. The hauling cable (driven by the motor) attaches to the carriers and pulls them along the fixed carrying cable. For the bicable system, the only

function of the carrying cable is to support the weight of the carriers and the payload. This method lessens the load on the cables since each cable is specialized to a specific task, as opposed to the monocable design, in which one cable is used for supporting and hauling.
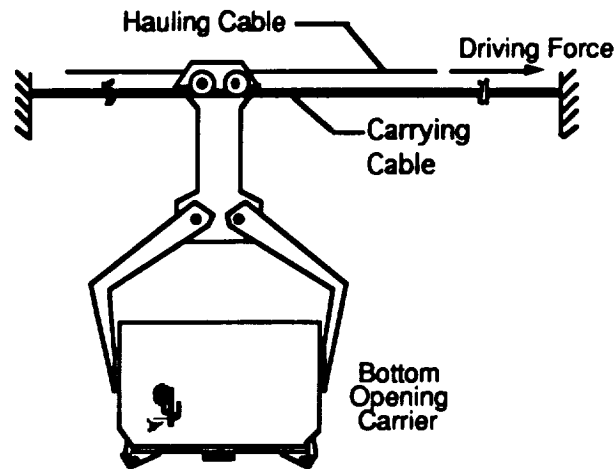
Figure 3.1.3. The Bicable System Setup

The bicable system can haul much greater loads than a monocable, but the existing monocable systems on Earth are already capable of transporting five times the mass required to support the base . Thus, a monocable system on Mars will be capable of transporting more than five times the required payload. For this reason, as well as the ease of construction and maintenance on monocable systems, FTS will design a monocable aerial tram for the transport of mining products.

3.2 Tram Structure

The monocable aerial tram will have trestles composed of some type of concrete structure that can be made from indigenous soil. The wire rope will be of round strand construction, composed of 114 steel wires. The carriers, illustrated in Figure 3.2.1, will be constructed out of the aluminum alloy, Al 2014 T6.
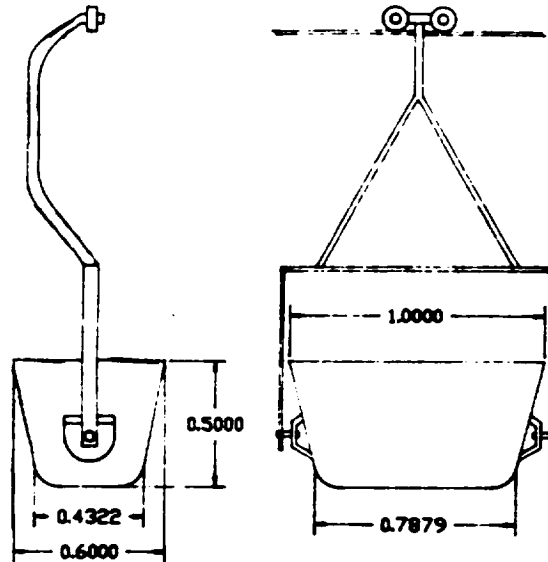
Figure 3.2.1. Two-wheeled carrier of monocable ropeway

3.2.1 Design Parameters

The following parameters resulted from the needs of the monocable tram. They collectively define the profile of the ropeway.

S_{br} = 31,900 kg

s = 5

d = 30 mm

w = 7.4 kg/m

l_s = 150 m

v = 2.5 m/s

n = 200

t = 3.0 mm

W = 300 kg

where S_{br} = Breaking force of the rope

s = Factor of safety

d = Diameter of the rope

w = Weight per unit length of the rope

l_s = Span length, or length between trestles

v = Travel speed of the ropeway

n = Number of cars on the route (per 15 km distance)

t = Thickness of sheeting material used to construct carrier

W = Carrier payload

A velocity of 2.5 m/s is recommended for continuously circulating ropeways with fixed grips in order to facilitate automation [3.1]. The thickness of the sheeting from which the carriers are constructed was dependent on the volume of the carrier [3.1, p. 385]. The grips were chosen to be fixed for simplicity in design. The spacing of the trestles provides a factor of safety of 10. The trestle spacing can be increased to up to 300 meters, while still ensuring a factor of safety of 5. This would greatly decrease the effort necessary for construction.

3.3 Automation

To maintain continuous transport of regolith to support the daily activities of the advanced Martian base, the aerial tram will be automated. Automated methods for both loading and unloading will be necessary. Characteristics such as low clearances at the loading site (the mine) and high clearances at the unloading site (the refining facility) are desirable to allow gravity to assist in the loading and unloading of the materials.

Our carriers are of a tilting bucket design. There is a catch gear fitted to the hanger to prevent the carrier from tilting upside down. This gear is automatically released at the refining facility. The carrier then tilts automatically, dumps it contents and may then be reverted to its working position. The axis of rotation must occur just below the center of gravity of a loaded carrier, while the center of gravity of an empty carrier will be below the fulcrum.

3.4 Command and Data Handling

To maintain and control the automation of the tram, the command and data handling system of the tram must be able to detect possible hazards or malfunctions within the system and control the transport of the regolith. Included among the duties of the computer system is to maintain the speed of the motor and the cable for correct distance between consecutive carriers, and to handle the loading and unloading procedures of the carriers. If malfunctions or hazardous situations arise, the computer will communicate with the base to update its status.

3.5 Power

The aerial tram will be mechanically driven by an electrical engine powered by the base's nuclear reactors, the reliability of which would

eliminate any need for refueling. Electrical cables could easily be strung along with the tram cables to provide power to intermediate stations (i.e. engines).

Electric motors are almost exclusively used for driving ropeways on Earth for the following reasons.

- Small dimensions, relative to the output
- A relatively wide speed control range, in pair with a wide output range. (The speed control is affected in an easy, quick and continuous manner, not requiring intricate and costly mechanisms such as gear boxes.)
- Easy to operate
- Large short-time overload capacity
- Protection arrangement by electric current is simple

A three-phase commutator motor was chosen to drive the ropeway because it is the best type for operating continuous ropeways. It has a shunt characteristic which facilitates continuous and economic speed control. The motor also has a laminated yoke to eliminate losses on hysteresis and eddy currents. This motor will provide the 16kW of power necessary to drive the system. We recommend that an internal combustion engine similar to those of our other vehicle designs be located at the refining facility as a backup system.

The motor will need to be protected from the environment. This should not be a problem, as the engine will be protected largely by the refining facility where it will be located.

4.0 Lifter

The lifter is designed to perform the loading and unloading processes within the base vicinity. The lifter must interact with several types of vehicles, ranging from the ascent/descent vehicle to the cargo rovers. FTS will require that there be at least three lifting vehicles. One would be located at the landing pad, one at the base, and one extra should be present at any given time in case of mechanical failure. A crane design was chosen after several lifting vehicles were evaluated. The following sections will discuss the components of the crane including structure, command and data handling, power, and safety factors.

4.1 Lifter Requirements

To operate efficiently and effectively, the crane should be able to survive the Martian environment for a nominal lifetime. Therefore, the crane must meet the following requirements.

- maximum lifting capacity of 30,000 kg
- capacity for cargo up to 6m wide and 10m long
- total range of 3 km
- fully telerobotic
- flexible
- durable
- low maintenance
- simplicity in design

4.2 Lifter Characteristics

In our evaluations, we looked for the least massive crane which still satisfied the original requirements. Trusses were selected as the main lifting component to reduce weight. The selected crane, shown in Figure 4.2.1, is a composite of many lifting vehicles, which currently exist on Earth. Figure 4.2.2 shows a front and a side view of the crane.
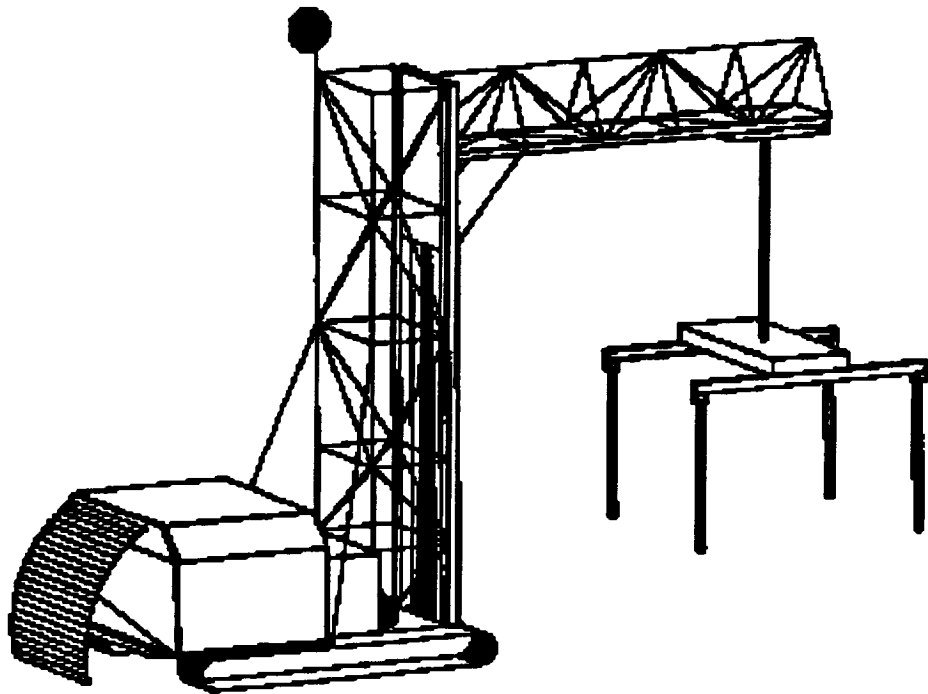
Figure 4.2.1. 3-D view of the Mars crane
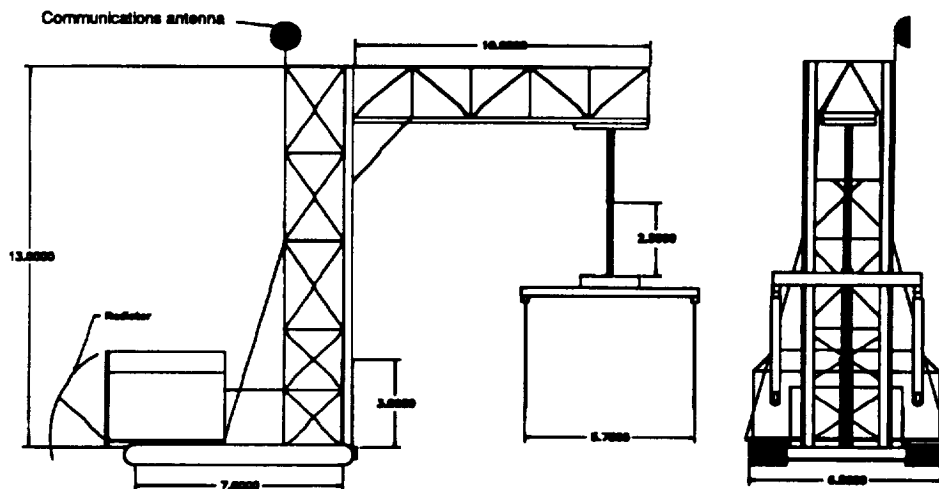
Figure 4.2.2. Front and Side View of Crane

As shown, the crane has a horizontal truss and a vertical truss structure similar to the tower configuration of lifting cranes. The horizontal truss moves along the vertical truss in a forklift type movement. In the back of the

14

crane is a large container which, by housing indigenous material, acts as a counterweight. The horizontal truss has a maximum extension of about 10 m which provides flexibility in reaching the payload, and the vertical truss has a height of about 13 m. The grasping mechanism which hooks onto the payload can vary in position along the horizontal truss.

The crane has a tracked wheel mobility system. We computed the empty weight of the crane to be no more than 30 MT. By adding regolith as counterweight, the total weight could go up to as much as 100 MT. The trusses and the grasping mechanism will be made mainly of aluminum alloy materials, which provide lightweight and high strength characteristics.

4.3 Grasping Mechanism

The grasping mechanism has three degrees of freedom that can accommodate a maximum cargo width of 6 m. As seen in Figure 4.3.1, the mechanism consists of four payload connectors that hook on to the side of the payload, assuming most payloads have universal trunnions on the side, similar to the Space Shuttle type payload trunnions.

For delivery, the grasping mechanism can swivel over restricted angles. The payload connector can travel along the length of the cargo depending on the locations of the trunnions, and they can also travel along the width, depending on the size of the cargo.

Payload Connector
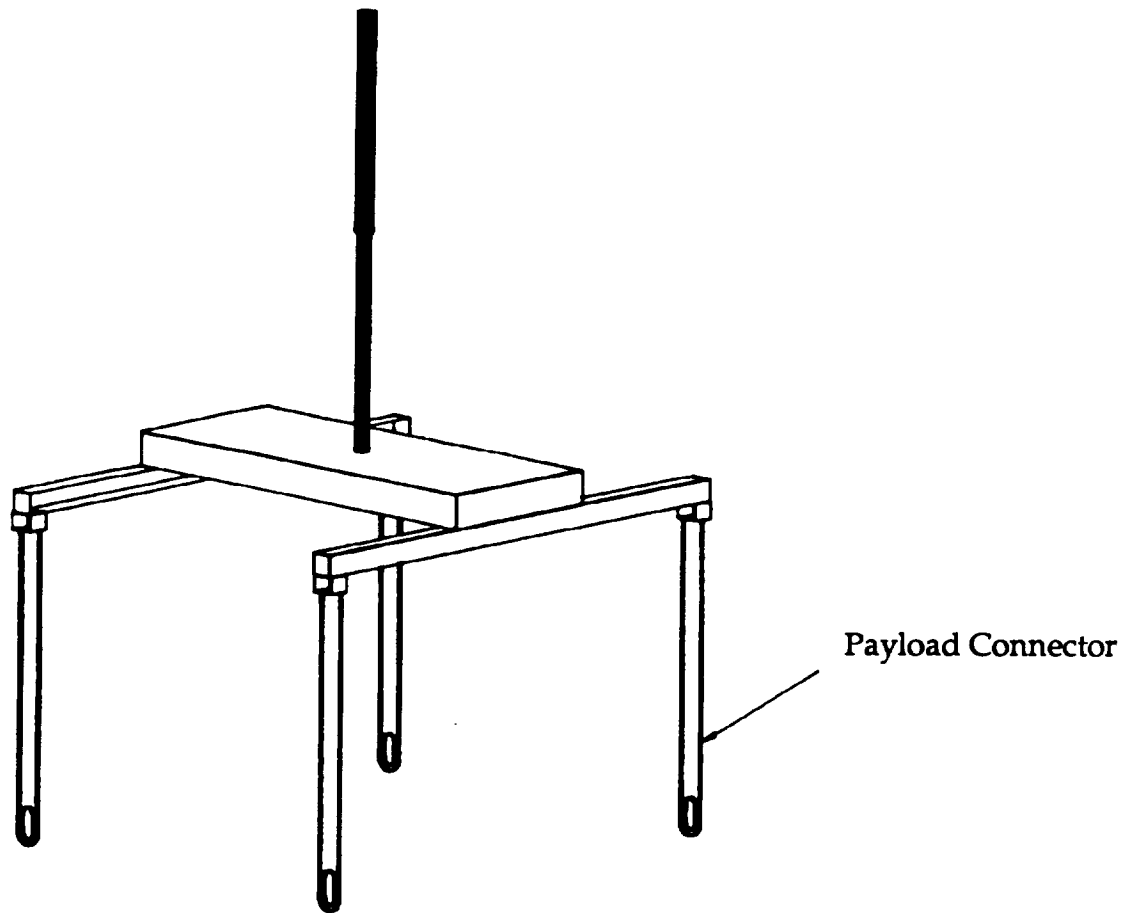
Figure 4.3.1. Grasping mechanism

4.4 Power Source

The heavy lifter will use an internal combustion engine similar to those used in the rovers discussed in Section 7.8, also using methane and oxygen as its fuel and oxidizer. Both the locomotion and the lifting power for the heavy lifter will be supplied by a single engine, requiring 422 kW of power for locomotion and 50 kW for maximum lifting. These power requirements are not additive, since the lifter will not be traversing while lifting or lowering a payload. The hoisting of the maximum cargo, 30 MT, using the grasping mechanism requires approximately 40 kW at a hoist rate of about 0.4 m/s. Also, the power required to translate the horizontal truss along the vertical truss with a 30 MT payload is about 50 kW at a rate of 0.3 m/s.

Power is calculated by multiplying the weight of the payload by the hoist rate, or

$$P = F * V$$

where F is the weight of the payload and V is the hoist rate. The required locomotion power was calculated in the same fashion as that needed for the rovers using a speed of 2 km/hr and is described in Appendix C.

4.4.1 Engine Specifications

The lifter's engine, although very similar to those used in the rovers, is different in one main aspect — engine speed. The lifter, being a very heavy and slow machine, will employ a low speed, high torque engine. Its engine will achieve maximum power output at 1500 RPM, as opposed to the rovers' 3000 RPM [7.2]. The lifters' engine will be geared such that it is driving only one mechanism at a time, whether it be the drive train, the vertical truss, or the grasping mechanism. Therefore, the lifter will not be capable of moving while lifting or lowering a payload. This situation would probably not be desirable anyhow, as it could create a situation in which the lifter would become unstable. The maximum speed achievable by the heavy lifter will be 2 km/hr. The engine will displace 25.2 liters and weigh approximately 500 kg (see Appendix C). The lifter will have a maximum range of 10 km , thus it will carry 500 kg of the methane/oxygen bipropellant, 435 kg of which is oxygen and 65 kg of which is methane. [7.1]

4.4.2 Engine Cooling

The engine will be cooled in a fashion similar to the rovers. It will have a curved radiator and will use propylene glycol as a coolant [7.5]. It was calculated that the radiator on the heavy lifter will have to dissipate 108 kW (see Appendix C). Using a coolant temperature equivalent to the rovers' 525°K will require a radiator surface area of 25.8 m². Since the radiator will be constructed of pure aluminum 1 cm thick and be coated with silverized Teflon, this translates into a radiator weight of 2300 kg.

4.5 Telerobotics

The crane will be controlled telerobotically by an operator from a command module. The module can either be placed in the habitation module or near the landing pad, where the majority of the loading and unloading processes will occur. To aide in telerobotics, the crane will need various sensors to accomplish the following tasks.

17

- avoid obstacles
- detect tilting of the vehicle due to uneven distribution of cargo mass
- detect the range to the obstacle during loading and unloading processes
- provide warnings of undue strains in support members

Many cameras will be placed at convenient places on the crane, ranging from a bird's eye view to acquisition cameras. The acquisition camera will have the capability to zoom in to small, critical places for accurate detail. Since the crane will operate within the base perimeter where most surfaces will be flat and hard, it does not require most of the surface sensors like the rover.

4.6 Command and Data Handling

The command and data handling system for the lifter will be much simpler than that of the other vehicles since the main mode of operation will be telerobotic. The computer system for the lifter is used mainly to detect the possible hazards mentioned above and alert the operator of possible mishaps. A more general description of the command and data handling subsystem is given in Section 8.4.

4.7 Safety Factors

There will be many redundant systems to confront all undesirable scenarios. One such scenario is a fatigued structure forced to withstand a moment applied by the uneven distribution of mass within the cargo. To prevent this, the crane should be inspected prior to any major lifting operation. One other possibility is the failure of the sensors, which is unpredictable and critical for the loading and unloading process. This scenario demands a second set of sensors to verify the first. Another scenario is the potential loss of control of the crane, endangering the cargo and any structures nearby. This worst case scenario could be prevented by a redundant system for operator override or shutdown.

18

5.0 Hopper

While the system of rovers covers exploration up to 100 km from the base, a new vehicle is required for exploration at greater distances. A ballistic rocket hopper was envisioned, providing a shorter transit time and a more flexible operating range. With a payload of 6.5 MT, this vehicle can realize two missions: carrying an autonomous, light rover with various scientific payloads, or carrying a light rover and a crew of two, with supplies for seven days. Our hopper can transport either payload to a site up to 1000 km from the base, where the rover would then enable exploration within a 100 km (10km for manned rover) radius around the landing site. Due to the fuel selection for our overall system, on-site refueling would not be feasible, and our hopper is limited to one hop away from and one hop back toward the base.

Since this hopper uses a ballistic trajectory, it has the potential to ascend 350 km vertically, making it virtually a suborbital flight. For this reason, previous ascent/descent studies were useful in evaluating the design. Also due to this trajectory height, the hopper would be grounded during solar particle events or Martian sandstorms.

5.1 Hopper Configuration

Of all the treatments we analyzed for Mars descent vehicles, most considered the importance of ease in unloading cargo as secondary. However, we elected to emphasize this area in our conceptual design to simplify the ingress and egress of cargo, whether it be autonomous or manned. The assumption was that the other systems (such as shielding and propulsion) could still be successfully addressed while working around the cargo area, and we feel that the final configuration bears out this assumption.

As can be seen in Figure 5.1.1, the cargo bay was placed at the vehicle's center. Then the hover engines were balanced around the bay in two equal, self-contained, and coordinated sets. This arrangement provided stability in firing, and the center of mass does not shift dramatically as fuel is consumed. Much of this configuration was derived from that of a previous Martian ballistic hopper [5.1].

19
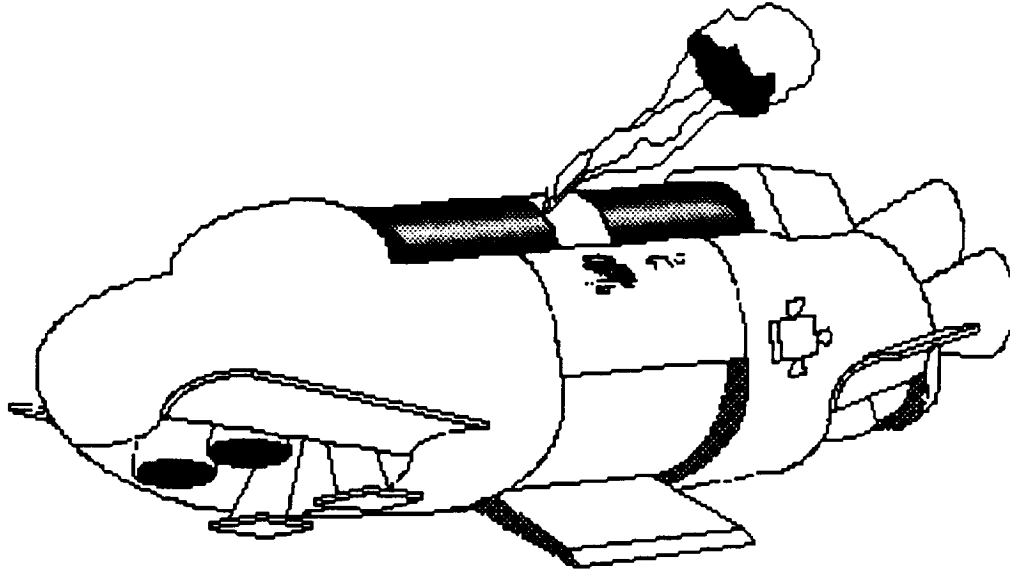
Figure 5.1.1. Rocket hopper conceptual design

The trajectory of our craft was modeled by three phases -- launch, ascent, and touchdown. During launch, all of the engines in the recessed undercarriage would fire until the vehicle attained an altitude of 50 meters, at which point the vehicle would pivot into the attitude required for the ascent phase. This pivot would include the firing of the RCS jets to point the nose in the intended direction of flight, and then a moment would be applied by the hover jets until a flight path angle of 50° was reached. As the clamshell doors are shut underneath, the main engines (aft) would fire, sending the hopper into a ballistic trajectory. The vehicle would then coast through the apex of the flight and the beginning of descent. At about 2/3 of the way through the flight, the undercarriage engines would fire at 35% thrust until it was under Mach 3 (about 800 m/s in the upper Martian atmosphere), at which point a parachute would be deployed. Under 100 meters of altitude, the chute would be released, and the final course corrections and touchdown would be powered. A sample descent was computed using the FORTRAN program [5.2] found in Appendix D, and some of the results for a 1000 km trajectory are summarized in Table 5.1.1 below.

Table 5.1.1. Example of descent, 1000 km trajectory

Alt. (km)	Vel. (m/s)	Type of Deceleration	Considerations
350	1950	atmospheric drag	low L/D; heating up to 1500 K
200	1600	powered	35% thrust
75	800	Rotofoil parachute	error compensation for trajectory
1	50	powered	100% thrust; hover and touchdown

These programs were also run to arrive at a total structural mass of 30 metric tons (MT). For a 1000 km mission, 87 MT of fuel (CH_4/LOX) would be required, yielding a take-off mass of 124,000 kg. These and other hopper characteristics are summarized in Table 5.1.2.

Table 5.1.2. Characteristics of the ballistic rocket hopper

Payload mass	6.5 MT
Structural mass	30 MT
Propellant mass	87 MT
Propellant volume	106 m^3
Approximate dimensions	5 x 10 x 4 m
Maximum range	1000 km
Service ceiling	350 km
Maximum acceleration	±29.4 m/s^2
L/D (ascent/descent)	1.5/0.8

5.2 Thermal Protection

During much of its trajectory, and especially in descent, the rocket hopper will experience extreme heat on the order of 1500°K, a figure that resulted from runs of the computer programs mentioned above. To combat this, most of the previous studies have used massive heat shields for their vehicles, and the shields usually wind up discarded after one use. To avoid this cost, we

21

propose the following material, which also provides a necessary preamble to the structure section.

One area of current research that has attracted much interest, especially in the Japanese scientific community, is Functionally Gradient Materials (FGM) [5.3]. These are being designed with the National Aerospace Plane in mind, a vehicle whose mission is not entirely dissimilar to that of our hopper. To this end, materials are being designed which will withstand 2000°K on the outer surface and a temperature difference of 1000°K across the material, which will be more than adequate for our needs. To accomplish this, materials could be combined as shown in Figure 5.2.1. Given 50 years of technological advance, this concept should be viable in terms of engineering and cost, and fully 90% of our hopper's shell could consist of FGM.
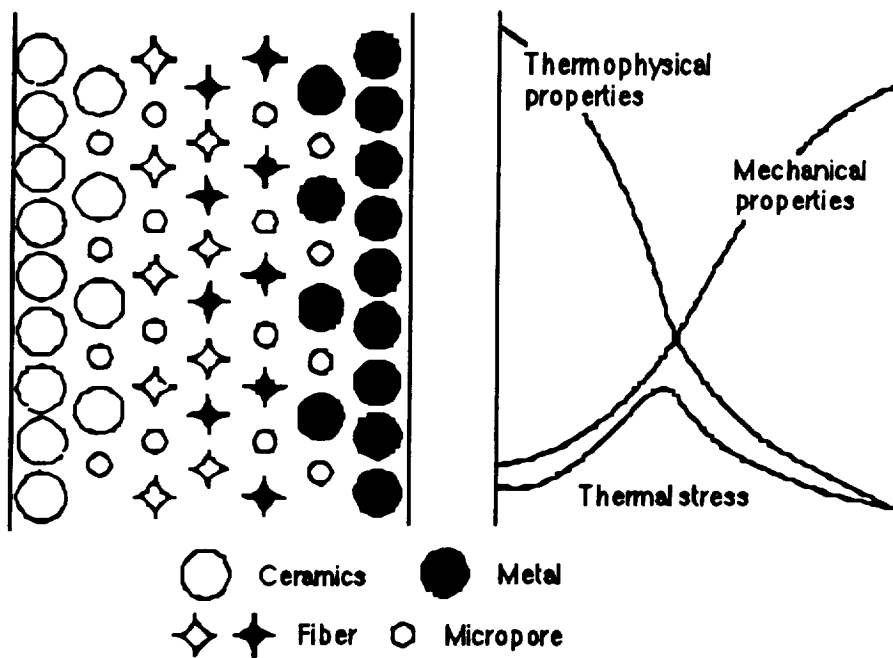
Figure 5.2.1. Concept behind Functionally Gradient Materials (FGM)

By combining a ceramic resistant to UV degradation with a metal such as titanium, an optimum shell could be created. Instead of relying on ablative heat shields, UV coatings, and a separate support structure, a heat-resistant load-bearing skin can be provided.

22

5.3 Structure

Our hopper is not comparable to any conventional aircraft or rocket, and is therefore not subject to conventional types of structural analysis. For instance, spars and wing boxes would have no real function in our craft, and treating it as a pressure vessel is impractical. The best approximation is to treat the hopper as a bare aircraft fuselage with bulkheads down the length and stringers tying them to the skin. However, engines have been placed at almost every conceivable place on the hopper, thereby creating the need for numerous load-paths. To handle this, a three-dimensional truss would have to connect each bulkhead, providing sufficient stiffness for all potential thrust directions. A crude depiction of these combined elements is in Figure 5.3.1.
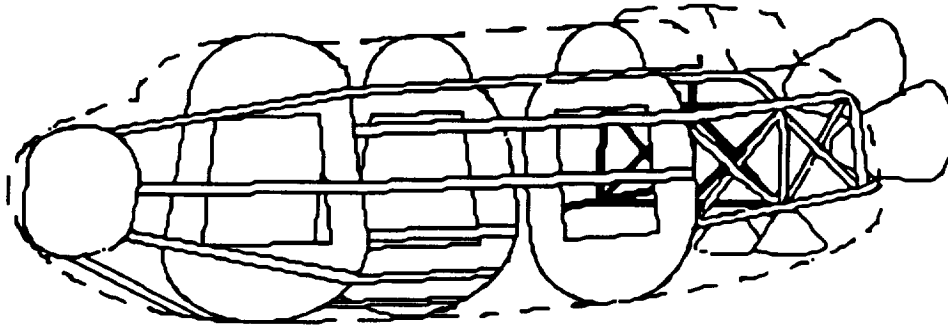
Figure 5.3.1. Sketch of some primary structure elements

The end result of our analysis consists of a partial load-bearing FGM skin supported by a graphite/Magnesium interior structure. The skin is limited in its ability to bear loads by two main considerations. First, the engines of the undercarriage are recessed, and the ascent and descent thrust cannot be carried by the exterior skin. Also, there are several panels in the skin (clamshell doors, payload door) which would have to be carefully supported so as not to provide weak points in the structure.

In order to properly evaluate our design, a complete thermodynamic analysis would be required, including NASTRAN static and dynamic studies and a CFD treatment. Because of time limitations, this analysis could not be included in within the scope of the SIMPSONS project.

5.4 Propulsion

The hopper propulsion system will be a sophisticated and integrated set of engines due to the Vertical Take-Off and Landing (VTOL) launch and landing

23

techniques selected. Two identical sets of main engines on the underside of the craft will provide hover and brake capability, as well as a launch capability up to 50 meters. These engines will require throttle capability as well as some degree of vectoring, and they will provide up to 500 kN of thrust. A minimum of four engines is recommended for stability, but more nozzles of smaller exit areas could be used to help disperse the Martian dust kicked up during approach. Finding ideal expansion unfeasible, we sized our nozzles by the available area, arriving at a 2.25 meter diameter.

In the rear will be placed a cluster of ballistic launch engines which will provide the main boost into the suborbital trajectory. These engines will provide a total of 3500 kN at peak thrust, and they are closer to 4m in diameter. In addition, maneuvering engines (RCS jets) will be placed at symmetric locations to provide stability, to prepare for ballistic ascent, and to provide minor course corrections during flight. The last two categories of engines will need to be throttled, but not vectored.

As described previously, all engines will use CH_4/LOX as propellant.

5.5 Aerobraking

Many designs of atmospheric entry vehicles rely on wings to provide aerodynamic braking. However, since the atmosphere on Mars is two orders of magnitude less than that of Earth, the wings required to significantly slow a vehicle of the mass we are considering would be on the order of tens of meters in span. Since this is obviously impractical, our vehicle will rely on retrorockets and parachutes, as well as on whatever drag can be obtained.

The deceleration mechanism of choice was the Rotofoil (Rotating Flexible Drag Mill) [5.4] parachute due to the supersonic speeds the hopper will encounter. Its performance should exceed that of conventional ribbon parachutes. Our hopper will carry two Rotofoils on each mission, one being 20 meters in diameter and the other 8m. The sizes of these chutes were selected to provide no more than three Earth gravities of deceleration and a total delta-v of about 700 m/s. Since the parachutes would not be cut free until the craft is within one kilometer from the ground, and the Martian winds are not significant outside of storms, it is conceivable that the parachutes can be retrieved. This would especially be true at the base landing areas, where the terrain would necessarily be rover-navigable, thereby giving a high probability that at least the smaller parachutes could be reused.

24

5.6 Life Support/Protection

Long range manned missions using the rocket hopper will last approximately 5 days. An ECLSS must be provided to supply life support for 2 astronauts for up to 7 days to include a safety factor for the astronauts. The partially closed ECLSS was chosen over the open system because it requires less mass, which decreases the size and fuel requirements of the rocket hopper. Refer to Section 8.3 for more information on the partially closed ECLSS. Table 5.6.1 lists power and mass estimates for a partially closed ECLSS for the rocket hopper obtained from a program written at the University of Texas at Austin [5.5].

Table 5.6.1. Power and mass requirements for rocket hopper ECLSS

Crew Size	2
Mission Duration (days)	7
Power Required (kW)	.495
Mass of Spares/Consumables (kg)	102.579
Mass of Systems Hardware (kg)	90.426
Total System Mass (kg)	193.005

To further support manned missions, the FTS hopper must provide adequate radiation shielding for its crew. Although the Martian atmosphere gives significant protection to vehicles on the surface, the rocket hopper is capable of reaching altitudes of 350 km. At this altitude, astronauts are not protected from the galactic cosmic or solar radiation. Astronauts will only be exposed to this radiation for a few minutes per mission, so the galactic cosmic radiation is insignificant due to its low intensity. Solar radiation, on the other hand, occurs in sudden, intense bursts. Shielding, similar in size to a Mars transfer vehicle, would be required for the hopper to operate during an solar particle event (SPE). To reduce the mass of the hopper, FTS has decided not to include radiation shielding on the hopper, but to restrict the hopper from flying during an SPE. This is a realistic assumption since these solar events occur approximately once every 10 years and last only one or two days.

5.7 Communications

The rocket hopper will communicate with the base via the satellite constellation (See Section 8.4 for description of communications system). The

hopper will utilize three sets of antennae, one for communications during flight, one to acquire navigational beacons, and one which will be deployed after landing.

Though the atmosphere of Mars is thin, the heating during re-entry may be significant enough to cause ionization, and this could interfere with or even black out hopper communications. If the problem of ionization does not occur, the hopper will use internally mounted antennas for communication during flight in order to protect them from the heat the hopper will undergo during aerobraking.

In the underside of the hopper would be placed a direction finding antenna, which would be used to acquire landing beacons. These beacons could either be those permanently installed at the base or those dropped by the Martian airplane in a previous reconnaissance mission, and the hopper would acquire them in the final descent stages.

Once the hopper has landed, a high-gain, high-frequency, steerable antenna may be deployed to permit transmission of scientific data which requires high data rates.

5.8 Autonomy and Telerobotics

At times, the crew may want to send an unmanned mission using the rocket hopper to reach distant sites for study. To do this, the AI must be capable of autonomous navigation to the desired location. Furthermore, the computer must also be able to select a favorable site to land and land there safely. In addition, telerobotic capabilities may be required to maneuver around the base or to navigate difficult flight missions. Although telerobotics require less AI, information regarding the state of the vehicle (such as velocity and altitude) must be relayed back to the human operator to allow him to navigate safely.

5.9 Command and Data Handling

To support autonomy and teleoperations, the following inputs will be required by the command and data handling system.

- Attitude
- Altitude
- Velocity and Position
- Surface Mapping

For a more general description on the command and data handling subsystem and on how the AI system architecture works, refer to Section 8.4.

5.10 GNC

The hopper will require an IMU capable of measuring the changes in attitude and position in every direction in order to fully know the state of the vehicle. This requirement will be met by 3 orthogonal gyroscopes and 3 orthogonal accelerometers. Time integration of the state will yield the base-relative position, heading, and attitude of the vehicle. The error in position accumulating through the integrator should be small enough, due to the short flight time, to be easily correctable during the hover portion of the flight plan, so position correction by satellite will not be needed.

Also aboard the hopper will be sensors for hazard detection and landing. Terrain avoidance radar should provide the hopper with enough information for safe clearance in both the horizontal and vertical directions. Also, landing beacons will provide the hopper with a direction toward the desired site. Finally, stereoscopic cameras will also aid the hopper in finding a suitably flat place to land, especially when it is doing so autonomously at the far end of the hop.

6.0 The Unmanned Martian Aircraft

Because the atmospheric pressure at the surface of Mars is equivalent to the pressure at 30 km altitude (100,000 ft) on Earth, aviation on the red planet may seem to be a difficult prospect. But, if the gravity difference is considered, the equivalent terrestrial altitude drops to 72000 ft, an altitude at which many reconnaissance aircraft are capable of sustained cruise. The thinner Martian atmosphere also makes it simpler to push an object as well, allowing long cruise ranges. The unmanned Mars airplane concept was studied at JPL in the late 70's and appeared to have no technical difficulties in designing and operating a remotely piloted Mars airplane. It also appeared that such a vehicle could be most useful in extending the capability of a Mars surface crew.

6.1 Applications

Thanks to its long range capability and versatility, the Mars airplane is well suited for long range scientific exploration, especially over rough terrain, and it can fulfill a wide range of missions such as surface imaging, atmospheric sounding, high altitude meteorology, and radio science. In addition, an unmanned Mars airplane can perform other useful functions such as the following.

- Deployment of remote observing stations (penetrators, fixed or moving surface stations) or navigation beacons, either by air drop or by landing
- Servicing of manned outposts and delivery of high priority hardware to crew far from base on a surface sortie, as well as return of priority samples from a rover crew to the base
- Search and Rescue (SAR) in the case of the loss of communication between a rover and the base

28

6.2 Constraints

The major constraint for the aircraft is the Mars atmosphere. Figure 6.2.1 shows density and temperatures (based on Viking I measurements) and calculated speeds of sound. The density of the Martian atmosphere at ground level is about 1% of the value at sea level on Earth. This low density requires the use of large wing areas (low wing loading), high cruise lift efficiency and high aspect ratios to fly at subsonic speeds at an acceptable level with limited power.

Due to this thin atmosphere and in order to keep the aircraft dimensions and power requirements reasonable, the payload cannot exceed a few hundred kilograms, restraining the concept to unmanned aircraft.

Mars gravity being only .377 of Earth's, some of the performance degradation due to the thin atmosphere is offset by a lower effective wing loading. The reduced gravity then gives the Mars aircraft a 2.65 times longer range for the same L/D.

The low density of the Mars atmosphere and the moderate flying speed of the aircraft result in very low Reynolds numbers (10^5 versus 10^7 for a light aircraft on Earth). At such low Re, the laminar boundary layer on the airfoil tends to separate easily in positive pressure gradients, increasing the drag and decreasing the lift. The Mars aircraft will thus have to use airfoils specially designed to operate efficiently at low Re.

Another constraint is that the composition of Martian atmosphere (95% CO_2) doesn't allow the use of air breathing engines. Since jet-engines can't be used, the aircraft will have to rely on propellers. Because the speed of sound is lower than that on Earth (about 70% of its value on sea level on Earth), the propeller's diameter and rpm are severely limited, considering that the limiting tip Mach number for efficient operations is not to be exceeded.

29
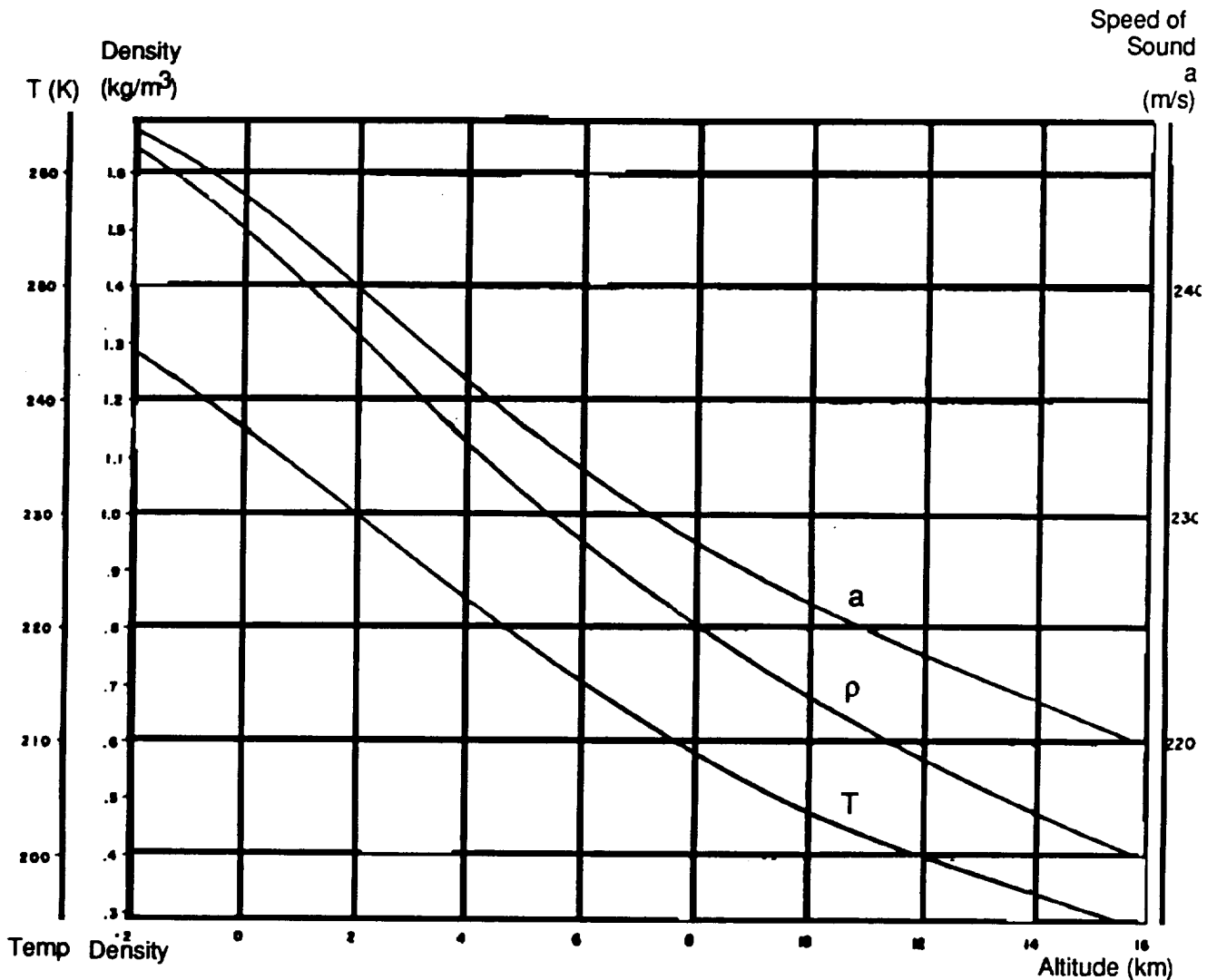
Figure 6.2.1. Mars atmospheric parameters

6.3 Operational Requirements

To enlarge the scope of operation, two different types of aircraft will be studied, both of which are unmanned.

- A heavy aircraft, operating from the base's runway with a payload capability of 300 kg and dedicated mainly to heavy scientific missions and servicing of outposts. The required range is at least 12000 km, allowing a 6000 km radius of operation around the base.

- A light aircraft, capable of several vertical takes-off and landings in one mission, with a payload limited to 100 kg. This version will be able to perform ground experiments and carry samples back to the base. It will also be dedicated to atmospheric sounding. The small aircraft is supposed to have a range of 8000 km, allowing it to reach the northern pole from the base, land, and return to the base.

Both aircraft will have an altitude range of -2 to 15 km to accommodate a wide range of scientific missions and a low cruise speed (90-130 m/s) in order to minimize the power requirement and allow longer cruise duration.

For both airplanes, the effort focused on minimizing the overall weight and optimizing the payload/range capability.

Table 6.3.1. Aircraft Requirements

	Small Aircraft	Large Aircraft
Speed (m/s)	90-130	90-130
Payload (kg)	100	300
Range (km)	8000	12000+
Operation altitudes(km)	-2 to 15	-2 to 15

6.4 Design Considerations

The following sections will describe both aircraft designs in extensive detail, from the basic airframe to each of the subsystems necessary for continued operation.

6.4.1 General Configuration

For both aircraft, a classical configuration was adopted since this configuration allows high lift-to-drag ratios and high stability. Moreover, the high tail volume can tolerate large shifts in the center of gravity resulting from payload deployment. Other features include:

- Inverted V-tail to reduce mass as well as drag
- High aspect ratio wings to minimize the induced drag (aspect ratio of 22, similar to the one used for the JPL Martian plane)

31

- Large propellers for efficient, high-altitude flight in the thin
  Martian atmosphere

The small aircraft will use a single engine, pusher propeller (see Figure
6.4.1.1). With this configuration, the nose of the aircraft is free of interference,
allowing operations such as atmospheric sounding. The large aircraft will be
equipped with two engines in a push-pull configuration, with a twin boom
tail (see Figure 6.4.1.2). This configuration allows conservation of the
aircraft's symmetry should one of the engines fail.
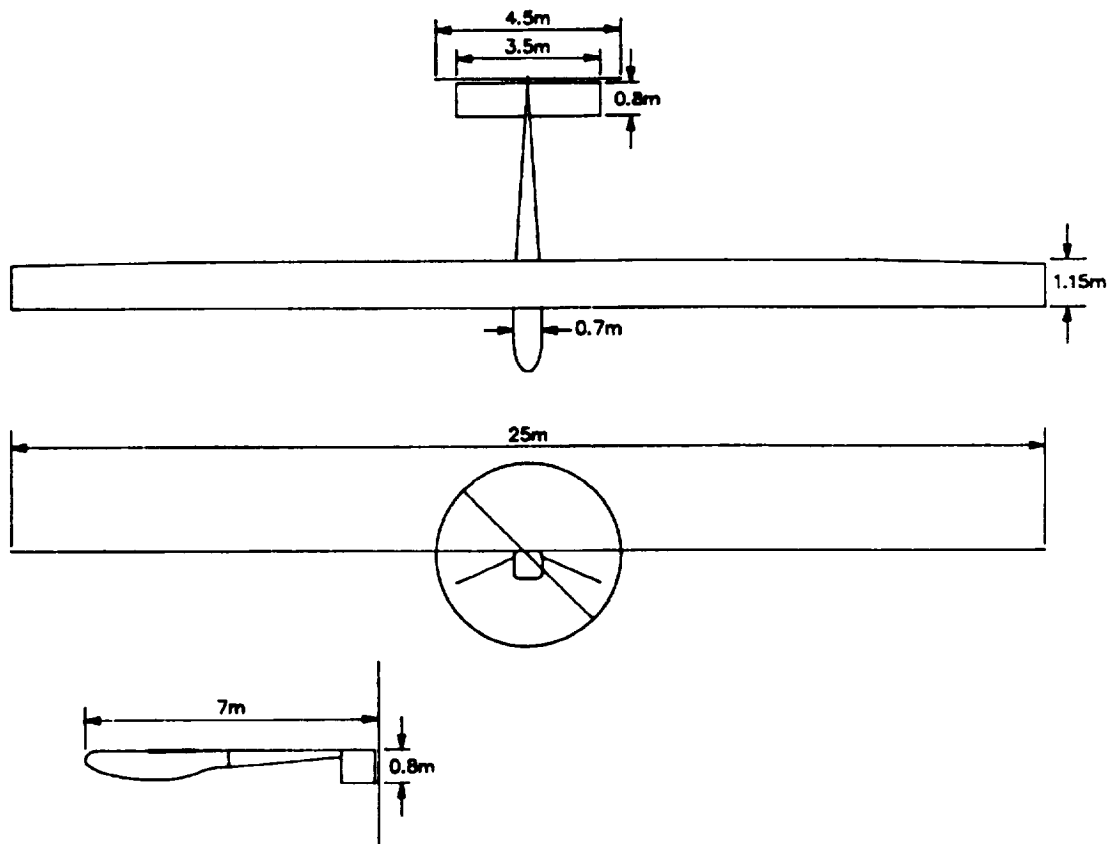
Figure 6.4.1.1. Small Mars Aircraft
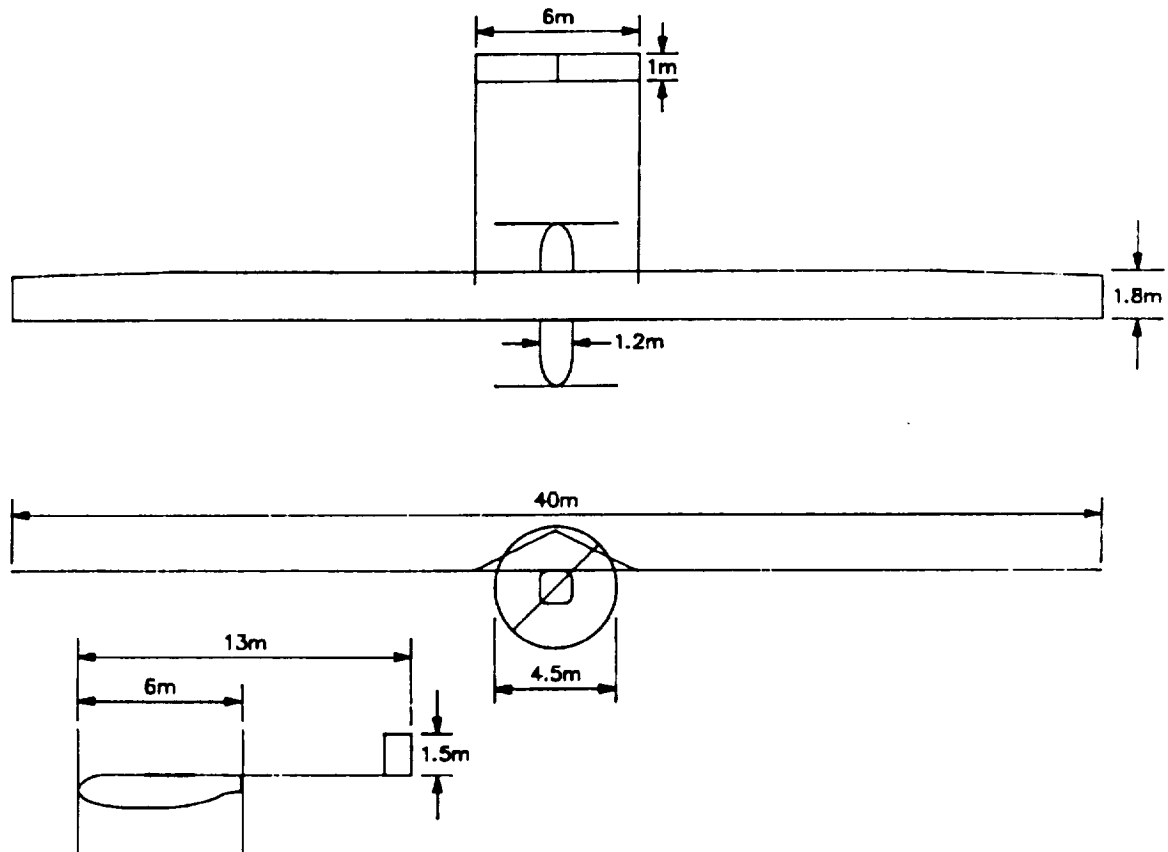
Figure 6.4.1.2. Large Mars Aircraft

6.4.2 Airfoil

The Eppler E61, designed at the University of Stuttgart by Richard Eppler, was chosen [6.1]. This thin airfoil (5.5%) designed for Reynolds numbers between 30000 and 160000, offers theoretical performances with high C_L and relatively low C_D (Figure 6.4.2.1 and Figure 6.4.2.2). Very limited wind-tunnel tests have revealed an L/D some 20% lower than the theoretical. But some other experimental results prove that tripping the boundary layer on the wing's upper surface improves both maximum lift coefficient and lift/drag ratio.
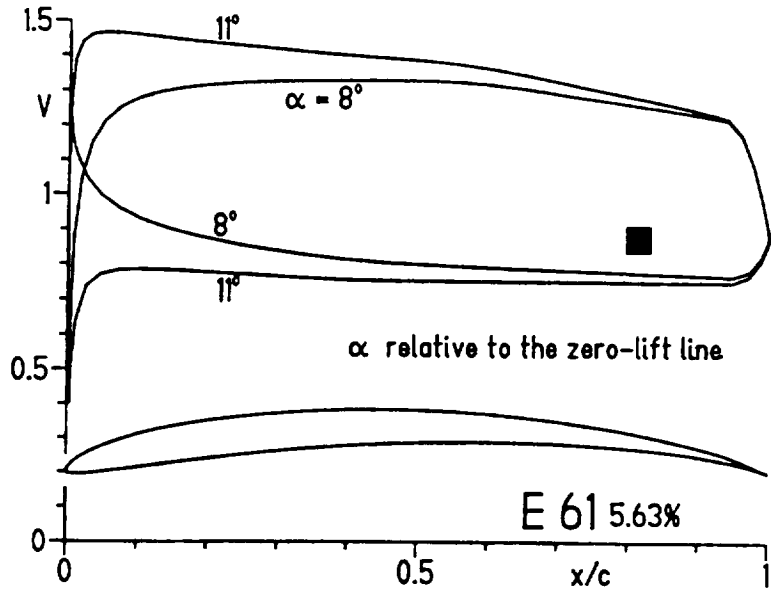
Figure 6.4.2.1. Eppler E61 Profile

Source: R. Eppler: "Airfoil Design and Data"
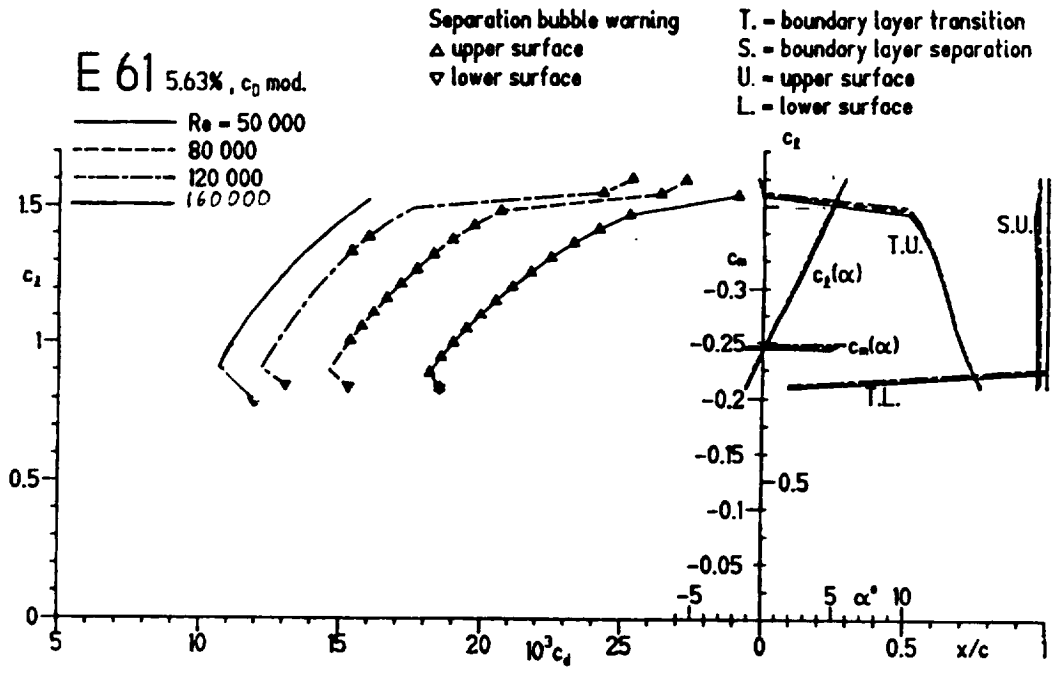
Figure 6.4.2.2. Characteristics of the Eppler E61 Profile

Source: R. Eppler: "Airfoil Design and Data"

34

6.4.3 Propulsion

Due to its high power/mass ratio, a closed loop, internal combustion engine (CH_4/O_2) was chosen. Modern day aircraft's reciprocating piston engines have a specific fuel consumption around 0.25 kg/kW-hr. We estimated a specific fuel consumption of 0.15kg/kW-hr would be achievable within the timeline defined for this project. But since our aircraft has to carry the oxidizer and, for a stochiometric reaction the fuel-air ratio is 1:4, our total cruise consumption will be approximately 0.8 kg/kW-hr. Both oxygen and methane are stored in spherical tanks inside the fuselage. As for the low Martian temperature and the expected duration of flight (around 50 hours maximum), we can assume that a passive thermal insulation will be sufficient to keep oxygen and methane cryogenic.

The propellers would be derived from the one designed by Peter Lissaman (aerodynamic designer of the Gossamer Condor) for the JPL Mars aircraft in 1978. This 4.5 m diameter, 0.5 m chord, two bladed, variable pitch propeller may attain a cruise efficiency of 88%, with a 0.8 tip Mach in cruise, and it operates between 340 and 950 RPM [6.2].

For the vertical take-off/landing procedures, the aircraft will use a combination of small thrusters similar to those of the Viking landers. These thrusters will use the same fuel from the same tanks as the aircraft's engines.

6.4.4 Structures and Materials

The primary goal in the Mars aircraft design was to achieve an ultra light weight vehicle with maximum percentage of the weight allocated to mission-performance related systems such as payload, avionics, and fuel. In order to cut the total weight, an all composite structure was chosen, using mostly high strength Thoronel 300 carbon-fiber and epoxy composites. This would allow for a structural weight fraction between 15 and 20 %.

Figure 6.4.4.1 shows a JPL wing structure for a Martian aircraft. Considering the large wing area needed, the wings comprise between 60 and 70 % of the Mars airplane's structural weight. For a 5.5 cm thick wing (Eppler E61) with an aspect ratio of 22, a wing structural weight of 1.5 kg/m2 can be assumed, based on a review of lightweight military RPVs.

Since the Mars atmosphere is relatively thin, it cannot offer much protection against UV radiation, which are very damaging to composites.

This may require the use of a special coating to protect the structure and systems of the aircraft.
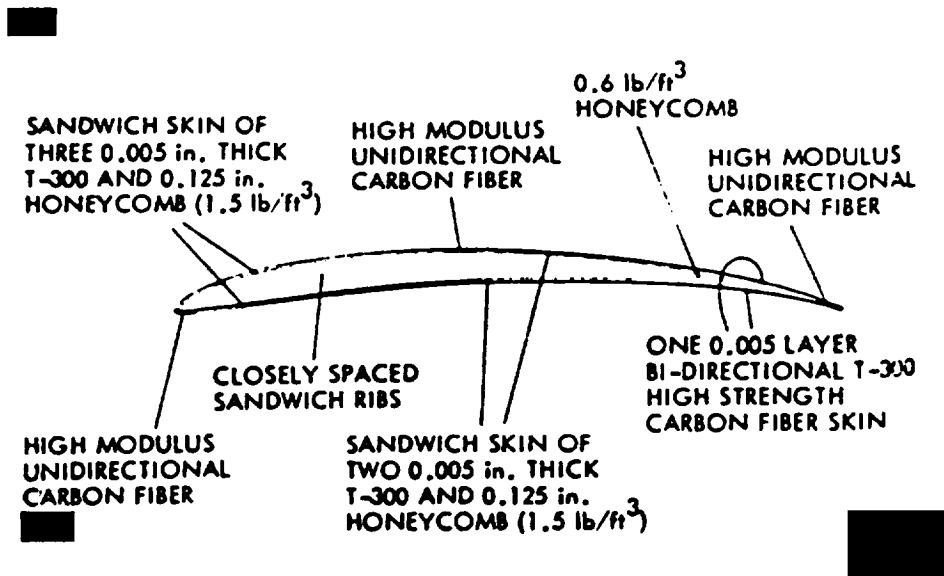
Figure 6.4.4.1. Wing Structure
Source: NASA CR 157942

6.4.5 Fuselage

Both aircraft have the same fuselage shape, the size and cross section of which are determined by the size of the cryogenic oxygen and methane fuel tanks (see Figure 6.4.5.1 and Figure 6.4.5.2). Those tanks are placed in such a way that the consumption of O2 and Ch4 during the flight will not affect the position of the center of gravity significantly. The main payload bay is also located in the vicinity of the CG in order to avoid large CG shifts during payload delivery.
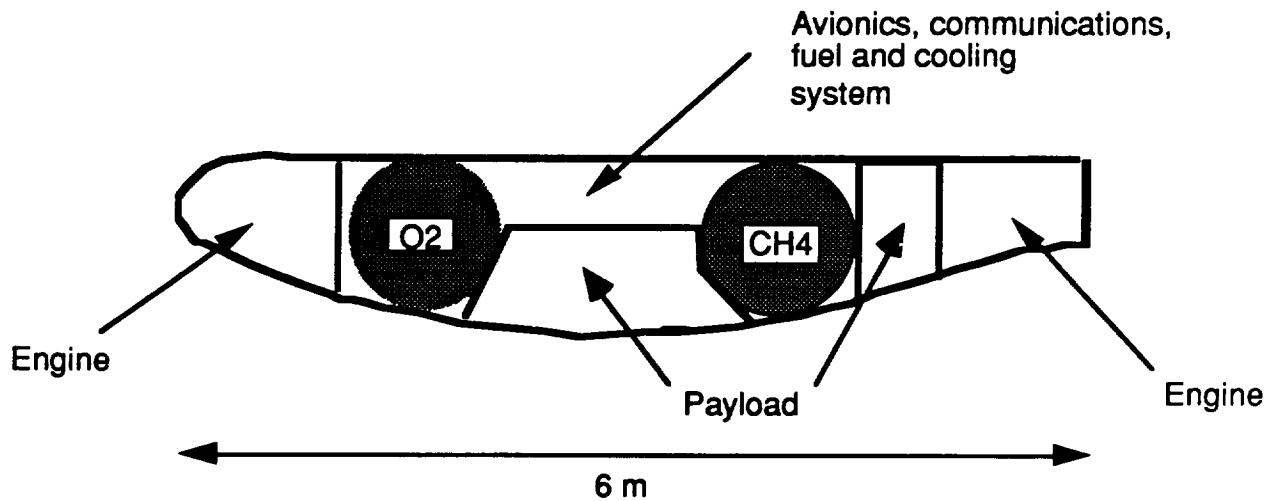
Figure 6.4.5.1. Large Aircraft Configuration.
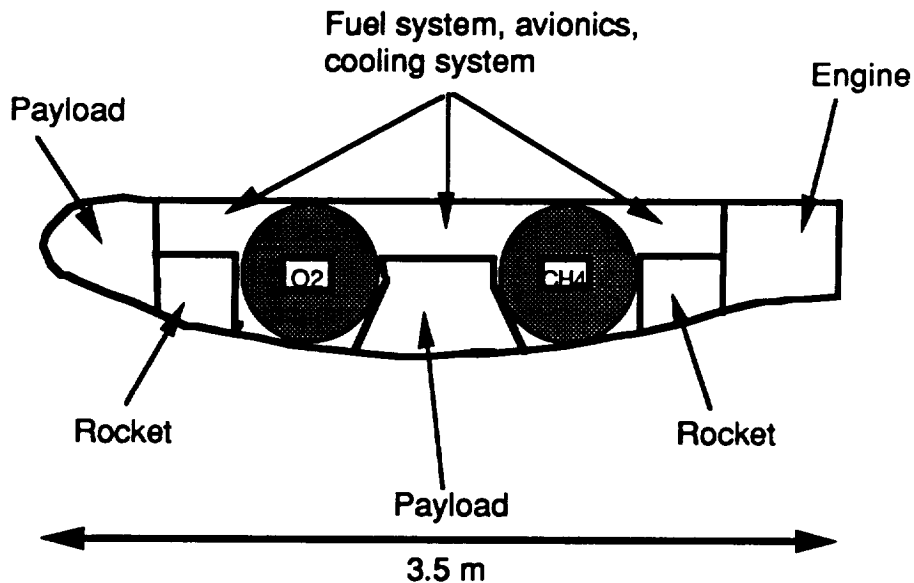
Figure 6.4.5.2. Small Aircraft Configuration

6.4.6 Take-off/Landing

To minimize the take-off distance and thus the runway length, both aircraft are supposed to use a short-take-off device, such as a catapult. The landing distance will also be shortened by using slow-down devices, such as nets. The landing gear for both aircraft will be a simple skid similar to those used on gliders.

To save fuel, the small aircraft will use its VTOL devices only on remote sites. These devices consist of two variable-thrust rockets mounted vertically in the fuselage and four constant thrust small rockets in the wing near the

37

inboard hinge point (two for roll control and two for yaw control). The landing gear includes 4 deployable, lightweight, tapered struts with tilting landing pads. Two struts are attached to the wing leading edge at the inboard hinge points, and two are attached to the tail's underfins. This configuration allows for good airplane stability against wind-blow-over and in the use as a drilling platform.

For landing, the aircraft will use the deep stall flying method. For the last four decades, this has been the standard way of retrieving free-flight models in updrafts. Deep stall flight has also been investigated by NASA as a way for light airplanes to descend to safety in the case of an emergency. During the rocket-controlled descent, the aerodynamics of the lander would have very little influence, and the landing would be identical to that of the Viking spacecraft.

For a take-off, the airplane would lift vertically using its rockets before diving for speed, and then it would perform a gentle pull-out (see Figure 6.4.6.1).
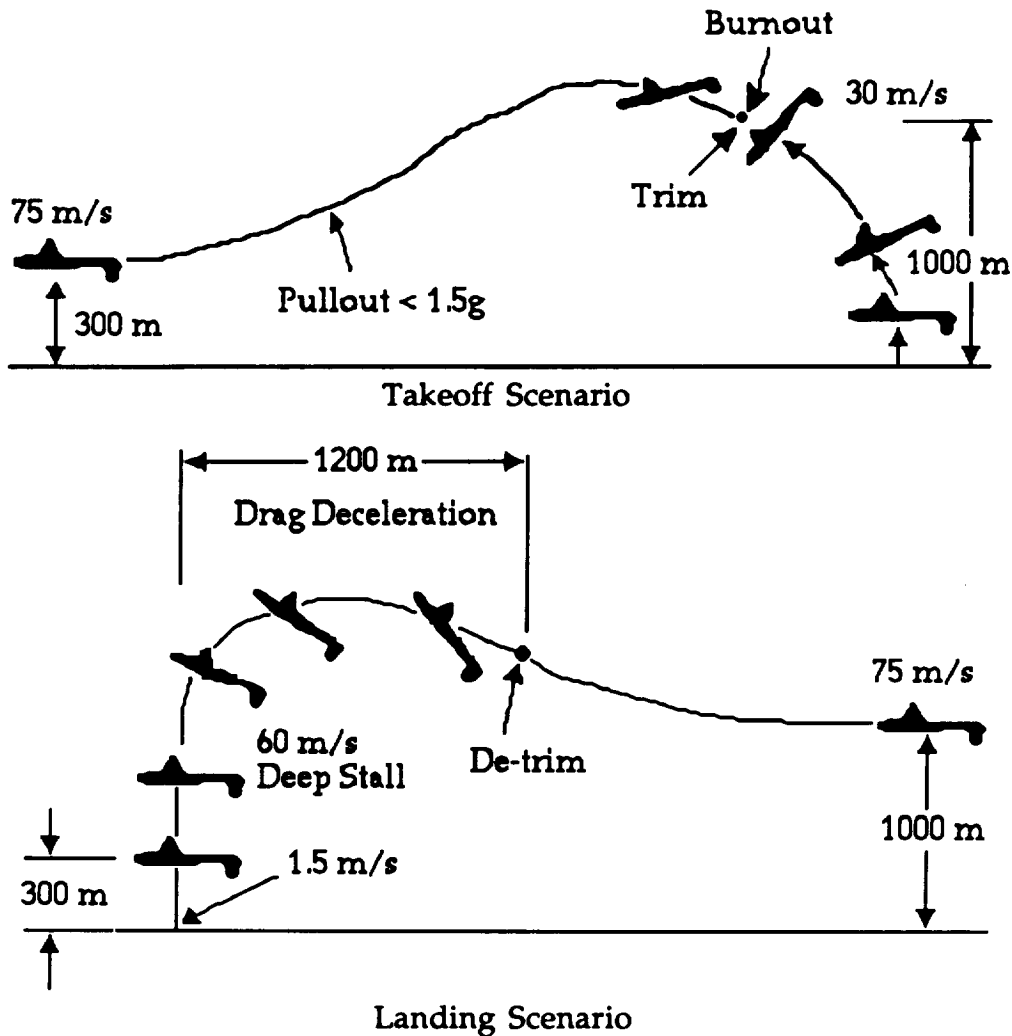
Figure 6.4.6.1. Example of vertical takeoff and landing scenarios using small variable thrust rockets (Viking lander type)

Source: NASA CR 157942

6.4.7 Engine Cooling

Because of the large amount of heat generated by the utilization of closed loop internal combustion engines, large radiators would be needed. To avoid any additional drag, the wingscould be used as a heat rejection surface The large amount of available wing area is well suited to this concept. As an example, a 20 m^2 area at 400 Kelvin would be needed to dissipate 35 kW, which closely corresponds to the heat generated by a 40kW O_2/CH_4 engine.

The radiator system needs to be specified in greater detail to obtain more accurate figures. In the current design, an approximation of the radiator mass has been incorporated in the weight breakdown.

6.4.8 Airplane Communications

Airplane communications with the base will be conducted through the line-of-sight (LOS) system when the airplane is in the LOS range and through a relay satellite while out of sight of the base. (The communications system is described in Section 8.2). The LOS system will be used to remotely pilot the vehicle during take-off and landing at the base. The range of the LOS system is dependent on the altitude at which the aircraft is flying.

The airplane will be equipped with a low power omnidirectional antenna. Although this will only allow low data rates to be transmitted, it will allow for continuous transmission of data through either system and eliminate the need for a complicated tracking system. A complicated tracking system including a steerable antenna would add a non-trivial amount of weight to the already weight-strapped airplane. Only long range missions near the north pole will be out of the field of view of the relay satellites. Nonetheless, continuous transmission of data throughout the majority of the mission will reduce the amount of data storage devices needed, thus reducing the weight and power requirements of the data collection subsystem. It is possible that a high inclination satellite will be included in the communications satellite network to handle this communication range.

6.4.9 Autonomy and Telerobotics

In consideration of its long range and the difficulty in establishing real-time communication with the base, the aircraft will have to be fully autonomous, including such procedures as VTOL. Like the rocket hopper, the aircraft (small) must have the capability to select a suitable site to land and to perform the landing autonomously. Nevertheless, a remotely piloted function should be available as an emergency back-up or for complex maneuvers.

6.4.10 Command and Data Handling

The computer will navigate mainly by a terrain-following procedure, using medium and high resolution images provided by previous or current remote-sensing satellites. The very high resolution images needed for high-

precision procedures (vertical landings, for example) would have to be provided by previous aircraft missions. The command and data handling system could also rely on ground-based beacons for navigation. In addition, the avionics also need aircraft attitude, attitude rates, position, and position rates for navigation.

6.4.11 Airplane GNC

The airplane's requirement to keep track of its position, changes in attitude and changes in position are much the same as those of the hopper. An IMU with three orthogonal gyroscopes and three orthogonal accelerometers will provide the changes in position and attitude of the vehicle, which will be time integrated to find the position. The accumulating error in position will reach 50 meters in approximately 47 minutes, then the position will be updated via satellite communication within a tolerance of 20 meters. Subsequent position updates will have to take place every 37 minutes (see Appendix E).

Similar to the hopper, a terrain avoidance radar will provide the airplane with enough information to clear any obstacles in the flight path in the horizontal and vertical directions. The altitude of the airplane will be measured by a radar altimeter (with a pressure sensor as a backup in case of failure), and then added to the planet's radius for use in the satellite updating process.

6.5 Mars Aircraft Characteristics

Table 6.5.1 and 6.5.2 display the main characteristics of the small and large aircraft which were calculated using the method described in Appendix F. The appendix also includes the charts displaying the aircraft parameters versus the altitude.

The aircraft are fairly large with 25m and 40 m wingspan, respectively. The small aircraft fuel budget of 150 kg includes 25 kg for one landing/take-off procedure. With this budget ,the goal of 8000 km is reached, providing an endurance time of 25 hours. The large airplane has a total range of more than 15000 km, with an endurance of 45 hours. For fuel, the small aircraft carries 30 kg of CH_4 (52cm diameter tank) and 120 kg of O_2 (58 cm diameter tank), while the large one carries 110 kg of CH_4 (80 cm diameter tank) and 440 kg of O_2 (90 cm diameter tank). This sizing was made assuming a density of 1140

41

kg/m^3 for liquid oxygen and a density of 417 kg/m^3 for liquid methane. The aircraft speed grows relatively fast with the altitude and it appears that, in order to avoid the transonic region, the ceiling of 15km cannot be reached at full gross take-off weight. In addition, the rate of climb is relatively low, especially at the maximum weight, so the aircraft may encounter a problem of keeping altitude in a strong down draft when flying along the wall of a canyon with a strong side wind.

Table 6.5.1. Mars Aircraft Main Characteristics

	Small Aircraft	Large Aircraft
Wingspan	25 m	40 m
Planform area	28 m^2	73 m^2
Mass	450 kg	1200 kg
Payload	100 kg	300 kg
Aspect ratio	22	22
L/D (H=1 km)	28.8	30.3
V$_{cruise}$ (H=1 km)	92 m/s	94 m/s
Range	7980 + 1 VTOL	15400 km
Propulsion	1 X 15 kW (pusher)	2 X 20 kW (push-pull)
Wing loading	60.4 N/m2	62 N/m2
Vertical speed	910 ft/s	1000 ft/s

Table 6.5.2. Mars Aircraft Mass Breakdown

(All masses in kg)	Small Aircraft	Large Aircraft
Airframe	70	180
Power plant	35	80
Cooling system	40	70
Avionics/Comm.	20	30
VTOL system	35	0
Payload	100	300
Fuel	150	540
Total	450	1200

7.0 Rovers

The seven rover configurations which are being considered for the SIMPSONS Project are: 1) fuel transport vehicle (FTV), 2) human-operated Mars exploration rover (HOMER), 3) materials transport vehicle (MTV), 4) heavy cargo vehicle (HCV), 5) manned, short-range vehicle (MSRV), 6) Mars autonomous rover for ground exploration (MARGE), and 7) light cargo vehicle (LCV). The following sections describe the mission of the rovers and the design of each major subsystem.

7.1 Rover Mission Profiles

FTS has chosen seven primary rover configurations to support the operation of an advanced Mars base. The following sections describe the mission of each of these vehicles.

7.1.1 Fuel Transport Vehicle (FTV)

The fuel transfer vehicle is designed to refuel lifters and rovers, as well as the Mars aircraft. A range of 10 km will allow the FTV to refuel any vehicle within the vicinity of the base. The FTV can carry 6000 kg of LOX and 1000 kg of liquid CH_4. This is enough fuel to fill the tanks of 3 heavy rovers in the HOMER configuration, which has the largest fuel capacity of any rover. Although fuel for the rocket hopper will be transported using pipelines, the FTV could serve as a backup in case of an emergency. The FTV will be operated telerobotically.

7.1.2 Human-Operated Mars Exploration Rover (HOMER)

The FTS vehicle network includes the HOMER which will be used for long range manned missions. HOMER will carry a crew of two astronauts along with equipment to explore the Martian surface as well as setup and resupply outposts. Life support will be provided for a 10 day mission (maximum) using a partially closed Environmental Control and Life Support System (ECLSS). HOMER has a top speed of 10 km/hr and range of 200km. At this speed, HOMER can reach its maximum distance from the base in less than 1 day.

7.1.3 Materials Transport Vehicle (MTV)

The primary function of the MTV is to transport regolith from the mining facility to the manufacturing facility should the tram become inoperable. A

43

range of 30 km will allow the MTV to make a round trip to the mine, which is located approximately 15 km from the base. The MTV can carry up to 7 MT of regolith for future refinement into oxygen and methane. A backup to the tram is essential because the base is dependent on the oxygen for life support. The MTV will be operated telerobotically.

7.1.4 Heavy Cargo Vehicle (HCV)

The heavy cargo vehicle will transport payloads of up to 10 MT within 20 km of the base. One mission of the HCV is to aid in base expansion by moving habitation modules from the descent vehicle to the base. The HCV will be operated telerobotically.

7.1.5 Manned, Short Range Vehicle (MSRV)

Basic transportation of astronauts around the base can be accomplished using the MSRV. The MSRV can also be carried by the rocket hopper up to 1000 km from the base. Astronauts can then use the MSRV for short range exploration around the hopper. The range of the MSRV will be 30 km which will give it adequate range for crew members to drive from the base to the mining facilities, power plant, launch pads, and manufacturing facilities. The MSRV will have a carrying capacity of 2 astronauts, plus 2000 kg of additional payload. However, it is not equipped with its own life support system, so astronauts must wear space suits while riding on the MSRV.

7.1.6 Mars Autonomous Rover for Ground Exploration (MARGE)

Long range unmanned exploration on Mars will be conducted by MARGE. This rover will be able to traverse obstacles up to 1 m in height to provide mobility over the rough terrain that will be encountered away from the Mars base. This capability will allow MARGE to operate autonomously at distances of up to 200 km from the base. MARGE can also be carried by the hopper, increasing its range by 1000 km. MARGE can carry 2500 kg of scientific equipment or experiments at a maximum speed of 10 km/hr.

7.1.7 Light Cargo Vehicle (LCV)

The light cargo vehicle is an autonomous/telerobotic rover whose main purpose is the transportation of light cargo around the base area. With a range of 200 km, the LCV will be able to set up outposts or deliver supplies to

44

outposts. The LCV will have a carrying capacity of 2500 kg and a maximum speed of 10 km/s.

7.2 The Lego Concept

The Lego concept has been incorporated into the structural designs of all rovers. The designs are created by adding "blocks" (subsystems) together to make the desired vehicle. A block is considered legoble if it may be easily connected to and disconnected from the chassis. The advantages of this concept are that the vehicles are completely modular, that the blocks can be used as spare parts on almost any vehicle, and that new configurations can be made in-situ to meet unforeseen needs of the base. The astronauts will be able to construct (with robotic aid) any new vehicle configurations within the maintenance facility.

7.3 Mobility System Design

FTS investigated three mobility systems for use on the rovers: 1) hemispherical wheels, 2) elastic loopwheels, and 3) tracks. The criteria for choosing a design included efficiency, simplicity, mobility (overcoming obstacles), as well as total mass. The following requirements were placed on the mobility of the heavy and light rovers.

> Heavy Rover:
> > Overcome 0.5m obstacle
> > Traverse 0.3m crevasse
> Light Rover
> > Overcome 1.0m obstacle
> > Traverse 0.5m crevasse

Because the mobility of a rover is dependent on chassis, as well as wheel, design, the mobility requirement was considered as a part of the chassis design. The track system was eliminated from the study early because it is both massive and complex. The elastic loopwheels were eliminated for two reasons. First, though loopwheels are more efficient than conventional wheels under normal conditions, the power required to drive a loopwheel system increases by orders of magnitude if debris is introduced into the loop. Second, the material which was being considered for the elastic loop degraded heavily under ultraviolet radiation [7.1]. Hemispherical wheels have the

advantages of being simple and of having low stress concentrations at the shaft joint [7.2]. Thus, the hemispherical wheel was chosen for the mobility system of both the heavy and light rovers.

7.4 Heavy Rover Chassis Design

The heavy rover chassis design was based on the heavy rover's payload and its mobility requirement. A drawing of the chassis frame is shown in Figure 7.4.1.
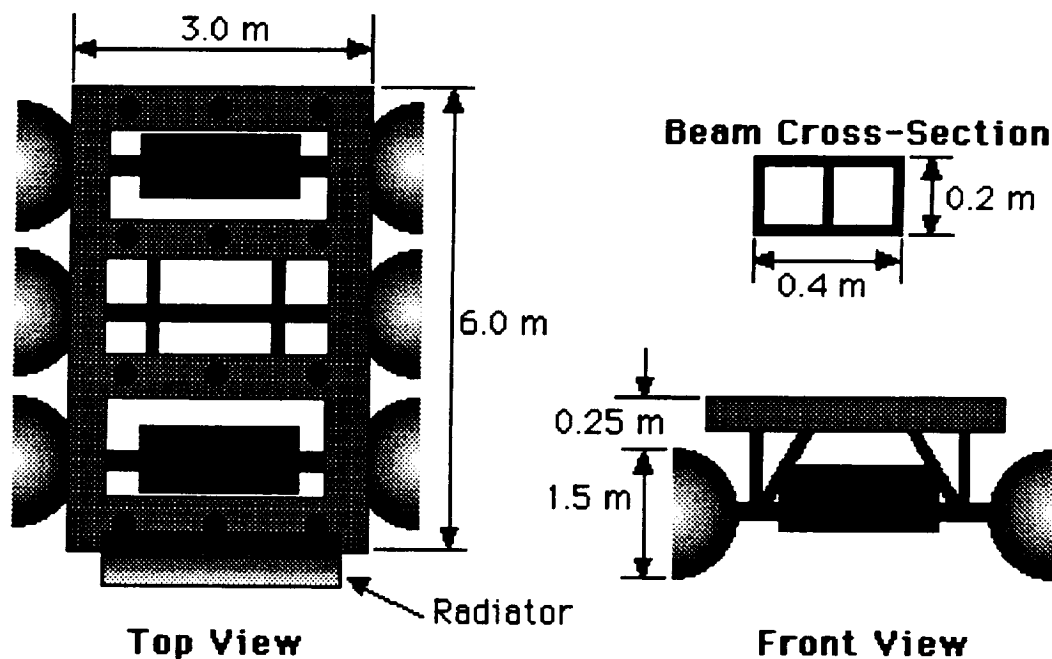
Figure 7.4.1. Heavy Chassis Design

Several materials were considered for the chassis frame, and the choice of material was based on density, strength, and cost. A decision matrix elaborating on the selection process appears in Figure 7.4.2. The decision matrix is based on a high score of 10, with each criterion weighted according to its relative importance to the rover chassis design.

Criteria	Aluminum 2014-T6	Stainless Steel	Structural Steel ASTM-A514	Titanium Alloy
Density (x 10)	9 / 90	1 / 10	1 / 10	5 / 50
Strength (x 6)	4 / 24	9 / 54	7 / 42	8 / 48
Cost (x 5)	9 / 45	7 / 35	8 / 40	2 / 10
Total	159	99	92	108

Figure 7.4.2. Chassis Material Decision Matrix

As seen in the decision matrix, the best material for the chassis is aluminum 2014-T6. It has a high yield strength, the lowest density among those considered, and it is a low-cost, easily-worked material. For support, the beams were chosen to be two-celled monocoques with a thickness of 5.0 mm. The dimensions of the chassis were determined by the size of the modules it would be carrying. The thickness of the cross-section was determined using a NASTRAN model of the chassis. This model and its associated NASTRAN output are detailed in Appendix G. A summary of the output may also be found in Table 7.4.1. Using the largest projected load, the maximum stresses in the chassis were compared to the yield strength of the aluminum 2014-T6, and a safety factor of 7.85 is provided by the chosen thickness and material. Figure 7.4.3 shows the maximum stress as a function of the beam thickness, and it includes the yield strengths of the aluminum and titanium alloys as a reference.

47

Table 7.4.1. Summary of Results for Heavy Chassis Using Aluminum and Titanium

Thickness (m)	Max Displacement for Al (m)	Max Displacement for Ti (m)	Max Bending Moment (N-m)	Max Stress (Pa)
0.005	-1.69E-02	-1.03E-02	2.43E+04	-5.22E+07
0.0075	-1.16E-02	-7.06E-03	2.43E+04	-3.60E+07
0.01	-8.98E-03	-5.46E-03	2.43E+04	-2.80E+07
0.0125	-7.41E-03	-4.50E-03	2.43E+04	-2.32E+07
0.015	-6.36E-03	-3.87E-03	2.43E+04	-2.00E+07
0.0175	-5.62E-03	-3.42E-03	2.43E+04	-1.78E+07
0.02	-5.07E-03	-3.08E-03	2.43E+04	-1.61E+07
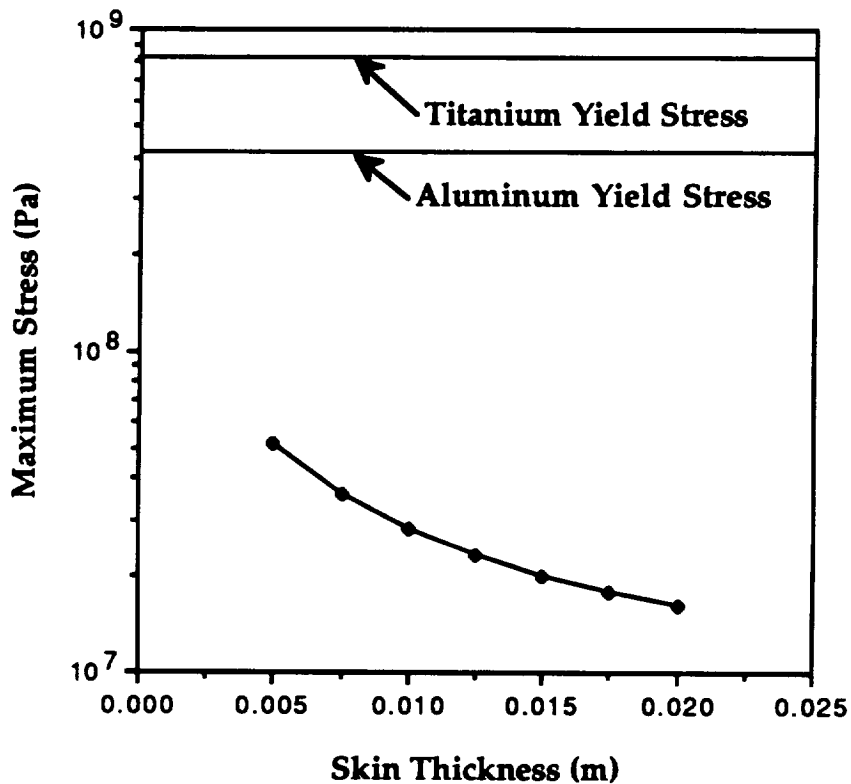
Figure 7.4.3. Maximum Stress in Heavy Chassis as a Function of Skin Thickness

Two of the three axles on the heavy chassis are powered (four-wheel drive). The chassis maneuvers using Ackerman steering (the same steering mechanism found in automobiles), in which wheels on powered axes are steerable. The black dots seen in Figure 7.4.1 are the structural interfaces used

to connect modules to the chassis. These interfaces will be discussed in greater detail in Section 7.7. The heavy rover has a ground clearance of 0.75m. The two thin, vertical beams in the top view of the chassis are supports for the fuel tanks. The fuel tanks will hang underneath the chassis, lowering the vehicle's center of gravity, and a mylar cover will protect them from dust and rocks kicked up by the wheels. For further detail on the tank designs, see Section 7.8.3.

7.5 Light Rover Chassis Design

The light rover chassis design was based primarily on the mobility requirement. Because the light rover is capable of operating autonomously, it will have to be more maneuverable than the heavy chassis. To meet its mobility requirements, the light chassis was separated into two sections. Like the heavy chassis, the light rover has two powered axles and Ackerman, four-wheel steering. A drawing of the chassis frame is shown in Figure 7.5.1.
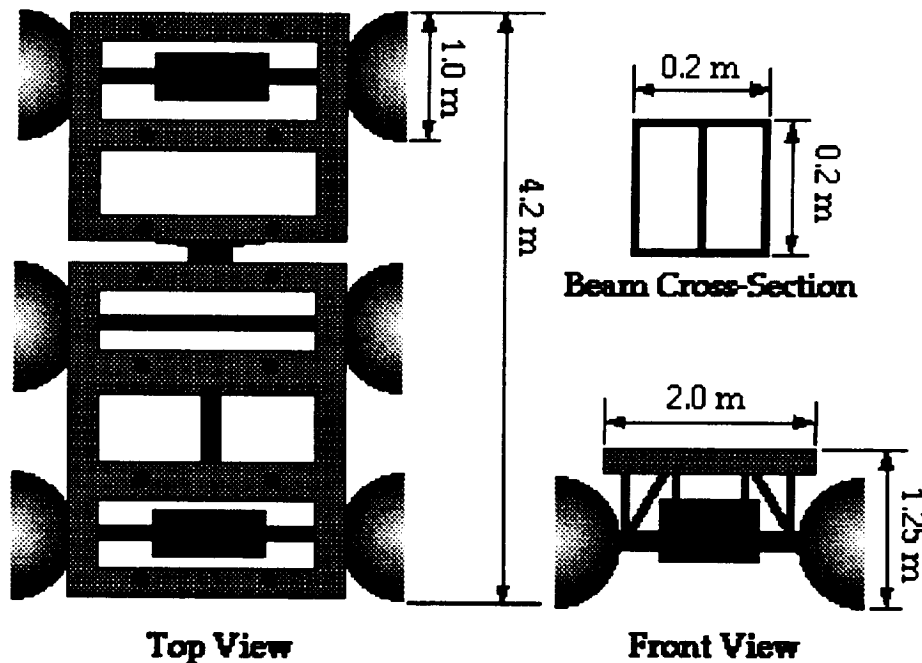
Figure 7.5.1. Light Chassis Design

Since the criteria for material selection was the same for the light chassis as for the heavy chassis, aluminum 2014-T6 was again chosen. As before, the overall dimensions were determined by the size of the modules being carried. The cross-section of the beams in the chassis is a two-celled monocoque with a thickness of 5.0 mm., where the thickness was determined using

NASTRAN in the same manner as for the heavy chassis (see Appendix E).
For a summary of the output, see Table 7.5.1. Using the largest projected load,
the maximum stresses in the chassis were compared to the yield strength of
the aluminum 2014-T6, and a safety factor of 8.5 is provided by the chosen
thickness and material. Figure 7.5.2 shows the maximum stress as a function
of the beam thickness, and it includes the yield strengths of the aluminum
and titanium alloys as a reference.

Table 7.5.1. Summary of Results for Light Chassis Using Aluminum and Titanium

Thickness (m)	Max Displacement for Al (m)	Max Displacement for Ti (m)	Max Bending Moment (N-m)	Max Stress (Pa)
0.005	-1.45E-03	-8.72E-04	-1.29E+04	4.69E+07
0.01	-7.91E-04	-4.74E-04	-1.29E+04	2.55E+07
0.015	-5.74E-04	-3.44E-04	-1.29E+04	1.85E+07
0.02	-4.69E-04	-2.81E-04	-1.29E+04	1.51E+07
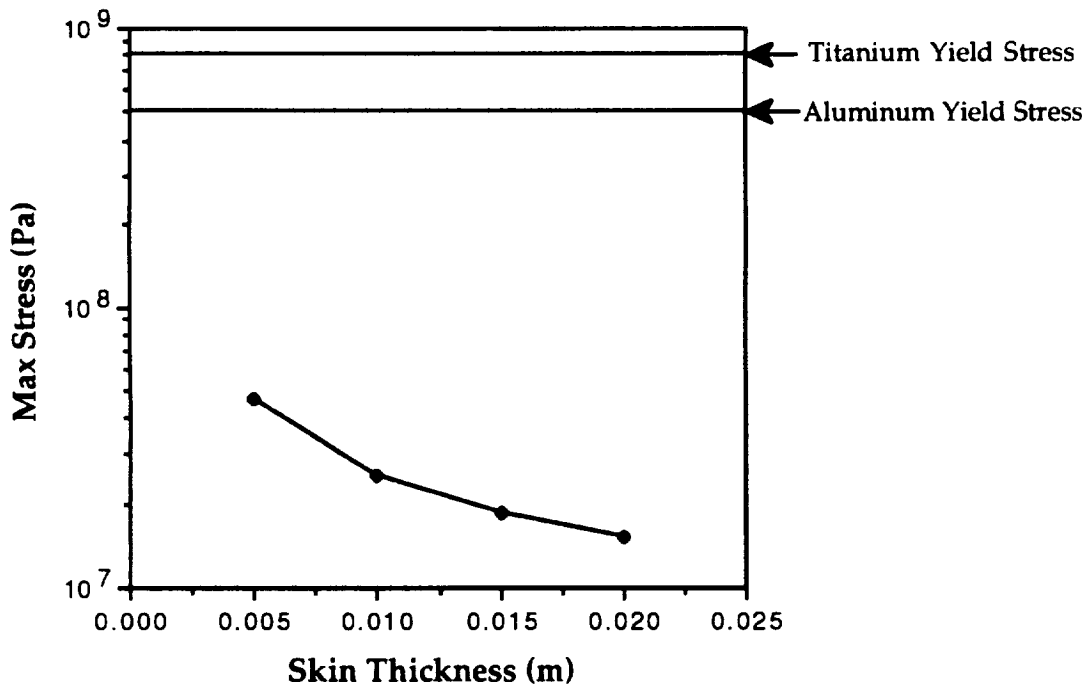
Figure 7.5.2 Maximum Stress in Light Chassis as a Function of Skin Thickness

50

The black dots seen in Figure 7.5.1 are the same structural interfaces as used on the heavy chassis. The light chassis has a ground clearance of 1.0 m. The connection between the two halves of the light chassis is a powered coupling with three degrees of freedom (roll, pitch, and yaw), which will enhance the light rover's maneuverability.

7.6 Lego Module Design

A major feature of the legoble rover design is the ability to place different types of modules on the same chassis to accommodate different missions. The following are a set of legoble modules designed by FTS to fit the mission profiles discussed previously.

7.6.1 HOMER Module

The HOMER Module is a pressurized, "shirt-sleeve" laboratory. The hull of the module is made of 1.0 cm thick aluminum and is covered by a layer of polyurethane insulation. The basic dimensions of the module are given in Figure 7.6.1. Inside the laboratory will be the life support systems, scientific equipment, and crew accommodations. All functions of the rover may be controlled from inside the HOMER module. The module is equipped with lights and stereoscopic cameras in the front and rear as well as structural interfaces on top of the module for connecting GNC, communications, or command and data handling modules.
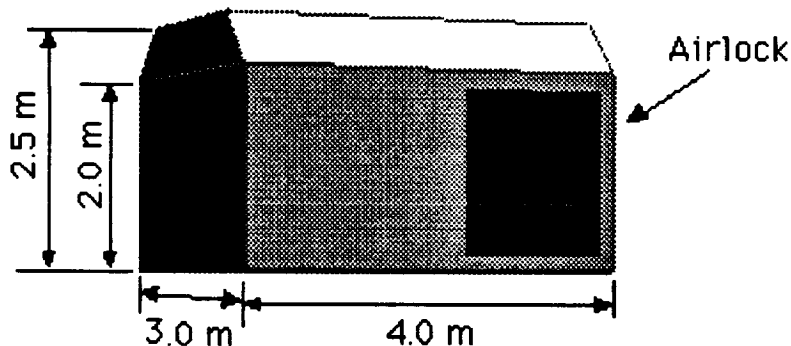
Figure 7.6.1. HOMER Module

7.6.2 Communications Module

The communications module for all rovers will be a steerable antenna as pictured in Figure 7.6.2, and it will be pointed using stepper motors. The 1.0

m diameter antenna is made of a graphite and aluminum and will be placed on a base containing transmitters and receivers (two of each for redundancy).
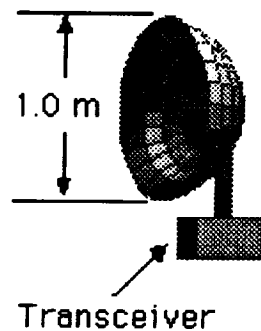
Figure 7.6.2. Communication Module

7.6.3 Fuel Transport Module

As shown in Figure 7.6.3, the fuel transport module consists of two stainless steel insulated tanks. The long, cylindrical tank is capable of holding 6000 kg of LOX, while the spherical tank carries 1000 kg of CH_4. These tanks have passive thermal control in the form of polyurethane insulation approximately 10 cm thick, and this module uses a pumps to transfer fuel from the FTV to the tank being refueled. The base of the fuel transport module is made of aluminum 2014-T6, which is 2.0 cm thick.
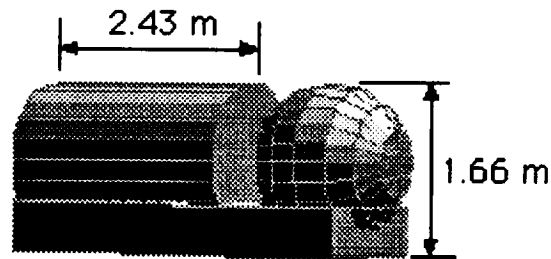
Figure 7.6.3. Fuel Transport Module

7.6.4 Regolith Transport Module

Capable of carrying 8000 kg of regolith, this module consists of a 1.0 cm thick aluminum bin which can be elevated by a hydraulic lever, as shown in Figure 7.6.4. The endplate at the low end of the bin raises to allow the regolith to spill out.
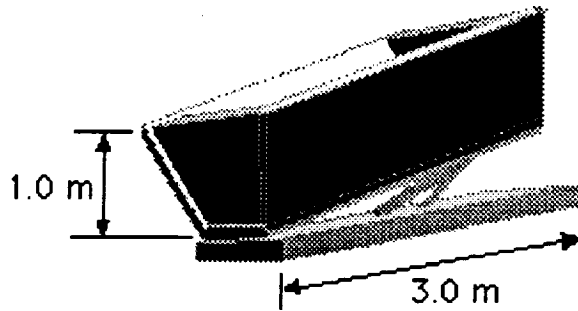
Figure 7.6.4. Regolith Transport Module

7.6.5 Cargo Modules

The design of both the heavy and light cargo modules are similar to that shown in Figure 7.6.5. Both are made of aluminum and have a door which slides open. The heavy cargo module has a carrying capacity of 8000 kg in a volume of approximately 18 m^3, and the light cargo module has a carries 2500 kg within approximately 4.5 m^3. In addition to the heavy and light cargo modules, there is a smaller cargo module (holding 1000 kg in a volume of approximately 1.2 m^3) for use on the MSRV.
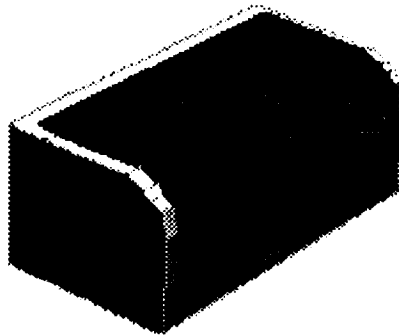
Figure 7.6.5. Cargo Module

7.6.6 Manned, Short-Range Module

The manned, short-range module, shown in Figure 7.6.6, contains seating for two astronauts in EVA suits and has room to carry a limited cargo. This module contains manual controls for driving the rover, as well as instrumentation to provide the astronauts with information on the rover's status and navigation.

53
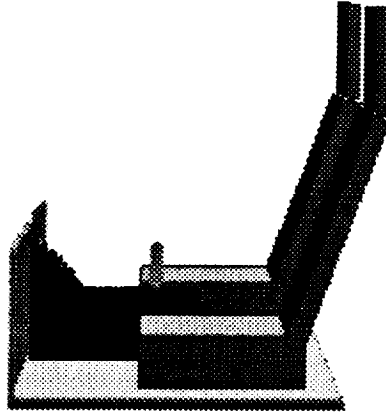
Figure 7.6.6. Manned, Short-Range Module

7.6.7 GNC Modules

The sensors which make up the GNC "module" do not reside in a single block. Rather, the sensors are broken into several modules, each connected by interfaces on the chassis or other modules. For example, the ground-penetrating radar sits directly on the chassis of all rovers. On the other hand, the IMU (inertial measurement unit) will be put in different places depending on the configuration. For further information on the sensing equipment, see Section 8.4.

7.6.8 Command and Data Handling Module

This module is the brain of the rover, a cube approximately 30.0 cm on each side. This cube will contain the CPU and associated data storage. Other subsystems, such as the HOMER module, may contain other computers or data storage devices, but this module contains the main computer.

7.6.9 Sample Configuration of Modules

As an illustration of the configurations possible using the legoble modules, Figure 7.6.7 shows the HOMER with the following modules attached to its chassis.

Command and Data Handling
Communications Module
GNC Modules
HOMER Module

54
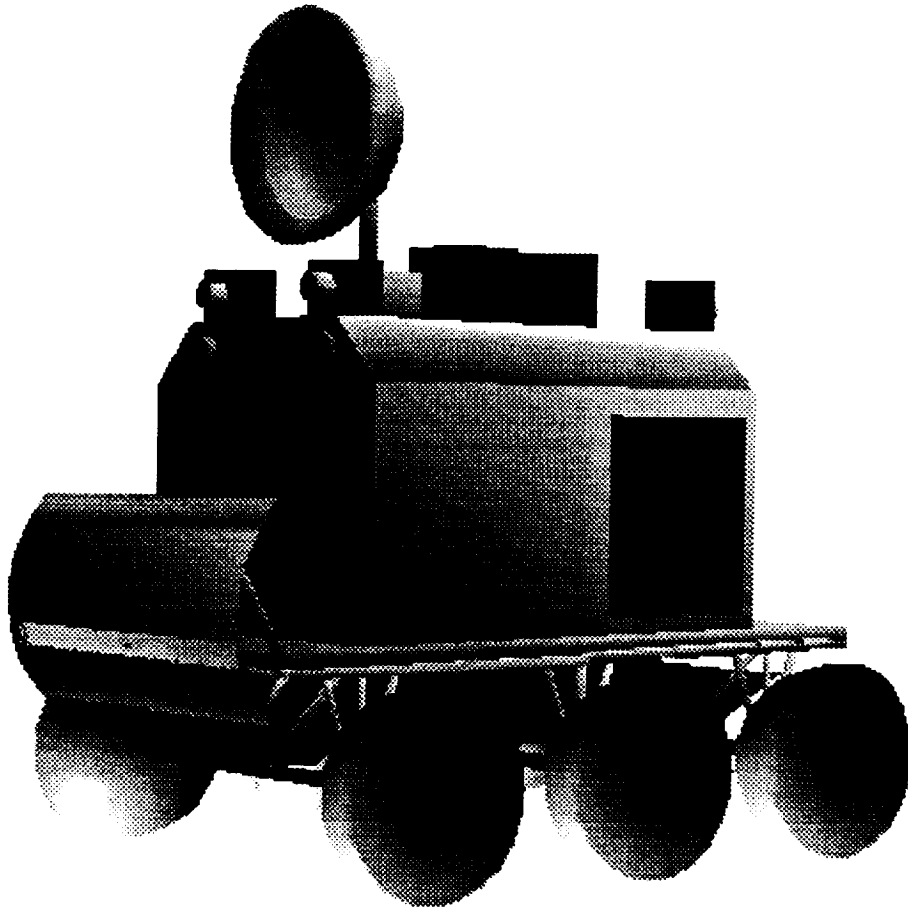
Figure 7.6.7 HOMER Configuration

A complete set of rover configurations is given in Appendix H along with mass and power breakdowns for each vehicle.

7.7 Structural Interface

The primary feature of FTS rover designs was the lego concept. To incorporate this concept, an interface was designed for securing various legoble blocks to a rover chassis. Besides physically holding the block to the chassis, the interface provides for power and data transmission between a legoble block and the rover chassis.

7.7.1 Interface Design

FTS designed the structural interface in Figure 7.7.1 for use with the rovers. In this design, the interface consists of a peg-like structure protruding from the rover chassis. The interface is made of aluminum 2014-T6. The interface was sized using a TK Solver model which examined the shear and

bending stresses. This analysis did not include dynamic loads which may induce transient stresses larger than those computed for the static model. The TK model and the resulting data are detailed in Appendix I.
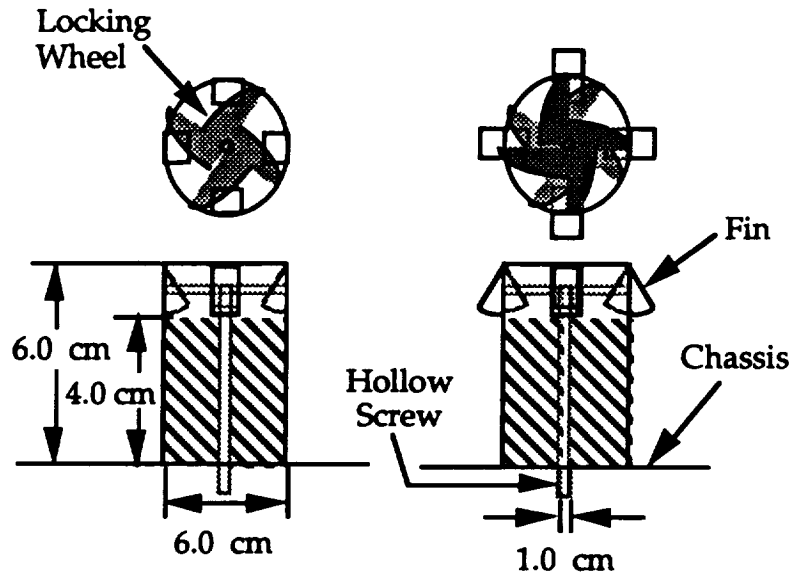
Figure 7.7.1. FTS Interface Design

Each interface has four triangular fins that are evenly spaced around the cylinder. The fins are able to pivot about a hinge which connects the top of each fin to the cylinder, enabling them to swing in or out of the cylinder. A ball-and-socket joint attaches the back of each fin to a locking wheel, which is located inside the cylindrical interface (see Figure 7.7.2).

Locked Postion   Unlocked Position
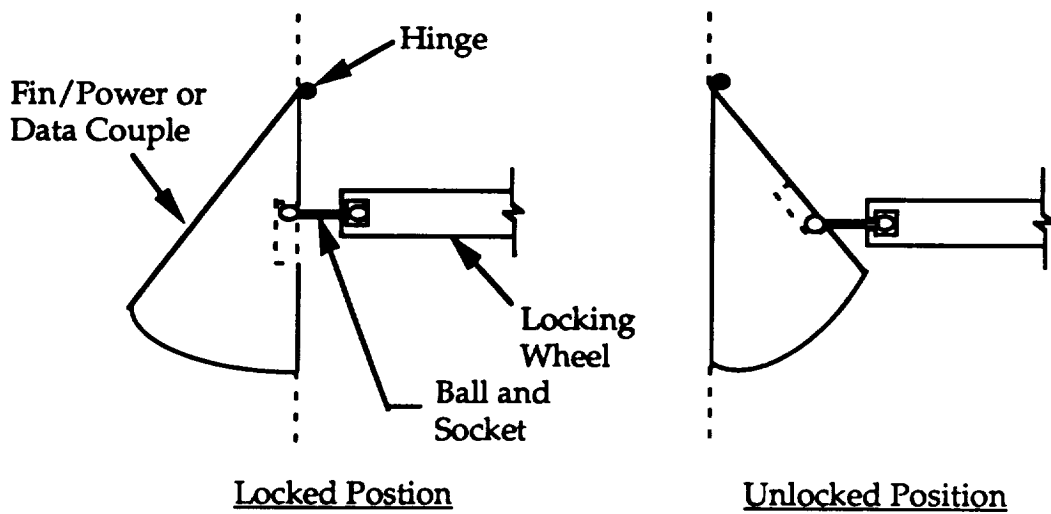
Figure 7.7.2. Structural Interface Fin Operation

One end of the ball joint is able to slide horizontally in a track which runs along the edge of the locking wheel. Therefore, as the locking wheel rotates, the ball-and-socket joint is pushed in or out due to the changing radius of the locking wheel. Meanwhile, the other end of the ball-and-socket attached to the fin can slide a small amount vertically to allow for differences in the height of the joint as the fin swings in and out. A hollow screw runs through the center of the interface and connects to the locking wheel (see Figure 7.7.1). An electric motor in the chassis can be connected to this screw to rotate the locking wheel. The following steps are required to attach a legoble block to a rover chassis.

1) Turn the locking wheel so that the four fins are in the unlocked position as in Figure 7.7.2.
2) Lower a legoble block onto the cylindrical structural interface (with robot assistance).
3) Extend the fins to the locked position by turning the locking wheel.

This will secure the block to the rover chassis as well as connect the data and power couples.

7.7.2 Power and Data Couples

The structural interface is capable of transmitting power and data between a rover chassis and a legoble block (see Figure 7.7.3).
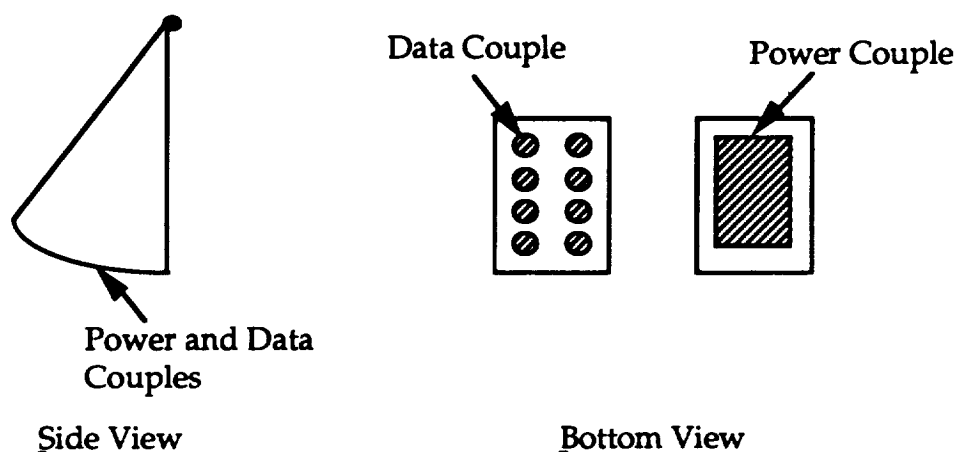
Figure 7.7.3. Power/Data Couple Design

A power connector consists of one flat metal plate located on the bottom of an interface fin, and another plate connected to the legoble block. When the fins are extended in the locked position, the two plates will come in contact with one another. Data couples work in the same manner, and the data couples will consist of a series of small, circular metal plates.

7.8 Rover Propulsion And Power

Locomotion, as well as electrical power for all rovers, will be provided by a partially closed internal combustion engine using a methane (CH_4)/oxygen bipropellant. The engine will be a reciprocating piston, spark-ignition engine capable of providing 108 kW of output power for the heavy rover, and 52 kW of power for the light rover. Due to the composition of the Martian atmosphere (95% carbon dioxide and only 1/150 the pressure of that at the earth's surface) the engine will be partially closed. This means that the rover must carry an oxidizing agent (oxygen) in addition to its fuel (methane), thus limiting the range of both the heavy and light rovers to a 200 km round-trip. It was determined that for long missions the amount of oxidizer would be nearly equivalent to half of the total weight of the rover, thus limiting the payload capability of either rover. For example, a 1000 km round-trip mission in the heavy rover (20 MT total mass) would require a total of 7500 kg of bipropellant [7.3].

A rotary engine was also investigated as a power source, and although it had a higher power to mass and higher power to volume ratio, it was approximately 10% less efficient. Therefore, it would not only require more fuel, but more importantly, it would require more oxidizer, making the weight penalty from the added fuel and oxidizer greater than the weight savings from the engine [7.4]. Other potential power sources and the selection process for the internal combustion engine are discussed in Section 8.1.

7.8.1 Engine Specifications

The engine will use a liquid methane, and liquid oxygen fuel mixture at an equivalence ratio of 0.6. Equivalence ratio is the ratio of the actual mass fuel-air ratio to the stoichiometric fuel-air ratio. An equivalence ratio of 0.6 is a conservative estimate of the minimum fuel-air ratio for methane in air that permits combustion [7.4]. Since the engine burns methane in oxygen and carbon dioxide, the equivalence ratio is assumed to be the same as that for

methane in air. Some of the other assumptions made for the analysis of the engine are

- Fuel was an ideal gas
- Isentropic compression and expansion
- Instantaneous and adiabatic combustion with a stationary piston
- No residuals in cylinders

The thermodynamic cycle used to model the engine was the ideal Otto cycle shown below in Figure 7.8.1.
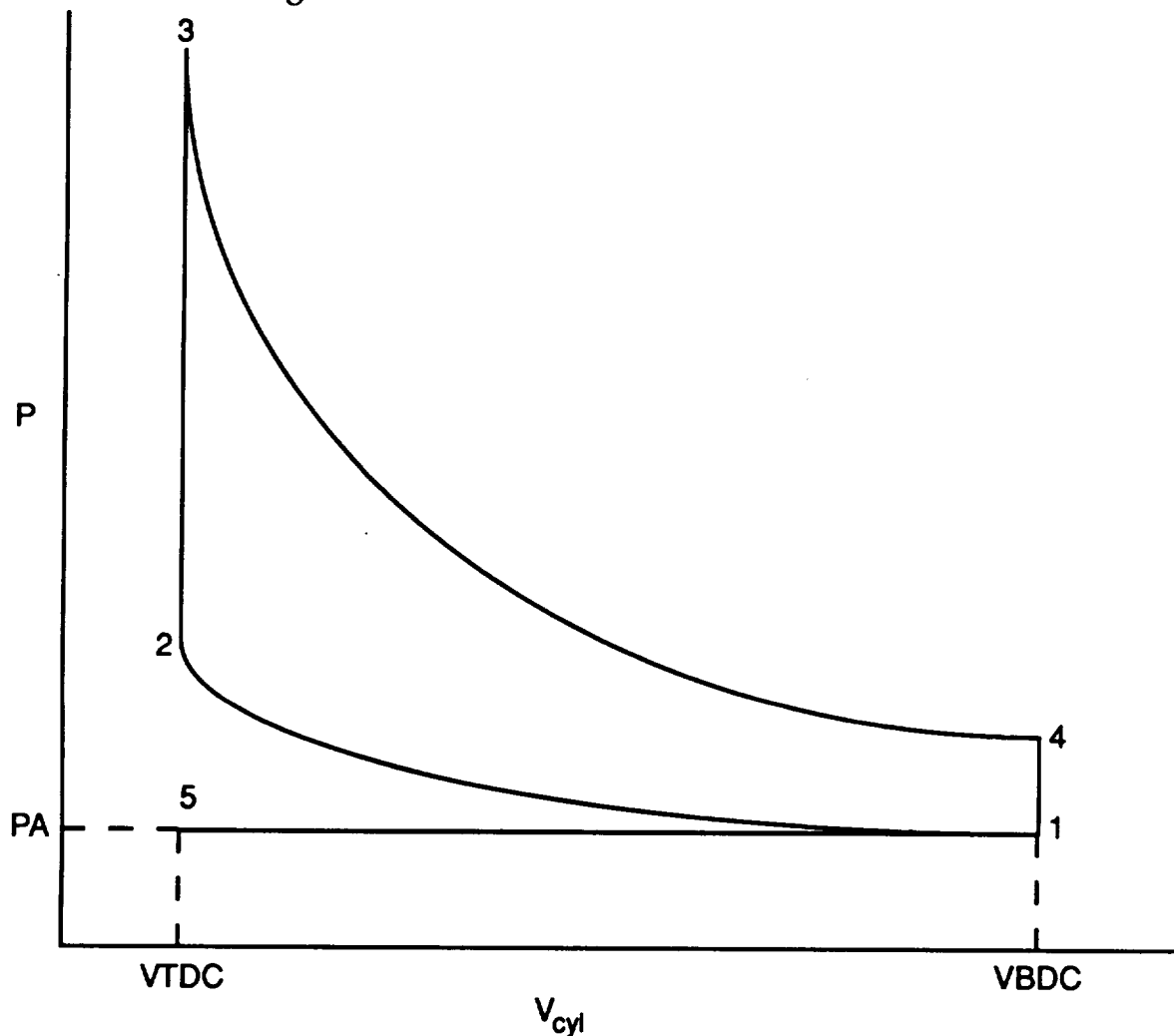
Figure 7.8.1 The Ideal Otto Cycle

This figure is a plot of pressure versus volume, where the values correspond to those inside of the cylinder. VTDC and VBDC correspond to the top dead center and bottom dead center of the cylinder, respectively. The cycle begins

59

with the induction of the methane-oxygen mixture from 5 to 1. Isentropic compression then occurs from 1 to 2, combustion from 2 to 3, isentropic expansion from 3 to 4, and finally exhaust to the atmosphere from 1 to 5.

The engine used on the both types of rovers will have a compression ratio of 9, intake pressure and temperature of 101.23 kPa and 300 K, respectively and the exhaust will be open to the atmosphere [7.5]. The engine block and cylinder heads will be constructed from aluminum to minimize the weight. The engines are estimated to weigh 110 kg for the heavy rover and 52 kg light rover [7.3] and will displace 3.2 L and 1.5 L, respectively [7.6].

Burning pure methane in pure oxygen produces a very high peak temperature in the engine, on the order of 4000 K. In fact, this temperature, even for an instant, may be high enough to melt the engine [7.7]. In order to avoid this undesirable condition, there will be a high pressure injection of carbon dioxide (CO_2) at the top of the compression stroke and just prior to ignition to dilute the pure methane and oxygen mixture, thus lowering the peak temperature to 3200 K in the engine and increasing the reliability and lifetime of the engine. The carbon dioxide is injected directly into the piston and is separated from the oxygen/methane fuel lines in order to avoid the possibility of the methane and oxygen tanks being directly exposed to the Martian atmosphere. A schematic of the engine is shown below in Figure 7.8.2.

60
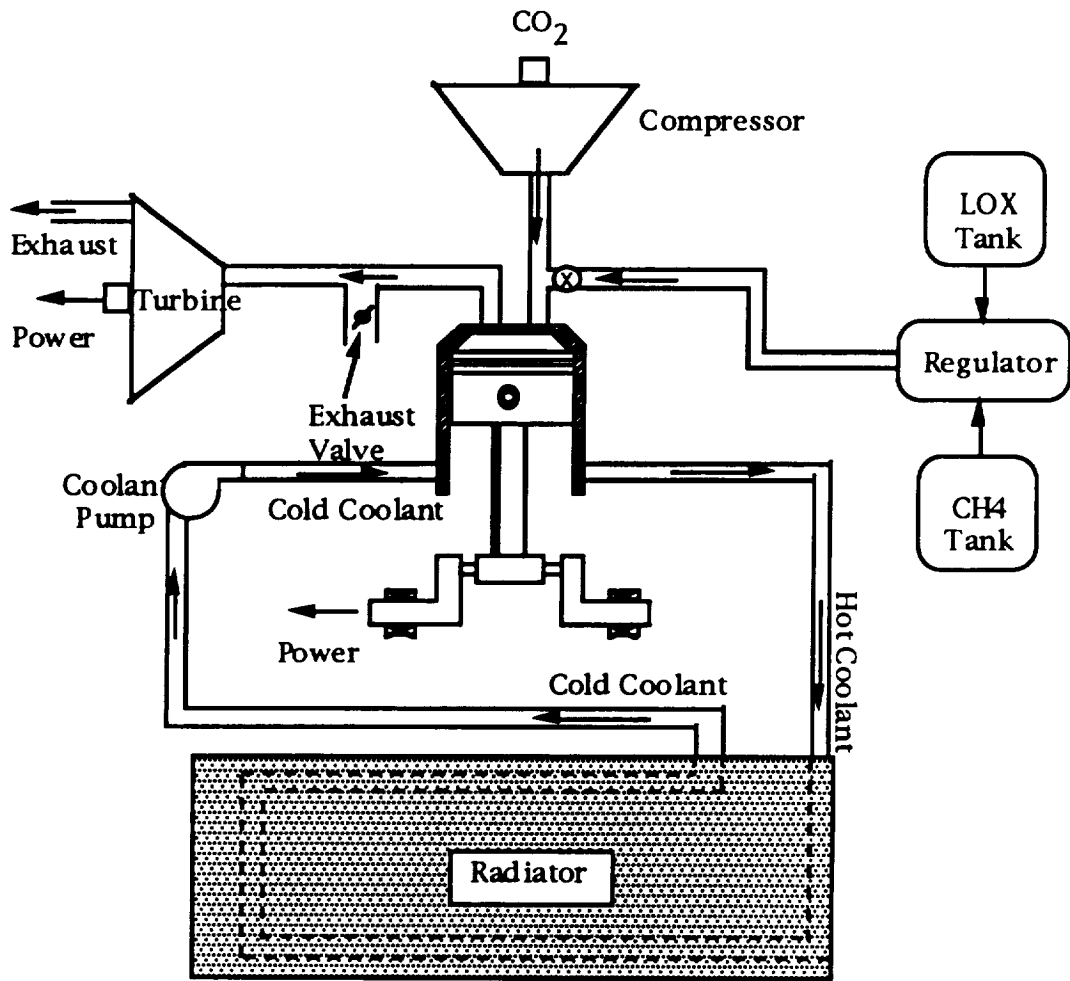
Figure 7.8.2 Engine Schematic

7.8.2 Propulsion and Cooling Systems

The absence of a significant atmosphere on Mars limits the cooling method for the engines to radiation, since convection would not be very effective. The radiator will be mounted at the end of the rover opposite to the scientific equipment and facing away from the rover. To minimize the amount of heat radiated onto the rover, the radiator will be in the shape of a circular arc stretched across the entire width of the chassis. A cross-section schematic of the heavy rover radiator is shown in Figure 7.8.3.
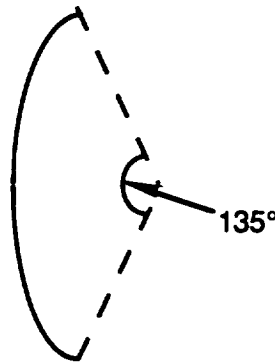
Figure 7.8.3 Schematic of heavy rover radiator

The heavy rover will be required to dissipate 36.3 kW of excess heat. This is based solely on a calculation of the energy released from the combustion of CH_4, O_2, and CO_2. The energy released from this combustion can be divided (approximately) into three parts, with 1/3 of the energy used for mechanical work, another 1/3 used for auxiliary power or cooling, and the remaining 1/3 is exhaust [7.4]. The calculation of the energy needed for locomotion and the amount released as excess heat is discussed in Appendix J.

The light rover radiator will be of the same shape as that of the heavy rover, however, it will only encompass a 90° arc and be 2 m wide. The coolant used in both systems will be propylene glycol, which is a very effective high temperature heat transfer agent [7.7]. The radiator specifications for both rovers are listed below in Table 7.8.1. Both will be constructed from pure copper 1 cm thick with a silverized Teflon coating giving the radiator an emissivity of approximately 0.97.

Table 7.8.1 Radiator Specifications

Rover	Area (m^2)	Weight (kg)	Radiated Heat (kW)
Heavy	10.0	900	36.3
Light	3.35	300	14

7.8.3 General Engine Fuel System

Because of the large amount of propellant required on both the heavy and light rovers, and the very limited amount of space on the rover, the methane and oxygen will be carried aboard the rover in liquid form. Carrying the fuel in liquid form reduces the amount of space taken up by the tanks and reduces the amount of internal pressure inside the tanks, both of which combine to make the tanks lighter. The engine fuel system consists of insulated storage tanks, cryogenic fuel pumps, a methane/oxygen regulator, and a high pressure carbon dioxide (CO_2) injector. The cryogenic fuels will require no active refrigeration units due to the amount of insulation provided, combined with the short mission duration (10 Earth days maximum) to minimize the amount of boiloff in the tanks. The methane and oxygen tanks will remain under a relatively constant pressure and temperature of 760 kPa and 1000 kPa and 113 K and 100 K, respectively. The tanks will only require a 1 cm thick stainless steel shell, covered by a 10 cm thick layer of polyurethane thermal insulation.

7.8.3.1 Heavy Rover Fuel System

On the heavy rover, both the methane and oxygen will be carried in insulated tanks below the center portion of the chassis. The weight of the tanks and fuel (2650 kg) is significant enough that it lowers the center of gravity of the heavy rover, thus increasing its stability. The tanks will be protected from boulder impacts by longitudinally and transversely mounted impact-resistant bars along with a mylar or kevlar netting to protect them from small rocks and debris kicked up by the wheels.

On the large rover both the methane and oxygen tanks will be located at the center of the rover and suspended from the bottom of the chassis. This allows fuel to be drawn by either of the two onboard engines. Having redundant engines and centralized fuel tanks improves the reliability of the

vehicle by allowing for the failure of one of the engines, while still allowing the functioning engine to use the remaining fuel to return to the base. A sample configuration of the heavy rover (HOMER) can be seen in Figure 7.6.7. The tanks will carry the amount of fuel necessary to complete a 200 km round trip (2000 kg [7.3]), including a 10% residual, while also allotting 10% of the tank volume as vapor space [7.8]. Based on a fuel-air ratio of 0.15 and adding the 10% residual, this amounts to 330 kg of methane and 1870 kg of oxygen for the rover in its HOMER configuration. The weight of the tanks will be 108 kg and 346 kg for the methane and oxygen tanks, respectively. The combined weight of the fuel and tanks will be approximately 2650 kg at the beginning of a full scale HOMER mission.

7.8.3.2 Light Rover Fuel System

The light rovers will have two fully redundant engines, but because its mission (unmanned exploration over potentially rough terrain), these rovers are unable to carry centralized fuel and oxidizer tanks underneath the chassis. Having only a single methane and oxygen tank carrying the maximum amount of fuel needed for a complete mission (625 kg of LOX, 95 kg of LCH4, in the MARGE configuration [7.3]) underneath the chassis would severely impair the light rovers mobility in the form of reduced ground clearance. For the same reason, it is not practical to place fully redundant tanks on each section of the rover. Instead, there will be two independent sets of tanks, one on each section of the rover. The large section will be capable of carrying 75% of the bipropellant (one on top of the chassis and one underneath) needed to complete a 200 km round-trip mission, while the smaller section will carry tanks capable of carrying 50% of the required bipropellant (both on top of the chassis). The individual tanks will weigh 161 kg and 139 kg for the methane and 269 kg and 213 kg for the oxygen.

FTS recommends that the mission scenario involve using the large section engine during the outbound half of a mission, and the small section engine during the return half of the mission. This leaves 25% of the fuel, which is 17.5 kg of methane and 117.5 kg of oxygen, in the large tanks. In this way, the large section engine may be used in contingency planning for the return trip in case of failure of the small section engine on the small section should fail while returning the rover to its point of origin. It is estimated that

25% of the fuel will be sufficient for the return trip by turning off all non-vital subsystems.

Because of the possible mission length of the light rover (up to 14 days) the light rovers will be equipped with rechargeable sodium sulfur batteries. These batteries have a specific energy density of 210 W-hrs/kg. Batteries will be used to power the on board systems during periods of scientific data gathering, since the engine cannot be run without the use of the emergency fuel reserve. The rover will be permitted to draw up to 5.4 kW, which is 75% of its peak power requirement (not including locomotion or the associated pumps), for up to 24 hours during these periods. This will require 620 kg of batteries [7.9]. The batteries will then be recharged as the rover traverses from one locale to another. It is important that the batteries have sufficient time to recharge in order to complete the ensuing experiments. This can be accomplished by traveling very slowly (2 or 3 km/hr) in the rover, thereby recharging the batteries while not depleting the limited fuel supply.

7.9 Rover GNC

The fleet of rovers requires instrumentation capable of determining base-relative position, heading, and sensing hazards and obstacles. The position and heading will be determined by an IMU, similar to that of the airplanes and hoppers. The IMU for the rovers will contain 3 orthogonal gyroscopes and accelerometers. The accelerometers and one of the gyroscopes will determine the state of the vehicle, which will be integrated to find the base-relative position. In order to keep the error in position doe to IMU output error (mostly due to the drift of the gyroscopes) below 50 meters, the position will be updated after the first 2.5 hours and every 1.5 hours afterward using the communications link with the satellite network. The reduction in time after the first update is due to the error associated with the updating method. The other two gyroscopes will also be used to measure the pitch and roll of the vehicle to avoid excess grade that may cause slippage or rollover.

Several types of sensors are needed to handle the hazard detection. Stereoscopic cameras will look forward to detect large obstacles and map the route for future missions. Ground penetrating radar will test the stability of the ground ahead of the rover to avoid soft surface material

65

that can cause the rover to sink or slip. Finally, pressure sensors will be placed in the wheels to warn the vehicle if it is leaving the ground.

8.0 Common Subsystems

Several subsystems were common to all vehicles and will be described in this section. These subsystems include propulsion/thermal, communications, life support, and command and data handling. Each subsystem is listed below with the vehicles that use them. In the following sections, a detailed discussion of these subsystems are presented.

- Propulsion/Power   Rovers
  Lifter
  Airplane
  Rocket Hopper

- Communications   Rovers
  Lifter
  Airplane
  Rocket Hopper

- Life Support   Rovers
  Rocket Hopper

- Command and   Rovers
  Data Handling   Lifter
  Tram
  Airplane
  Rocket Hopper

8.1 Rover Power Sources

Table 8.1.1 lists the power requirements for the ground vehicles in the transportation system. A number of power sources were considered for use on the advanced Martian rovers. These included a closed-loop internal combustion engine, fuel cells, solar arrays with batteries, and a radio-isotope thermoelectric generator (RTG). The selection of the rover power source was based on the following criteria.

- Maximum power capacity
- Power-to-mass ratio
- Commonality between vehicles

67

Table 8.1.1. Power Distribution of Vehicles

Type of Use	Heavy Rover	Light Rover	Lifter
Locomotion	110 kW	42 kW	422 kW
Lifting payload	N/A	N/A	50 kW
Allowable for Scientific Equipment	31.2 kW	44.6 kW	N/A
Airlocks	5 kW	N/A	N/A
Life Support	.4 kW	N/A	N/A
Communications	1 kW	1 kW	1 kW
GNC	.2 kW	.2 kW	.2 kW
C&DH	.2 kW	.2 kW	.2 kW
Pumps	2 kW	2 kW	2 kW
Total Peak Power	150 kW	90 kW	475.4 kW

8.1.1 Criteria Description

Maximum power capacity, defined as the maximum amount of power that can be supplied by a given power source, is the most important criterion. The rover will have to overcome obstacles and conduct exploration activities (drilling or sample return), which will require a substantial increase in power usage. Therefore, the chosen power source must be capable of efficiently supplying the additional power.

High power-to-mass ratio was the second most important criterion, since this would result in a powerful, light-weight engine as well as a more efficient means of providing excess power. Power-to-mass ratios for several candidate power sources are shown below in Table 8.1.1.1 [8.1].

68

Table 8.1.1.1. Power-to-Mass Ratios of Possible Rover Power Sources

Power Source	Power/Mass (W/kg)
RTG	5
Photo voltaic	16
H_2/O_2 Fuel Cell	55
Internal Combustion Engine	1000

Commonality is the third most important criterion. Using the same fuel for all vehicles would simplify fuel production and refining. Also, the use of a common type of propulsion system greatly enhances the maintainability of the vehicles. Therefore, the power subsystem should be common to all rovers and be capable of using indigenous fuel.

8.1.2 Selection Process

On the basis of current research and Figure 8.1.2.1, the most likely candidate as a rover power source is a methane/oxygen closed-loop internal combustion engine. Figure 8.1.2.1 shows the decision matrix used to compare the various types of power sources, where ten and zero are the high and low scores respectively. The internal combustion engine scored the highest in each of the three categories. Fuel cells ranked second, followed by solar cells and RTG's.

Criteria	Internal Combustion		Fuel Cell		Solar Cell with Batteries		RTG	
Max. Power (x 10)	9	90	7	70	5	50	1	10
Power/Mass Ratio (x 8)	10	80	7	56	4	32	2	16
Commonality (x 5)	9	45	7	35	2	10	0	0
Total	215		161		92		26	

Figure 8.1.2.1 Decision Matrix for Rover Power Source

8.1.3 Internal Combustion Engine

With respect to maximum power capacity, the internal combustion engine will produce a lower weight penalty than the fuel cell system for power capability beyond the average power consumption. For example, a rover requiring 50 kW of power nominally may have a peak power of 75 or 100 kW. Based on the power-to-mass ratios shown in Table 8.1.1.1, the weight penalty for the additional power capacity using fuel cells would be 450-900 kg. Using the internal combustion engine, however, would result in the addition of only 25-50 kg. This savings in weight enhances the value of each mission by allowing larger scientific payloads, sample returns, or fuel capacity.

The internal combustion engine is easy to implement as a common power source because its high power-to-mass ratio permits different engine sizes to suit the power range needed by the various rovers. As described in Sections 7.4 and 7.5, two chassis will be designed to support the various rover missions of the advanced Martian base. A small engine will be designed for missions using the light chassis, and a larger engine for those missions using the heavy chassis. The use of similar engines in all vehicles would facilitate the recycling of failed engines for spare parts.

Also, safety would be enhanced during hazardous missions, since the low weight of the engine makes it possible for a redundant engine to be carried. The addition of a redundant engine would also increase the maximum power capacity, thereby allowing the rover to overcome greater obstacles than it could with a single engine, or to undertake more power-intensive exploratory missions. Other power sources would not be able to provide this capability as efficiently as the internal combustion engine.

A methane/oxygen bipropellant was chosen as the fuel for the internal combustion engine because it can be produced from Martian resources, is easier to store in cryogenic form than other fuels (liquid hydrogen), and will provide adequate performance.

8.1.4 Other Power Source Candidates

Fuel cells were also considered as a rover power supply, since they scored the second highest score in Figure 8.1.1.1. They have a slightly lower fuel consumption rate than the internal combustion engine, but they also have a much lower power-to-mass ratio. The excess weight of the fuel cells,

however, greatly outweighs the savings in fuel over the internal combustion engine for a nominal mission (< 200 km). Fuel cells would be more efficient as a long-range (> 1000 km) power source, but this would require the construction of rovers with specialized power subsystems. Since these specialized subsystems would require specialized rovers, the commonality benefits of the lego concept would be lost. For these reasons, fuel cells were eliminated as a candidate power source.

Solar cells with batteries were disqualified for use on light rovers due to their low power-to-mass ratio, as well as their vulnerability to the Martian environment. Since the base will be located at 30 ° N Latitude, a reduction in solar cell efficiency is expected, thus creating the need for a relatively larger array. These arrays would be difficult to protect from Martian dust storms, and would therefore degrade at an accelerated rate. Large arrays will also substantially increase the weight of the vehicle, thus increasing the power requirement and reducing vehicle performance.

Radio-isotope thermoelectric generators (RTGs) were disqualified due to their extremely low power-to-mass ratio. The amount of power required by even the light rover (90 kW) could not be generated by an RTG without severe weight penalties for both shielding and cooling.

8.2 SIMPSONS Communications Systems

The communication system for the advanced Martian base will have to meet the following requirements.

- Continuous communication with manned vehicles
- Simultaneous communication with multiple sites
- Navigation beacons for aircraft and rovers
- Communication with mobile ground sites
- Transmission of high data rates

The proposed system consists of a line-of-sight system, a constellation of five Mars-synchronous satellites, and the orbiting node. Five synchronous satellites are needed to provide continuous coverage of Mars. It may be necessary to include satellites with inclined orbits in order to communicate with polar aircraft missions. The base will act as the control facility for all communications.

71

8.2.1 Line of Sight System

The line-of-sight (LOS) system will consist of an RF transmitter 50 meters tall operating in the Ka band (17-31 GHz), located near the center of the base. Using Ka band would put the communications links outside the bandwidth of galactic noise, which ranges from 100 MHz to 10 GHz. The tower will have four gimbaled, parabolic dishes one meter in diameter oriented 90° apart with each dish responsible for a 90° field of view. A 50 m-tall tower would provide line-of-sight capability to rovers within 20 km of the base if they are equipped with a 1 meter, steerable, parabolic antenna mounted 1 meter above the ground. Unmanned rovers could then be safely teleoperated from the base within the range of the LOS system. Although the range of the LOS system could be extended due to ground propagation, it was decided that, since the geography surrounding the base is unknown at this time, the effects of ground propagation and reflection on the range could not be estimated. The base's main unmanned facilities (mining and manufacturing) are also within the 20 km range of the LOS system, giving the crew the capability to remotely monitor and control their operations from the safety of the base. The range of the line-of-sight system for the aircraft and the hopper increases with increasing altitude of the vehicles. This will be particularly useful for remotely piloting the airplane to a safe landing.

8.2.2 Relay Satellite Constellation

The relay satellite constellation, consisting of five Mars-synchronous satellites, will be used for those missions extending beyond the 20 km range of the line-of-sight system. These satellites will use the Ka band to permit the transmission of high data rates generated for scientific exploration, telerobotic operations, and vehicle health. For safety reasons, the system will provide continuous coverage of manned rovers. Real-time communication with unmanned rovers and the capacity to transmit high data rates will permit astronauts to safely teleoperate these rovers from the base during complicated hazard avoidance maneuvers. The satellites will be capable of simultaneously transmitting to several ground sites by generating multiple beams or employing a beam hopping technique. This is accomplished using a parabolic reflector antenna with an offset shaped subreflector with feed array for scanning [8.1]. The satellite will also be equipped with a tracking capability in order to maintain continuous communication between the base and fast-

moving vehicles such as the airplane and rocket hopper. Global coverage will be provided through the use of satellite cross-link antennae.

The orbiting node could be used as a communications relay during emergency situations, such as the failure of one of the Mars-synchronous satellites. This may be done in one of two ways. One, the node may be used as a direct relay from a remote site to the base. Two, the node may be used along with a functioning satellite cross-link in order to extend the range of emergency coverage. Although the node would not be capable of providing continuous coverage, it would be able to provide a number of communications windows for a remotely located vehicle to communicate with the base during an emergency situation.

8.3 Life Support

FTS has designed a transportation network that is capable of supporting long range, manned surface missions. For this to be possible, an environmental control and life support system (ECLSS) must be an integral part of the manned vehicles. The primary objectives of an ECLSS system are to maintain the cabin atmosphere, provide potable and waste water, and to supply food for the astronauts.

The three types of ECLSS are open, partially closed, and closed. In the open system, the food and water needed by the crew are stored. Air can be purified by removing CO_2 using Lithium Hydroxide and catalytic oxidizers and filters. For the partially closed system, all food items are again stored, but some amount of atmosphere revitalization and water recycling is used. Finally, the closed system includes atmosphere and water recycling as well as a food source. FTS will use a partially closed system because it requires less mass than an open system. Therefore, the remainder of this section will discuss only partially closed systems. A closed system was not considered because these systems are still conceptual.

8.3.1 Cabin Atmosphere

In the partially closed system, several techniques are used to recycle the cabin atmosphere. First, CO_2 is removed from the atmosphere. This CO_2 is then combined with hydrogen to form water and methane. The methane is then removed from the cabin. Electrolysis separates the water into O_2 and hydrogen. The hydrogen can then be used for CO_2 reduction process. The

ECLSS must also provide for control of humidity, temperature, ventilation and trace contaminant levels. Below is a list of technologies that can be used for atmosphere control [1].

Function	Description

CO2 Removal

- Electrochemical Depolarized Cell (EDC) Cell (EDC)

Chemical Battery
$2CO_2+4H_2+2H_2O=2CO_2+2H_2O+$elec. energy$+$heat

- Solid Amine Water Desorbed (SAWD)

CO_2 adsorption on a porous substrate

CO2 Reduction

- Sabatier Reactor

$CO_2+4H_2=2H_2O+CH_4+$heat

O2 Generation

- Static Feed (SF)

Liquid water is split by Electrolysis: $2H_2O=2H_2+O_2$

- Water Vapor Electrolysis (WVE)

Water Vapor from cabin air is split by electrolysis

- Solid Polymer

Liquid water split by electrolysis, O_2 is supplied at pressures sufficient for storage bottle recharge.

Nitrogen Storage/Generation

- Hydrazine dissociation

$N_2H_4=N_2+2H_2$
N_2 is directed to the O_2/N_2 control panel

Trace Contaminant Control Combination

- Activated Charcoal

Absorbs contaminants

- Catalytic Oxidation

C_6H_6,CO,CH_4,H_2 combined to form CO_2 and H_2O

- Chemical absorbers

Absorption of contaminants

- Bacterial Filters

Microbial filters

Cabin Ventilation and Humidity Control

- Air revitalization

Air pulled from major sources of

subsystem (ARS)	contamination into ARS for processing
• Condensing heat Exchanger and Water/gas separator	-Heat exchanger water coolant
	Centrifugal separation of condensate and cooled air

Source: *Dugan, James, Nathan Nottke,"Environmental Control and Life Support System"*

8.3.2 Water Management

The mass of the partially closed ECLSS can be greatly reduced by recycling water to varying degrees. The following technologies are available to perform water recycling in the ECLSS.

Function	Description
Hygiene Water Distillation	
• Vapor Compression Distillation	-Phase change purification -Conserves latent heat in an -Initial processing treatment
• Thermoelectric Integrated Membrane Evaporation Subsystem (TIMES)	-Phase change purification -Uses thermoelectrics to save -Initial processing treatment
Hygiene Water Filtration	
• Multifiltration (MF)	-Activated charcoal adsorption -Iodine impregnated resin -Ion-exchange resin -Organic oxidation
Potable Water Production	
• Cabin Humidity Control	-Condensation removed directly from cabin air
• CO_2 reduction	-From atmosphere revitalization system
Potable Water Treatment	
• Multifiltration (MF)	-Activated charcoal adsorption -Iodine impregnated resin -Ion-exchange resin

-Organic oxidation

Source: Dugan, James, Nathan Nottke,"Environmental Control and Life Support System"

8.3.3 Food

In order to maintain the health of astronauts, the caloric intake is 2200-2800 kCal/man-day. Dehydrated and intermediate moisture foods can satisfy the astronaut's needs while reducing the mass of stored items that must be carried. Another advantage of these foods is reduced storage space and long shelf lives. Thermostabilized or heat pasteurized food is another alternative. These foods are stored in aluminum cans or flexible pouches and can be heated and eaten from the container. Thermostabilized food does not require additional moisture. Finally, vacuum packed food, which is ready to heat, is another alternative. This type of food does not have a long shelf life, but it can be used for short duration missions [8.2].

8.4 Command And Data Handling

The Command and Data Handling subsystem (C & DH) receives, processes, and initiates commands to other subsystems for a particular course of action by the vehicle. It also gathers, stores, and sends measurement data received from the onboard instruments. The network of subsystems connected to the C & DH includes GNC, thermal, ECLSS, communications, and other relevant subsystems.

For this project, the C & DH subsystem is of particular importance since most of the vehicles designed for the Martian integrated transportation system will require a high degree of autonomy. As a result, use of artificial intelligence (AI) will significantly influence the computational needs for the C & DH subsystem. Therefore, a major concern is the capability to handle the requirements of AI. Details about the AI reasoning process are described in the next section.

8.4.1 Use of Artificial Intelligence

The use of artificial intelligence (AI) and robotics is an essential part of the integrated Mars transportation system. Although this area is still under development, FTS assumes that the technology will be present by the time the advanced Martian base is established.

8.4.1.1 The Algorithm

An intelligent, autonomous system working in an unstructured, dynamic environment requires models for navigation, planning, object recognition, and internal process control. Many different algorithms have been suggested to control the AI and its reasoning capabilities for this purpose. For example, different programs have been written just for obstacle avoidance. On the micro levels, these algorithms are specific to the method; however, on the macro scale, the decision process must overcome very similar problems. For path planning, the common problems include the following three hierarchical parts.

- Action planning
- Global path planning
- Local path planning

In the next sections, a general overview of the AI reasoning process is described and the hardware requirements are given.

8.4.1.2 Action Planning and Reasoning Process

Figure 8.4.1.2.1 shows the overview of the AI decision methodology. Included are the World Model, the Environment Model, Sensors, Control, Action Planning, and Human Interface.
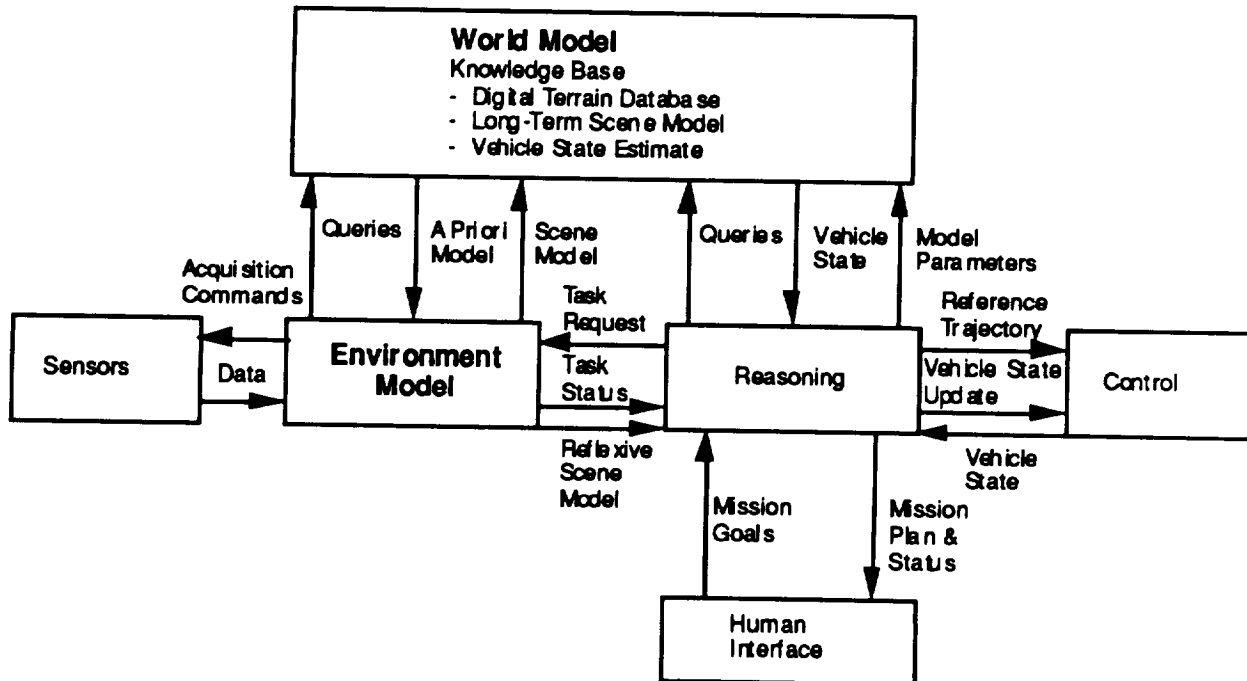
Figure 8.4.1.2.1. AI System Architecture

World Model. The World Model (WM) is a global database that represents all the information known *a priori* about the environment. The information contained in the WM are relatively fixed and include such knowledge as the work space, objects, properties of objects, relationships among them, events that can occur, and any other relevant information.

Environment Model. The Environment Model (EM) contains information that is more detailed, dynamic, and explicitly task oriented than the WM. The EM has an explicit 3D spatial representation that allows for the representation of moving objects and other dynamics within the surrounding environment.

Reasoning and Action Planning. The Reasoning area is the core of the AI system architecture. The Reasoning, which is also referred to as Action Planning, receives information from the WM, EM, and Control blocks and analyzes it according to the current mission goals. Commands are then sent to the other areas to begin an action or to obtain more information about the environment.

Sensors. The Sensors block is responsible for the gathering of information about the environment. This area detects the presence of hazards such as obstructions in the path (rocks, crevasses, etc.), as well as ground traction and stability, and other required inputs. This information is fed to the EM so that it can form a representation or perception of the surrounding.

Control. When an action plan has been finalized by the Reasoning, commands are transmitted to the Control to perform the specified operations. These include for example the speed and navigation of the vehicle. In addition, the Control also relays the vehicle's state back to Reasoning so that an ongoing analysis of the situation can be performed.

Human Interface. The Human Interface allows the human operator to specify the mission goals and the mission constraints that should be factored into the decision process. The interface is linked directly to the Reasoning center of the AI architecture.

78

8.4.1.3 System Architecture

The system starts by receiving inputs about the mission goals and mission constraints via the Human Interface. The Reasoning will dissect this information into operations that can be fed to the EM. Obtaining data from the Sensors and the WM, the EM returns a representation of the environment to the Reasoning, where a course of action is determined. Commands are then sent to the GNC subsystem to initiate the desired action.

8.4.2 Hardware Requirements

The area of computer hardware is difficult to finalize since the computer technology is constantly improving. In 50 years, when the advanced Martian base is expected to be established, more powerful and smaller computers will most likely make the hardware in existence today obsolete. For this reason, we will describe in the following section the requirements of the computational needs of the C & DH subsystem rather than specific hardware.

8.4.2.1 CPU

Several main concerns need to be addressed.
* Computational power
* Sizing and weight
* Power consumption
* Heating dissipation of the processor
* Mechanical reliability due to vibration

Moreover, the CPU must have the capability of real-time processing to react to a dynamic environment. The CPU must be able to process visual images , satellite digital images, or surface mapping in real-time. This requirement involves a large amount of data and high data rates. In a report on a Martian rover, JPL predicts that a range of 10-25 Mips will be required for a semi-autonomous vehicle, with 10 Mips being the most probable. For a complete autonomy, the latter speed, 25 Mips, should be the approximate computing power required [8.3]. In addition, the computer must be small and light enough to be accommodated by the vehicle, particularly the Martian airplane or the rocket hopper. Also, since the designed vehicles will have a limited power supply, minimal power must be consumed by the processor. In this

way, power consumption and heat generation are reduced. Currently, spacecraft CPUs require from 5-30 Watts of power.

FTS will assume that these problems will be overcome within the next 50 years. With the current rate of advances in computer technology, the CPU requirements should not be a difficult problem to surpass.

8.4.2.2 Data Storage Hardware

A data storage device is also required to store data for later processing or transmission to the remote base. It also serves as a storage bank for data specific to the mission that can be used for later analysis by the astronauts. The size and storage capacity of this device will depend on the technology in 50 years. With the current technology, an optical storage device is suitable for this purpose.

9 Conclusion

As the advanced Martian base becomes reality in the near future, an integrated transportation system will be required to provide support and maintainability of the base. The purposes of the transportation system include the transport of raw materials for the manufacturing of essential products (such as oxygen and water), the transfer of crew and cargo around the base, and the support of scientific exploration and research. Among the vehicles deemed necessary to carry out these objectives are the following.

Vehicle	Main purposes
• Aerial tram	Continuous regolith transport
• Heavy-lift crane	Loading and unloading of heavy payloads
• Rocket Hopper	Support of scientific exploration and outposts
• Martian Airplane	Support of scientific exploration and surface mapping
• Rovers	Support of scientific exploration and transfer of cargo

For the purpose of commonality, the main power system for all vehicles with the exception of the rocket hopper and the tram were designed to run on a methane/oxygen internal combustion engines. This commonality in power source will facilitate maintenance of the vehicles and will also simplify the production of fuel since a common fuel is utilized. In addition, a lego concept facilitates maintenance and introduces redundancy into the system, since spare parts are more readily available when needed.

All these vehicles, when working together, will provide the support required for the sustenance of the advanced Martian base and indirectly, will lead the way to the settlement of Mars.

9.1 Recommendations for Future Work

Due to the time frame and scope within which this project was undertaken, further analyses of each vehicle and its subsystems should be performed. Although this project gives an overall design for each of the vehicles which will be included in the integrated Martian transportation system, future studies will be required to develop these vehicles beyond the preliminary design stage. FTS recommends that a specific project be assigned for each of the five types of vehicle discussed in this report. With this in mind, the recommendations for future work on these vehicles are presented in the following sections.

9.1.1 Tram Future Work

FTS recommends that the following areas be examined in more detail for the aerial tram.

- Material properties of the carriers and the carrying rope with respect to the Martian environment

- The possibility of creating some type of concrete with Martian soil

- Reliability of the continuous mining process

The materials need to be examined to see how much effect radiation has on them. The wire ropes can be coated with other materials such as zinc for protection. Also, the use of in-situ materials to form Martian concrete to construct the tram structures (such as the trestles) will eliminate the need to deliver from Earth some of the heavy components of the tram. Finally, the parameters of reliability and their application in the analysis of a continuous mining system's capacity are given in Pavlovic's *Continuous Mining Reliability* [9.1]. In this book, a general code is given to determine many aspects of a mining system's reliability. This code was far too complicated to implement within the given time frame of this project. However, FTS recommends its use in further analysis of an aerial tram.

9.1.2 Lifter Future Work

In this area, future work will involve a more detailed analysis of the overall system before the crane can reach its final configuration and fulfill its designed task. First, a more detailed structural analysis of the grasping mechanism and the truss stability should be conducted. Also, there is a need to work out an assembly method that will deploy and assemble the crane on Mars. Other analyses should include a determination of how often and at what cost the crane will require maintenance.

9.1.3 Hopper Future Work

The rocket hopper is a very specialized vehicle, in terms of mission and configuration. The following areas, most of which have been addressed above, must be studied further in order to realize a complete vehicle.

- Vehicle lift-to-drag ratios
- Materials research/analysis
- Aerobraking
- Thermostructures
- IMU calibration

Also, several simplifying assumptions were made on the mass-sizing, such as no drag and constant mass during thrust. For a more accurate sizing , these factors must be taken into account in future analyses.

9.1.4 Airplane Future Work

The airplane has several areas which require future analysis. These include

- Thermal system
- State estimation
- Takeoff/Landing
- AI for surface terrain following

9.1.4.1 Thermal

Because CH_4/O_2 bipropellant delivers a very high gas temperature, heat dissipation should be a major emphasis for future study, since only preliminary designs of the thermal system were addressed in the discussion.

Terrestrial experience with aircraft engines has shown that cooling drag can be a large percentage of total aircraft drag. However, this problem is exacerbated at Mars by the reduced density of the atmosphere. Several alternatives will have to be investigated, including using the entire aircraft's skin as a heat rejection surface.

9.1.4.2 State Estimation

Because the error in attitude and position determination increases with time, methods must be developed to update the state using inertial measurement systems. This update could come from a ground-based beacon (which will not be available everywhere) or from orbiting communication satellites (which may not always be in view of the aircraft). Star sensors, trackers and the like have already been eliminated because they only provide attitude determination.

9.1.4.3 Takeoff/Landing

Several aspects of the take-off and landing processes will have to be studied further, including runway distance and excess power available. Once these aspects have been studied, they will provide a clearer picture of what kind of stresses the structure undergoes, what thrust vectoring may be required, the amount of fuel needed, and the vulnerability of the aircraft at these times to dust and debris.

9.1.4.4 Artificial Intelligence

Areas in AI, such as terrain mapping and its accuracy for autonomous flight and landings, should be better studied to determine the aircraft's dependency on back-up systems such as teleoperation.

9.1.5 Rover Future Work

In the rover arena, much work is left for future projects. First, in the area of structural design, dynamic analysis of the chassis and structural interface is required. Also, the mobility and suspension system should be examined morely closely to determine the performance of each chassis. Finally, since the CG location of the rovers were only estimated in this analysis, a more precise study of stability is warranted.

10.0 Management Proposal

10.1 SIMPSONS Project Organization

Figure 10.1 indicates the organizational structure for the SIMPSONS project. In order to ensure communication between the subsystems, an integration group composed of five team members was responsible for the vehicle subsystems' interfaces. This group was responsible for determining which subsystem needed to be reevaluated when iterating to meet all design requirements. Since there were five basic types of vehicles being designed, each person in the integration group was responsible for the integration of one vehicle. Eric Carlson was in charge of the hopper, Matthew Kaplan was in charge of the rovers, François Duvergne was in charge of the aircraft, David Le was in charge of the aerial tram, and Kent Allen was in charge of the lifter. Beyond this point, our team was broken down into subsystems, with group managers for each subsystem as indicated in Figure 10.1.

10.2 Program Schedule and Critical Path

All of the tasks and milestones necessary for the successful completion of this project have been identified and diagrammed in Figures 10.2 and 10.3. The program schedule (Figure 10.2) groups the tasks by milestone and describes the proposed time allotted for each. The schedule set deadlines and made note of slips in the schedule. Furthermore, the schedule and the critical path chart of Figure 10.3 indicate those tasks which can be performed simultaneously and those that cannot.

Chief Administrator
Sherie Bradfute

Project Manager
Matthew Kaplan

Chief Engineer
Eric Carlson

Integration

*Eric Carlson   Matt Kaplan   David Le   Kent Allen   Francois Duvergne

Structures

*Sherie Bradfute
Matt Kaplan
Quan Nguyen
Francois Duvergne

GNC

*Brett Thornhill
Matt Kaplan

Propulsion/Power

*Francois Duvergne
Bert Hernandez
Brett Thornhill

Communications

*Bert Hernandez
Sherie Bradfute

Robotics

*David Le
Quan Nguyen

Safety

*Kent Allen
Eric Carlson

(* indicates Technical Manager)

Figure 10.1 SIMPSONS Management Structure
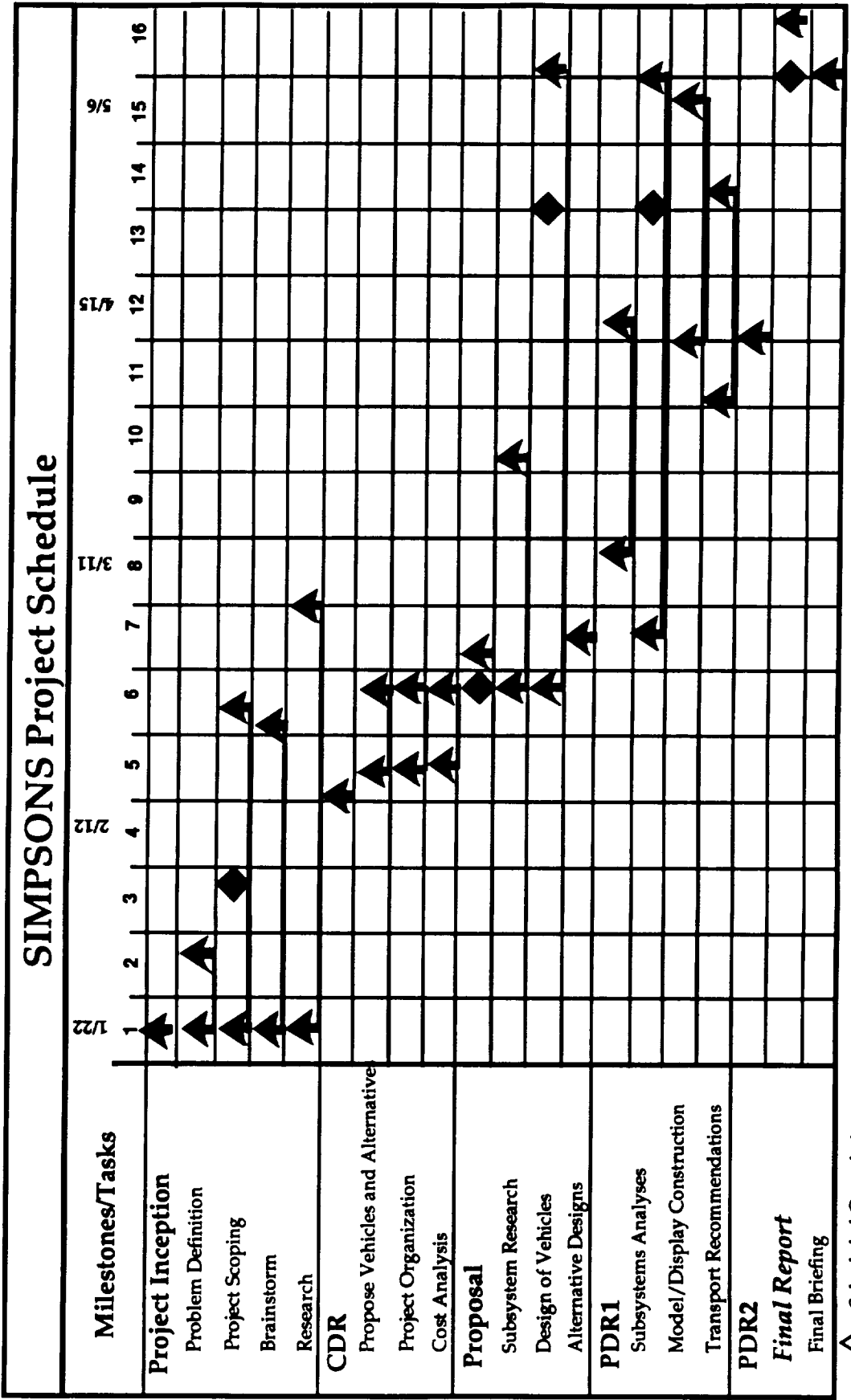
Figure 10.2 SIMPSONS Project Schedule

87
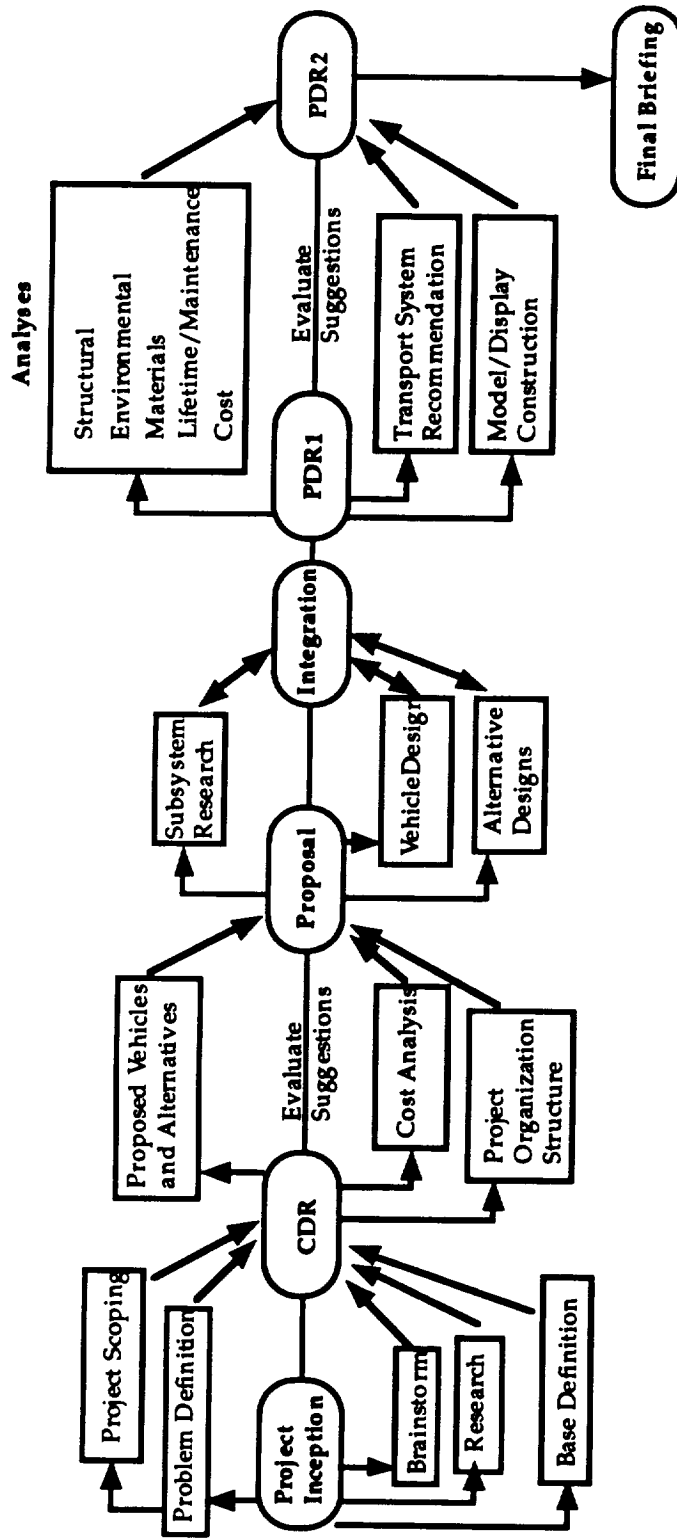
Figure 10.3 Critical Path Chart

10.3 Cost Proposal

The cost of this project has been divided into personnel costs and material costs. A detailed breakdown of the estimated costs within each category and the total cost is given below.

10.3.1 Personnel Costs

The personnel cost for this project is based on the salaries listed in the Request for Proposal. The estimated and the actual personnel cost are indicated below.

Position	Projected Hours per 16 Weeks	Actual Hours per 16 Weeks	Estimated Cost	Actual Cost
Project Manager	384	451	$9600	$11,275
Administrator	320	389.5	$7040	$8,569
Chief Engineer	320	369.5	$7040	$8,129
Engineer	1536	1193	$23040	$19,088
Consultants	16	22	$1200	$1,650
Total			**$47,920**	**$48,711**

10.3.2 Material Costs

The costs for materials were based on computer hardware and software needs of the project as well as materials required for presentations and documentation.

Macintosh Hardware, Software & Peripherals	$2,700
Main Frame CPU Time (@ $50/hour)	$200
Photocopies (@ $0.06 ea.)	$10
View graphs(@ $0.50 ea.)	$65
Final Presentation Models	$50
Miscellaneous Supplies	+ $5
Total Material Cost	$3,030

10.3.3 Total Project Cost

The total cost of the project was $51,741 (the cost of materials and personnel). The personnel cost was slightly over budget; the material cost, however, was lower than the $3,145 originally estimated in our proposal. The SIMPSONS project was within budget with the additional ten percent included for contingencies in our estimated total cost.

References

Section 3

3.1. Schniegert, Zbigniew, *Aerial Tramways and Funicular Railways* , Pergamon Press LTd., Headington Hill Hall, Oxford, 1966, p197.

Section 5

5.1 Wolf, C.V., et al., *Conceptual Design of a Mars Logistics Lander Convertible to a Rocket Hopper,* The Department of Mechanical Engineering, The University of Texas at Austin, 1988, p. 63.

5.2 Monroe, D., et al., *A Manned Mission to Mars: PDR 2,* Texas Space Services, The University of Texas at Austin, 1986, p. 206.

5.3 Niino, M. and Maeda, S., "Recent Development Status of Functionally Gradient Materials," *ISIJ International,* Vol. 30, No. 9, 1990, p. 700.

5.4 Shelton, J., et al., *PDR2: Manned Mars Mission Project,* GOTC Corporation, The University of Texas at Austin, 1985, p. 63.

5.5 Dugan, J. and Nottke, N., "Enviromental Control and Life Support System,"*Spacecraft Subsystems,* Department of Aerospace Engineering, The University of Texas at Austin, 1992.

Section 6

6.1 "Airfoil Design and data"; R Eppler; Springer-Verlag Ed; 1990.

6.2 "A concept study of a remotely piloted vehicle for Mars exploration"; Final technical report; Developement Science Inc.; NASA CR 157942; Aout 1978.

Section 7

7.1 Bickler, Don, Jet Propulsion Laboratory, personal conference, April 22, 1992.

7.2 Detwiler, M., et al., *Conceptual Design of Equipment to Excavate and Transport Regolith from the Lunar Maria: Final Report* , Mechanical Engineering Department, University of Texas at Austin, 1990, p.54.

7.3. Zubrin, Robert M. and David A. Baker and Owen Gwynne, "Mars Direct: A Simple, Robust, and Cost Effective Architecture for the Space Exploration Initiative", 29th Aerospace Sciences Meeting, Reno, Nevada, January 7-10, 1991.

7.4. Matthews, Dr. Ron, Professor of Mechanical Engineering, University of Texas at Austin, Personal Conference, April 22, 1992.

7.5. Campbell, Ashley S., *Thermodynamic Analysis of Combustion Engines*, John Wiley & Sons, Inc., New York, NY, 1979.

7.6. Acker, George, Southwest Research Institute, Personal Conference, April 1992.

7.7. Varghese, Philip, Professor-Aerospace Engineering/Engineering Mechanics, University of Texas at Austin, Personal Conference, April 1992.

7.8. Vance, R. W. and W. M. Duke, ed., *Applied Cryogenic Engineering*, John Wiley & Sons, Inc., New York, NY, 1962.

7.9 Wertz, James R. and Wiley J. Larson, et al, *Space Mission Analysis and Design*, Kluwer Academic Publishers, Dordrecht, The Netherlands, 1991.

Section 8
8.1. Davies, Richard S., 1991. "Communications Architecture", *Space Mission Analysis and Design*. Dordrecht, The Netherlands: Kluwer Academic Publishers.

8.2 Zubrin, Robert M. and David A. Baker and Owen Gwynne, "Mars Direct: A Simple, Robust, and Cost Effective Architecture for the Space Exploration Initiative", 29th Aerospace Sciences Meeting, Reno, Nevada, January 7-10, 1991.

8.3 Pivirotto, D., et al., *U.S. Planetary Rover Status:1989* , Jet Propulsion Laboratory, May 1990.

Section 9
9.1 Pavlovic, Vladimir, *Continuous Mining and Reliability*, Ellis Horwood Limited, Chichester, West Sussex, England, 1989.

Bibliography

Bekker, M.G., *Introduction to Terrain - Vehicle Systems* , University of Michigan Press, Ann Arbor, 1969.

Bekker, M.G., *Off - the - Road Locomotion; Research and Development in Terramechanics* , University of Michigan Press, Ann Arbor, 1960.

Brat, Guillaume, ed., *Spacecraft Subsystems*, Department of Aerospace Engineering, The University of Texas at Austin, 1992.

Day, J., Jet Propulsion Laboratory, personal conference, May 10, 1992.

Detwiler, M., et al., *Conceptual Design of Equipment to Excavate and Transport Regolith from the Lunar Maria: Final Report*, Mechanical Engineering Department, University of Texas at Austin, 1990.

Gere, J., et al., *Mechanics of Materials*, 2nd Ed., PWS-KENT Publishing, Boston, 1984.

Johnson, Richard C. and Henry Jasik, eds., *Antenna Applications Reference Guide*, McGraw-Hill, Inc., New York, NY, 1987.

Lowrie, James W., et. al. "Autonomous Land Vehicle (ALV) Preliminary Road-Following Demonstration," *Intelligent Robots and Computer Vision*. Washington: SPIE--The International Society for Optical Engineering, 1985, pp. 338-350.

Parodi, Alexandre M., "A Route Planning system For an Autonomous Vehicle," *The First Conference on Artificial Intelligence Applications*. Silver Spring: IEEE Computer Society Press, 1984, pp. 51-56.

Pivirotto, D., et al., *U.S. Planetary Rover Status:1989*, Jet Propulsion Laboratory, May 1990.

Probert, S.D. and D.R. Hub, *Thermal Insulation*, Elsevier Publishing Co. LTD., Barking, Essex, England.

Roth-Tabak, Yuva, and Terry E. Weymouth. "Environment Model for Mobile Robots Indoor Navigation," *Mobile Robots V*. Washington: SPIE--The International Society for Optical Engineering, 1990, pp. 453-463.

Thomson, Ron, *Mars Rover Report*, The University of Wisconsin Final Report. 1988.

Wertz, James R., et. al. *Space Mission Analysis and Design*. London: Kluwer Academic Publishers, 1991, pp. 342-348.

Wilcox, Brian, Jet Propulsion Laboratory, personal conference, March 13, 1992.

"Preliminary design of a long-endurance Mars aircraft"; A. Colozza; NASA CR 185243; April 1990.

"Fundamental of aircraft design", L. Nicolai, University of Dayton, Ohio;1975

"Aircraft design: A conceptual approach" D. Raymer; AIAA education series,1989

"The Ad-Hoc Mars airplane science working group"; Final report; V.C. Clarke, JPL; NASA CR158000; Nov. 1978.

"High-Flying Mini-Sniffer RPV: Mars Bound?"; D. Reed; Aeronautics & Astronautics; p 27-39; June 1978.

Appendix A
Ascent/Descent Vehicles

Most of the literature concerning transportation on Mars focuses solely on ascent and descent (A/D) vehicles due to the following reasons.

- They will be the first manned vehicles on Mars
- A/D can exist without an extensive transportation system, but such a system cannot exist without A/D vehicles
- each variable concerning payload, on-site refueling, aerodynamic braking, lift-to-drag ratios, terrain, and guidance and control requires in-depth study

For each of the above reasons, A/D vehicles demand more attention than our group could devote to it within the given time constraints. Fully addressing this issue would have compromised the rest of our transportation system, and vice versa. Since a relatively strong foundation already exists for it, we elected to minimize the A/D part of our scope and focus more upon the surface transportation aspects of our system.

Much of the research devoted to A/D was applied directly to the design of our ballistic hopper, but our base will require a separate ascent/descent vehicle based on different design criteria.

- 30 MT payload from orbit to Martian surface
- 15 MT payload from Martian surface to LMO (100km)
- Capacity for six crew
- 3 g_{earth} maximum acceleration
- 3 min./5 km hover
- Ease of loading/unloading
- Stability in flight
- Stability on surface, bad terrain
- Reentry heat dissipation

Additional and less specific design criteria would include: mission flexibility, system redundancy, reusability, and commutability of parts. A relatively unique requirement for our design is in-situ refueling, which most studies do not assume.

Evaluation of Past Designs

In our research, the one Mars A/D design which appeared most frequently was the bent biconic, or lifting body, design. This concept was specifically engineered for the reentry aspects of the flight, and is thus well-suited for the necessary L/D ratios, atmospheric heating, gliding flight in Martian atmosphere, and hover. However, no version of this design passed all the critical areas of maximum g-loading, 30 MT payload, surface stability and flight stability, and all of them also presented unloading difficulties.

The other design that received the most study was a "flattened Apollo" or "UFO" type craft. These designs seemed to address all of the deficiencies mentioned above with the exception of g-loading, but they added the inability to send a sufficient amount of payload into orbit. In addition, several studies questioned their own results, and it remains uncertain just what the performance characteristics of such a craft would be without further research.

The other concern is on-site refueling, which most of the previous studies do not assume. Since we are dealing with an advanced surface base (for which indigenous fuel is part of the definition), ascent fuel does not have to be carried down, and the vehicle can thus land "dry." This can significantly reduce the required fuel, which in one study was estimated at over 300 MT. On the other hand, descent fuel must be carried on ascent, where most previous studies provide fuel in low Martian orbit. Since fuel mass is often an overriding factor in spaceship design, the detailed ship design is left for future consideration.

Bibliography

Burgess, E., *Return to the Red Planet*, New York: Columbia University Press, 1990.

Monroe, D., et al., *A Manned Mission to Mars: PDR 2*, Texas Space Services, The University of Texas at Austin, 1986.

Carter, P., "Mars Cargo Descent Vehicle Sizing Analysis," NASA Johnson Space Center, 1985.

Pham, C., *Final Design Review Report for a Mars/Phobos Transportation System*, Star Truk Company, The University of Texas at Austin, 1989.

Carter, P., *A Manned Mars Mission*, Spacecraft Design Group, The University of Texas at Austin, 1985.

Shelton, J., et al., *PDR2: Manned Mars Mission Project*, GOTC Corporation, The University of Texas at Austin, 1985.

Appendix B
General Description of Martian Base

Base Selection

The principal Martian base site possibilities are as follows.

(a) 5° S. to 5° N. Latitude, 65° to 75° W. Longitude

(b) 10° to 40° N. Latitude, 240° to 280° W. Longitude

(c) 20° to 50° N. Latitude, 140° to 170° W. Longitude.

The selection of the base location is based on the following criteria.

- Relatively mild weather conditions (i.e., lower temperature variations and frequency of dust storms)
- Ground stability (i.e., low probability of landslides, lava flow, etc.)
- Mineral and liquid oxygen mining sites nearby
- Relatively level ground for landing sites and ease of debris removal

All base location choices are restricted to the northern hemisphere due to the more severe weather in the southern hemisphere. Also, an area of stable ground will minimize the possibility of damage or injury to the base and its crew.

Since water ice is nearer to the surface at northern latitudes, the base must be situated as far north as possible for easy mining of water; however, the base site must also facilitate accessibility to/from the Martian node, which is at 25° of inclination. These criteria disqualify option (a) from consideration.

Although both remaining options satisfy the previous three criteria, the final criterion eliminates option (c) due to its proximity to Olympus Mons. Not only is Olympus Mons the largest mountain on Mars (as well as the solar system), it is also surrounded by ejecta which makes landing and debris removal very difficult. Therefore, location (b) was selected as the primary base site. In addition, more radiation protection is provided at this location due to its low altitude (-1 km).

Base Elements

The advanced Martian base described here is baselined on the Genesis lunar base proposed by the University of Wisconsin. The base includes the following principal components.

- Modules (in series or individually) to support crew, hygiene facilities, exercise and health maintenance equipment, biosphere facility, safety and systems monitoring, logistics, EVA, mission operations, research workstations, storage, plus additional supportive functions
- Launch and Landing Facilities for crew/payload transfer
- . Vehicle Maintenance and Base Garage to store and maintain vehicles when not in use, along with repairing of damaged vehicles
- Surface Mining Operations to support processing, refining, and storage
- Power Plant
- Communications Facility

General Layout

The habitat area, including the communications facility, is situated at the center of the base. Approximately 3-5 km south of the base lie the launch and landing facilities, a distance we required to protect the base from blast effects or possible catastrophic incidents. Located 1 km to the west of the main base is the manufacturing facilities (MF) where water, oxygen, and other material needs of the base are produced. Raw materials for the MF are provided from the mining facilities, which are located 1-10 km west of the MF. To the east of the central node is the garage and maintenance facilities. Finally, two 1 MW nuclear power plants are positioned 1 km to the north for supply of all the base's power needs.

Base Growth

Figure B1 shows the configuration of the initial habitat area of the base. As more scientific missions and operational tasks are planned, growth of the base is expected. Shown in Figure B2 is possible expansion of the initial base, and this fashion can be used to expand the base to meet the needs of the crew and the additional operational missions.
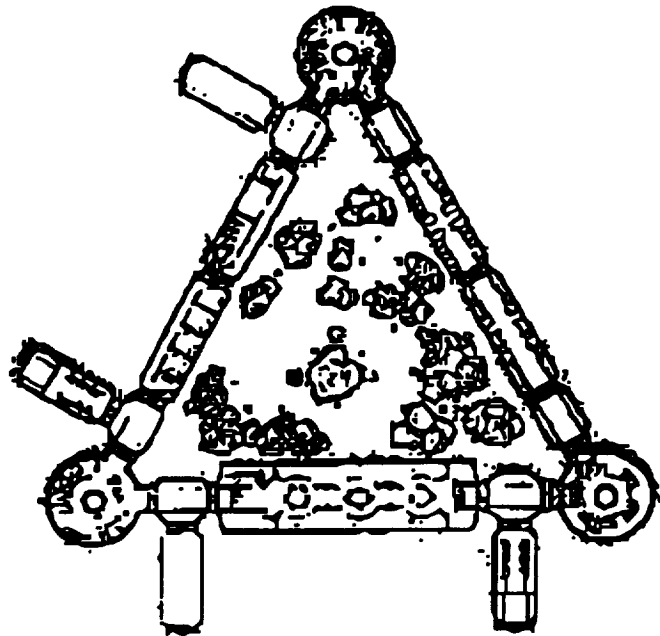
Figure B1 Proposed expandable module arrangement.

Source: "Aerospace Architecture: A Comparative Analysis of Five Lunar Habitats"
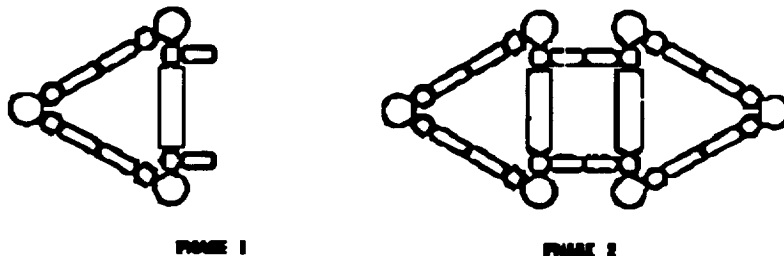
Figure B2 Example progression for base expansion.

Source: *Genesis Lunar Outpost*

Bibliogragpy

Amos, J., et al., *Robotic Construction of a Permanently Manned Mars Base: Final Report*, M.I.N.G., The University of Texas at Austin, 1989.

Soule, V., *Final Report II: A Mars Base*, École Polytechnique Feminine, NASA/USRA Advanced Design Program, 1989.

U.S. Department of the Interior, *Shaded Relief and Surface Markings of the Eastern and Western Regions of Mars*, Published by the U.S. Geological Survey, 1985.

Hansmann, T. and Moore, G.T., eds., *Genesis Lunar Outpost: Criteria and Design*, Space Architecture Design Group, University of Wisconsin-Milwaukee, 1990.

Moore, G.T. and Rebholz, P.J., "Aerospace Architecture: A Comparative Analysis of Five Lunar Habitats," University of Wisconsin-Milwaukee, 1992.

Appendix C
Ground Vehicle Propulsion and Power Calculations

The following are calculations and equations used for calculating the power required, fuel needed or heat dissipated by the internal combustion engines used by all ground vehicles.

1.0 Locomotion Power

The following equation was obtained from [C.1] used for calculating the power needed for locomotion of all of the ground vehicles:

for all calculations

$g= 3.7278 \text{ m/s}^2$ (Martian gravity)

$n= 1$

The power (P) required to propel the vehicle is

$$P=FV \tag{A1}$$

where

F= force required to propel the vehicle

V= velocity of the vehicle

and

$$F=R_C \tag{A2}$$

where

R_C= the rolling resistance per wheel

and is given by

$$R_c = \frac{\left[\dfrac{3Mg}{\sqrt{D}}\right]^{\frac{2n+2}{2n+1}}}{[3-n]^{\frac{2n+2}{2n+1}}[n+1]\left[K_c + bK_\phi\right]^{\frac{1}{2n+1}}} \tag{A3}$$

where

M= total mass divided by number of wheels or tracks

D= hemispherical wheel diameter

b= wheel width

n=soil deformation factor

$k_{\emptyset}$= coefficient of frictional deformation modulus

K_C= coefficient of cohesive deformation modulus

The values of the following constants are the same for all vehicles

$k_{\emptyset}$= 8100 Pa/m

K_C= 20855 Pa

n= 1

for the heavy rover

M=2500 kg

D=1.5 m

b=.75 m

V= 10 km/hr

This gives

R_C=4286.9 N

Total R_C=25721 N

Multiplying this by the maximum velocity, V, gives the power needed for level rolling

P= 71.4 kW

Adding 30% for peak power requirements, such as acceleration or traveling up inclines gives

P= 93 kW

Using the same equation for the light rover and using these values for the constants

M=1083.3 kg

D=1.0 m

b=.50 m

V= 10 km/hr

gives

R_C=1891 N

P= 41 kW

Using the same equation for the heavy lifter and using these values for the constants, and allowing only a 10% increase over the nominal power for peak power

M=50,000 kg

D=0.75 m

b= 1.50 m

V= 2 km/hr

gives

R_C=345 kN

P= 422 kW

2.0 Heat Dissipation

The amount of heat dissipated by the internal combustion engines was calculated from the chemistry of the combustion. The stoichiometric equation for the combustion of methane in oxygen is

$$CH_4 + 2O_2 = 2H_2O + CO_2 \qquad (A4)$$
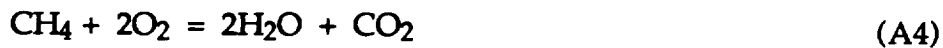
Since we are diluting the pure methane and oxygen mixture with carbon dioxide (CO_2) and using an equivalence ratio of 0.6 the combustion equation becomes

$$0.6\,CH_4 + 2O_2 + CO_2 = 1.6\,CO_2 + 1.2\,H_2O + 0.8\,O_2 \qquad (A5)$$

This means that we need 64 kg of oxygen and 44 kg of carbon dioxide for every 9.6 kg of methane burned, giving us a mass fuel-air ratio of 0.0889. The heat of reaction is calculated by summing the heats of formation of the products and subtracting the heats of formation of the reactants. If the resultant is negative, then the reaction is exothermic and energy is given off by the reaction. The heat of reaction for equation (A5) is -481,722 kJ/kmol [C.2]. In order to calculate the amount of energy that was released as heat, the heat of reaction was first divided by the molecular weight of methane, then multiplied by the mass flow rate of methane and multiplied by one-third. The mass flow rate of methane used was that for the combustion of methane in oxygen, which gives a mass fuel-air ratio of 0.15, since these are the two components we are carrying. The mass flow rate was calculated by multiplying the fuel consumption rate of 0.5 kg/km-ton from [C.3] by the weight of the vehicle and its velocity, then by the percentage of methane in the total fuel mixture. As an example, the mass flow rate for the maximum weight configuration of the heavy rover (20,000 kg) is 0.00362 kg/sec. This comes from

$$\dot{m} = \left(0.5 \frac{kg}{km-ton}\right)(20t)\left(10\frac{km}{hr}\right)\left(\frac{1hr}{3600s}\right)\left(\frac{1}{7.67}\right) \qquad (A6)$$

Using the following equation,

$$Heat = \left(481,722 \frac{kJ}{kmol}\right)\left(\frac{1kmol}{16kg}\right)\left(.00362\frac{kg}{sec}\right)\frac{1}{3} \qquad (A7)$$

the amount of waste heat was 36.3 kW. For the light rover the mass flow rate of methane was 0.0012 kg/s, and the waste heat 12 kW. For the heavy lifter, the mass flow rate of methane is 0.014 kg/s and the waste heat is 108 kW.

3.0 Radiator Calculations

The radiator was modeled as a graybody with an emissivity of 0.97 using Stefan-Boltzmann's law [C.4].

$$Q = \varepsilon \sigma T^4 A \qquad (A8)$$

where

ε = emissivity

σ = Boltzmann's constant = 5.67E-8 W/m^{2}K^4

T = absolute temperature in Kelvin

A = area of radiating surface

Assuming a coolant temperature of 525 K, which was reasonable [C.5], it was calculated that an area of 8.7 m^2 would be sufficient to radiate the required amount of energy. An area of 10 m^2 was chosen to allow for inefficiencies in the radiator due to dust accumulation on the surface or fluctuations in coolant temperature.

4.0 Engine Displacement

The displacement of each engine was calculated using the following estimation [C.5]:

$$D_p = \left(\frac{PM_w Vol}{E_f H_r \rho RPS}\right) \times 1000 \qquad (A9)$$

where

D_p = displacement of engine in liters

P = Power output in kW

M_w = molecular weight of methane

Vol= number of volumes flowing through engine (3.6 from Eq. (A5))

E$_f$= efficiency of engine (25% as a conservative estimate)

H$_r$= Heat of reaction of combustion

ρ= density of methane as it goes into engine (@ STP ρ=0.648 kg/m^3)

RPS= Intake strokes per second (.04 @ 3000 RPM, 4 stroke engine)

For the heavy rover, P=108 kW, the displacement was calculated to be 3.2 l.
For the light rover, P=52 kW, the displacement was calculated to be 1.5 l, and
the heavy lifter's displacement, P=427 kW, the displacement was 25.2 l.

5.0 Fuel Tank Dimensions

The following calculations were performed in sizing the fuel tanks for all
ground vehicles.

All fuel tanks for the ground vehicles were approximated to be cylindrical or
spherical in shape. The only one not in this shape is the liquid oxygen tank
on the heavy chassis. It is approximated as a rectangular block with rounded
ends. In order to calculate the thickness of the fuel tank, the maximum
internal stress must be calculated in the tank shell. Equations A10 and A11
were used to calculate the maximum stresses in the tank shells for spherical
and cylindrical pressure vessels, respectively [C6].

$$\sigma = \frac{pr}{t} \tag{A10}$$

$$\sigma = \frac{pr}{t} \tag{A11}$$

The stresses in the shell of the rectangular block were calculated by
determining the resultant force acting on the area of one of the faces. This
resultant force was then divided by the cross-sectional area of the shell, (i.e.
thickness times perimeter) perpendicular to the resultant force to determine
the stress in the shell.

The volumes of the tanks were calculated by dividing the density of both
liquid oxygen (1140 kg/m^3) and liquid methane (417 kg/m^3) by their
respective amounts carried on board each vehicle.

6.0 TK Model

The following TK Solver model was used to calculate the peak temperature using equations for variable specific heats taken from [C.7]. Chemistry information was taken from [C.2]. The model assumes that the reference temperature is the intake temperature of 300 K and that T2 is 611 K. T2 was calculated by hand for the isentropic compression of the carbon dioxide, oxygen and methane mixture. All specific heats are on a molal basis and are taken with respect to constant pressure in kJ/kmol. The heats of reaction of the reactants and products were then subtracted from their respective enthalpies [C.8].

References

C.1. Detwiler, and Chee Seng Foong and Catherine Stocklin, *Conceptual Design of Equipment to Excavate and Transport Regolith from the Lunar Maria*, Final Design Report, Mechanical Engineering Department, University of Texas at Austin, Fall 1990.

C.2. Davis, Raymond E. and Kenneth D. Gailey and Kenneth W. Whitten, *Principles of Chemistry*, CBS College Publishing, Philadelphia, Pa, 1984.

C.3. Zubrin, Robert M. and David A. Baker and Owen Gwynne, "Mars Direct: A Simple, Robust, and Cost Effective Architecture for the Space Exploration Initiative", 29th Aerospace Sciences Meeting, Reno, Nevada, January 7-10, 1991.

C.4. Chapman, Alan J., *Heat Transfer*, Macmillan Publishing Company, New York, NY, 1984.

C.5. Acker, George, Southwest Research Institute, Personal Conference, April 1992.

C.6. Gere, James M. and Stephen P. Timoshenko, *Mechanics of Materials*, Wadsworth, Inc., Belmont, California, 1984.

C.7. Howell, John R. and Richard O. Buckius, *Fundamentals of Engineering Thermodynamics*, McGraw-Hill, Inc., New York, NY, 1987.

C.8. Varghese, Philip, Professor-Department of Aerospace Engineering/Engineering Mechanics, Personal Conference, April 1992.

Appendix D
FORTRAN Listings

Program Mars is a program adapted from previous ascent/descent vehicle studies. All units are metric. Given several initial parameters, it integrates the equations of motion and can output the state after every integration step. Our version allows the vehicle to freefall until a specified altitude, at which the retrorockets then fire. These engines provide a constant decelerative thrust until the second specified altitude, at which the engines are cut and the parachute (Rotofoil) is deployed. The vehicle then descends to an acceptable hover height (on the order of tens of meters), where the engines would re-ignite for final approach. The program does not handle this last part of the descent — it is just used to find the velocity after parachute release.

<u>Input</u>: initial mass, initial flight path angle, initial velocity, lift-to-drag ratio, coefficient of lift, emissivity of vehicle surface, altitude at which retrorockets fire, total thrust of retrorockets, altitude and velocity at which parachute deploys, diameter of parachutes, fuel mass flow rate, planform area, and number of steps.

<u>Output</u>: acceleration, mass, time, velocity, stagnation temperature, azimuth, flight path angle, altitude, fuel burned, roll, distance down and crossrange.

Program Hopper uses a approximation of a typical trajectory to complete a mass sizing of the vehicle. All units are metric. First, the trajectory is modeled in three sections, then simplifying assumptions are made to compute the fuel mass needed to complete two hops. In deference to a manned crew, the acceleration is never allowed to exceed ±3 gees.

<u>Assumptions</u>: constant mass during burns, constant gravity, negligible drag during ascent, flat Mars.

<u>Input</u>: payload mass, mission range, hover altitude at take-off, hover time at end of hop, and specific impulse.

<u>Output</u>: total wet mass, mass of propellant, and final structural mass.

```
      PROGRAM MARS
***********************************************************
*      This is the main program of a Mars vehicle descent
*      simulation originally written by Preston Carter,
*      and it calculates in meters, kilograms and seconds.
*      It has been modified by several ASE 174M groups,
*      and our version starts a propulsive burn at the
*      first given altitude, then cuts power and deploys
*      a Rotating Flexible Drag Mill at the other.
***********************************************************
      COMMON/RO/RO
      COMMON/RHOO/RHOO
      COMMON/HMAX/HMAX
      COMMON/E/E
      COMMON/BALLCL/BALLCL
      COMMON/BALLCD/BALLCD
      COMMON/G/G
      COMMON/AMO/AMO
      COMMON/HEQUIL/HEQUIL
      COMMON RB
      COMMON/PROP/FFR,DM,PALT,THRUST
      COMMON/PARA/BALCDR,PALT2,RDR,VDR
      COMMON/TEMP/TEMP
      COMMON/ROLL/ROLL
      DIMENSION X(7),DX(7)
      REAL LD,S
      RB = 3.9
      ROLL = 0.0
      DX(4) = 0.0
      GMAX = 0.0
      TWMAX = 0.0
      G = 3.72
      RO = 3393300.0
      RHOO = 1.56E-2
      HMAX = 100.0
      DT = 1.0
      PRINT*, 'Coefficient of Lift?'
      READ*, CL
      PRINT*, 'Planform area?'
      READ*, S
      PRINT*, 'Lift/Drag?'
      READ*, LD
      H = 350000.0
      X(3) = H+RO
      PRINT*, 'Original velocity?'
      READ*, X(4)
      PRINT*, 'Flight path angle?'
      READ*, ANGLE
      X(5) = 0.017453*ANGLE
      PRINT*, 'Pullout altitude?'
      READ*, HEQUIL
      HEQUIL = HEQUIL*1000.0
      PRINT*, 'Emissivity of surface?'
      READ*, E
      PRINT*, 'Original mass?'
      READ*, AMO
      BALLCL = AMO/(CL*S)
      BALLCD = BALLCL*LD
      PRINT*, 'Fuel mass flow rate?'
      READ*, FFR
      PRINT*, 'Minimum altitude, Rotofoil deployment?'
      READ*, RDR
      RDR = RDR*1000.0
      PRINT*, 'Maximum velocity, Rotofoil deployment?'
```

```
      READ*, VDR
       PRINT*, 'Diameter, Rotofoil?'
      READ*, RFDMD
       RFDMS = 0.3926991*(RFDMD**2)
       BALCDR = AMO/(1.17*(S+RFDMS))
       PRINT*, 'Altitude for engine firing?'
      READ*, PALT
       PALT = PALT*1000.0
       PALT2 = PALT
       PRINT*, 'Thrust provided?'
      READ*, THRUST
       DX(7) = 0.0
       X(1) = 0.0
       DX(4) = 0.0
       X(2) = 0.0
       X(6) = 0.0
       X(7) = AMO
       TMAX = 5000.0
       TERMH = 0.0
       PRINT*, 'Number of steps?'
      READ*, NSTEPS
       TIME = 0.0
      CALL OUTPUT(TIME,X,DX,TW,IUNIT)
       H = X(3)-RO
******* Loop for descent begins *********************************
200   IF ((TIME.LT.TMAX).AND.(H.GT.TERMH).AND.X(4).GT.0.0) THEN
       IF (X(3)-RO.LE.100.) DT = .25
       DO 300 I=1,NSTEPS
           CALL RK(X,DX,DT,7)
           TIME = TIME+DT
       IF (DX(4).LT.GMAX) GMAX = DX(4)
300   CONTINUE
      CALL OUTPUT(TIME,X,DX,TW,IUNIT)
      IF (TW.GT.TWMAX) TWMAX = TW
          H = X(3)-RO
      ELSE
          GMAX = GMAX/9.81
          IF (IUNIT.EQ.6) GOTO 444
            PRINT*, '**********FINAL**********'
          PRINT*, 'TIME',TIME
          PRINT*, 'ALT',H
          PRINT*, 'GEES',GMAX
          PRINT*, 'TEMP',TWMAX
          PRINT*, 'FUEL',AMO-X(7)
          PRINT*, 'VEL',X(4)
444   CALL OUTPUT(TIME,X,DX,TW,6)
      GOTO 999
      ENDIF
      GOTO 200
******* Loop for descent ends **********************
999   CONTINUE
      STOP
      END

      SUBROUTINE OUTPUT(TIME,X,DX,TW,IUNIT)
***************************************************************
*      This routine outputs an ephemerous of the descent.
***************************************************************
      COMMON/RO/RO
      COMMON/ROLL/ROLL
      COMMON/PROP/FFR,DM,PALT,THRUST
      COMMON/RHOO/RHOO
      DIMENSION X(7),DX(7)
      RADDEG = 57.29578
```

D-3

```
      THETA = ROLL*RADDEG
      DRG = X(1)/1000.0
      CRG = X(2)/1000.0
      H = (X(3)-RO)/1000.0
      V = X(4)
      GFORCE = DX(4)/9.81
      GAMA = X(5)*RADDEG
      AZE = X(6)*RADDEG
      RHOF = DENS(X(3))
      IF (H.LE.1.0 .OR. V.LE.1.0) RHOF = -9999.0
      CALL FRY(X,RHOF,TW)
      PRINT*, 'TIME',TIME
      PRINT*, 'ROLL',THETA
      PRINT*, 'MASS',X(7)
      PRINT*, 'DOWNR',DRG
      PRINT*, 'CROSSR',CRG
      PRINT*, 'ALT',H
      PRINT*, 'VEL',V
      PRINT*, 'GAMMA',GAMA
      PRINT*, 'AZE',AZE
      PRINT*, 'ACCEL',GFORCE
      PRINT*, 'TEMP',TW
      RETURN
      END


      SUBROUTINE RK(X,DX,DT,N)
******************************************************
*       This is a Runge-Kutta 4th order integrator which
*       expects the subroutine DERIV to be supplied.
******************************************************
      REAL X(7),U(7),F(7),D(7),DX(7)
      CALL DERIV(X,D)
      DO 1 I = 1,N
      D(I) = D(I)*DT
1     U(I) = X(I)+0.5*D(I)
      CALL DERIV(U,F)
      DO 2 I = 1,N
      F(I) = F(I)*DT
      D(I) = D(I)+2.0*F(I)
2     U(I) = X(I)+0.5*F(I)
      CALL DERIV(U,F)
      DO 3 I = 1,N
      F(I) = F(I)*DT
      D(I) = D(I)+2.0*F(I)
3     U(I) = X(I)+F(I)
      CALL DERIV(U,F)
      DO 4 I = 1,N
4     X(I) = X(I)+(D(I)+F(I)*DT)/6.0
      DX(4) = D(4)
      DX(7) = D(7)
      RETURN
      END


      SUBROUTINE DERIV(X,DX)
******************************************************
*       This subroutine supplies the equations of motion.
******************************************************
      COMMON/BALLCL/BALLCL
      COMMON/BALLCD/BALLCD
      COMMON/G/G
      COMMON/AMO/AMO
      COMMON/RO/RO
      COMMON/PROP/FFR,DM,PALT,THRUST
      COMMON/PARA/BALCDR,PALT2,RDR,VDR
```

```fortran
      COMMON/ROLL/ROLL
      DIMENSION X(7),DX(7)
      Q = 0.5*DENS(X(3))*X(4)**2
      HDOT = X(4)*SIN(X(5))
      IF (X(3)-RO.LE.PALT.AND.X(4).GT.10.0.AND.X(3)-RO.GT.RDR) THEN
            DX(7) = -FFR
            PTHRUST = THRUST/X(7)
      ELSE
            DX(7) = 0.0
            PTHRUST = 0.0
      ENDIF
      CALL CMROLL(X(7),X(3),X(4),X(6),HDOT,Q,ROLL)
      DX(1) = X(4)*COS(X(6))*COS(X(5))
      DX(2) = X(4)*SIN(X(6))*COS(X(5))
      DX(3) = HDOT
      DX(4) = -Q/(BALLCD*X(7)/AMO)+G*SIN(X(5))-PTHRUST
      DX(5) = Q/(BALLCL*X(7)/AMO)/X(4)*COS(ROLL)-G/X(4)*COS(X(5))
     &        +X(4)/X(3)*COS(X(5))
      DX(6) = Q/(BALLCL*X(7)/AMO)/X(4)/COS(X(5))*SIN(ROLL)
      CALL CHUTES(X(3)-RO,X(4),DX(4),Q)
      RETURN
      END


      SUBROUTINE CHUTES(R,V,A,Q)
************************************************************
*     This subroutine determines whether the Rotofoil is
*     deployed and computes the deceleration encountered.
************************************************************
      COMMON/PARA/BALCDR,PALT2,RDR,VDR
      IF ((R.LE.RDR).AND.(V.LE.VDR)) THEN
            A = A-Q/BALCDR
            PRINT*, 'CHUTES OUT'
      ELSE
            PRINT*, 'CHUTES IN'
      ENDIF
      RETURN
      END


      FUNCTION DENS(R)
******************************************************************
*     This function contains an analytical model of the density
*     of the Martian atmosphere which was developed at JPL from
*     a best fit of the Viking I and II flight data.
******************************************************************
      COMMON/RHOO/RHOO
      COMMON/HMAX/HMAX
      COMMON/RO/RO
      RHO1 = 0.01601
      H = (R-RO)/1000.0
      IF (H.EQ.0.0) THEN
            DENS = RHO1
      ELSE IF ((H.GT.0.0).AND.(H.LE.5.0)) THEN
            DENS = RHO1*EXP(-0.0515306*H)
      ELSE IF ((H.GT.5.0).AND.(H.LE.50.)) THEN
            DENS = RHOO*EXP(-(-0.5314+0.1083*H+2.188/H))
      ELSE IF ((H.GT.50.0).AND.(H.LE.HMAX)) THEN
            DENS = RHOO*EXP(-(-2.881+0.1396*H+42.55/H))
      ELSE IF (H.GT.HMAX) THEN
            DENS = 0.0
      ENDIF
      RETURN
      END


      SUBROUTINE CMROLL(W,R,V,AZE,HDOT,Q,ROLL)
```

```
***********************************************************
*        This subroutine controls the roll of the vehicle during
*        descent assuming a constant L/D and angle of attack.
*        For this simulation, the vehicle's lift is modulated by
*        the bank angle.  Also, this routine controls the craft's
*        rate of descent and flight azimuth according to the
*        trajectory profile requirements.
***********************************************************
        COMMON/BALLCL/BALLCL
        COMMON/G/G
        COMMON/RO/RO
        COMMON/HEQUIL/HEQUIL
        COMMON/AMO/AMO
        H = R-RO
        IF (ROLL.EQ.0.0) THEN
         SGN = 1.0
        ELSE
        SGN = ROLL/ABS(ROLL)
        ENDIF
        IF (Q.EQ.0.0) THEN
        ROLL = 0.0
        ELSE IF ((H.LT.HEQUIL).AND.(HDOT.LT.0.0)) THEN
        ROLL = 0.0
        ELSE IF (H.GT.HEQUIL) THEN
        ROLL = ACOS(0.0)
        ELSE
            COSEQG = ABS(G*(BALLCL*W/AMO)/Q*(1.0-V**2/(G*R)))
            IF (COSEQG.GT.1.0) THEN
            ROLL = ACOS(0.0)
            ELSE
            ROLL = ACOS(COSEQG)
            ENDIF
        ENDIF
        IF (AZE.GT.1.57079) THEN
        ROLL = -1.0*ROLL*SGN
        ENDIF
        RETURN
        END


        SUBROUTINE FRY(X,RHOF,TW)
***********************************************************
*        This is the aeroheating subroutine.  It uses an equation
*        for convective heating from Corning's Aerospace Vehicle
*        Design to calculate the stagnation temperature.  Radiative
*        heating effects are assumed to be negligible since the
*        vehicle is flying mush slower than 10000 m/s.
***********************************************************
        COMMON RB
        COMMON/RO/RO
        COMMON/E/E
        COMMON/RHOO/RHOO
        COMMON/TEMP/TEMP
        DIMENSION TEMP(101)
        DIMENSION X(7)
        IF (RHOF.EQ.-9999.0) THEN
            TW = 0.0
            GOTO 555
        ENDIF
        RBF = RB*3.2808
        VC = 10831.5
        SBK = .48E-12
        ONE = 17600./SQRT(RBF)
        TWO = SQRT(RHOF/RHOO)
        THREE = (X(4)/VC)**3.25
```

```
      TW4 = ONE*TWO*THREE/(SBK*E)
      TW4 = ABS(TW4)
      TW = SQRT(SQRT(TW4))
      TW = TW/1.8
555   CONTINUE
      IH = INT((X(3)-RO)/1000.)
      IF (IH.LT.1) IH = 1
      TT = TEMP(IH)
      TW = TW+TT
      RETURN
      END
```

.

```fortran
      PROGRAM HOPPER
      REAL*8 MH,MHPR,MPL,MHST,G,GE,I,TH,EPS,UPPER,LOWER,MHTO
      REAL*8 MLTO,MLPR,MLPL,TL,MLST,ALT,ML,THR,PREV1,PREV2
      REAL*8 MATO,MAPR,MAST,MAPL,THR2,TA,MA,RANGE,SF,VEL,PL
      COMMON SF,G,GE,I
      PRINT*, 'This program will estimate the mass required for a'
      PRINT*, ' ballistic Martian hopper, given 5 initial parameters.'
      PRINT*, 'So answer the questions, and dont give me any trouble.'
      PRINT*, 'Ultimate range (km): '
      READ*, RANGE
      RANGE = RANGE*1000
      PRINT*, 'Launch height (m): '
      READ*, ALT
      PRINT*, 'Specific Impulse (sec): '
      READ*, I
      PRINT*, 'Payload mass (kg): '
      READ*, PL
      MPL = PL
      PRINT*, 'Hover time (sec): '
      READ*, TH
      SF = .15
      EPS = 10
      G = 3.72
      GE = 9.81
*****************************************************************
*         Okay, here's how this thing works.  First, the fuel is
*         computed for the final hover for the second hop.  Then
*         this fuel is considered payload for the ascent phase, and
*         the fuel for that is determined.  This new fuel total is
*         all payload for the launch sequence, and then it's all
*         repeated for the initial hop, for a total of six phases.
*         By now, the total structural weight is way beyond what
*         was originally assumed, and the entire process is repeated
*         until you get two total masses within 10 kg of one another.
*****************************************************************
5     MHPR = 0
      MHST = SF*MPL
10    MHTO = MHPR+MPL+MHST
      CALL HOVER (MHTO,TH,MHPR,MHST,MLST,MAST,MPL)
      UPPER = MHTO+EPS
      LOWER = MHTO-EPS
      IF (MH.LT.UPPER.AND.MH.GT.LOWER) GOTO 20
      MH = MHTO
      GOTO 10
20    PREV1 = MAST
      MAPL = MH-PREV1-PREV2
      MATO = MH-PREV1-PREV2
50    CALL ASCENT (MATO,MAPR,MAST,MAPL,RANGE)
      UPPER = MATO+EPS
      LOWER = MATO-EPS
      IF (MA.LT.UPPER.AND.MA.GT.LOWER) GOTO 80
      MA = MATO
      GOTO 50
80    PREV2 = MLST
      MLPL = MA-PREV1-PREV2
      MLTO = MA-PREV1-PREV2
100   CALL LAUNCH (MLTO,MLPL,ALT,MLPR,MLST)
      UPPER = MLTO+EPS
      LOWER = MLTO-EPS
      IF (ML.LT.UPPER.AND.ML.GT.LOWER) GOTO 200
      ML = MLTO
      GOTO 100
200   UPPER = MLST-PREV2
```

```
      IF (UPPER.LT.EPS) GOTO 220
      MHST = MHST+MAST+MLST-PREV1-PREV2
      GOTO 10
220   IF (MPL.NE.PL) GOTO 300
      MPL = ML
      GOTO 5
300   PRINT*, 'Masses -- Total: ',ML
      PRINT*, 'Prop.: ',MHPR+MLPR+MAPR,'  Str.: ',MHST+MLST+MAST
      END


      SUBROUTINE HOVER (MHTO,TH,MHPR,MHST,MLST,MAST,MPL)
*************************************************************************
*        This routine determines the amount of fuel (and storage
*        structure required) to hover the vehicle for the given
*        time.  Assuming constant mass yields a conservative estimate.
*************************************************************************
      REAL*8 MHPR,MPL,MHST,G,GE,I,TH,EPS,MHTO,MLST,MAST,SF
      COMMON SF,G,GE,I
      MHPR = MHTO*G*TH/(I*GE)
      MHST = SF*(MHPR+MPL)+MLST+MAST
      MHTO = MHPR+MPL+MHST
      RETURN
      END


      SUBROUTINE LAUNCH (MLTO,MLPL,ALT,MLPR,MLST)
*************************************************************************
*        This routine uses a thrust equal to 110% of the take-off
*        mass to lift the vehicle to the given height.  It then
*        calculates the fuel required, using a constant mass for
*        a conservative estimate.
*************************************************************************
      REAL*8 MLPR,MLPL,MLST,G,GE,I,TL,EPS,MLTO,ALT,THR,SF
      COMMON SF,G,GE,I
      TL = 4*ALT/G
      THR = 1.1*MLTO*G
      MLPR = THR*TL/(I*GE)
      MLST = SF*MLPR
      MLTO = MLPL+MLPR+MLST
      RETURN
      END


      SUBROUTINE ASCENT (MATO,MAPR,MAST,MAPL,RANGE)
*************************************************************************
*        This routine treats the vehicle as a projectile and
*        calculates the velocity needed to achieve the desired
*        range.  It then uses a constant acceleration of three
*        Earth gravities to determine the thrust and fuel needed.
*************************************************************************
      REAL*8 SF,G,GE,I,MAPR,THR2,TA,MAST,MATO,MAPL,RANGE,VEL
      COMMON SF,G,GE,I
      THR2 = 3*MATO*GE
      VEL = SQRT(G*RANGE/1.17)
      TA = VEL/(7.2*G)
      MAPR = THR2*TA/(I*GE)
      MAST = SF*MAPR
      MATO = MAPL+MAPR+MAST
      RETURN
      END
```

Appendix E
Gyroscopic Drift Error Analysis
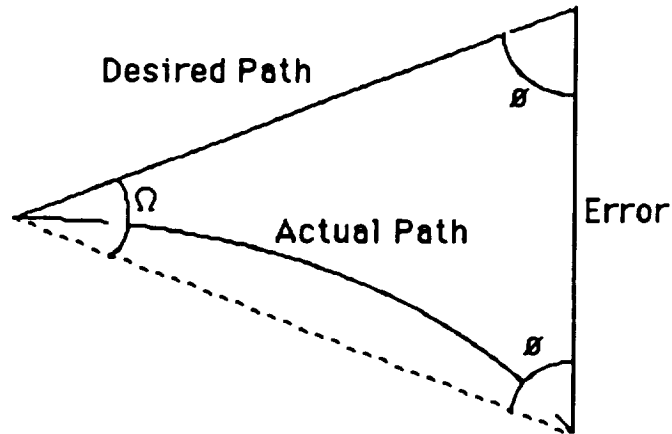
Figure E.1

Figure E.1 shows the deviation of a vehicle from its desired path due to gyroscopic drift. The symbols in the figure are defined as follows.

- Ω = angular error due to drift = ß * time radians
- ß = gyroscopic drift = 4.84E-8 radians/second
- Path length = Velocity * time = V * t
- ø = (PI - ß)/2 radians

Using the law of sines, the following equation is derived.

$$(\text{Error}) * \sin \text{ø} = V * t * \sin \Omega = V * t * \sin (\text{ß} * t)$$

Assuming that Ω is small, so that the approximations of $\sin \Omega = \Omega$ and $\sin \text{ø} = 1$ are valid, the final equation solved for time is:

$$t = \text{sqrt}(\, \text{error}/ \,(V * \text{ß})\,)$$

The allowable error is 50 meters, however, the position update is only accurate to 20 meters, so after the first update, the allowable error is only 30 meters. The calculations for the rovers and airplanes yielded the following results for the time between position updates.

Rovers: Cruise Velocity = 8.94 m/sec,   Allowable error = 50 meters

        First update in 3 hours
        Subsequent updates every 2 hours 20 minutes

Airplanes: Cruise Velocity = 130 m/sec,   Allowable error = 50 meters

        First update in 47 minutes
        subsequent updates every 37 minutes

Appendix F

Aircraft aerodynamics

The basic flight equations are:

$$L = \text{Lift} = 1/2 \, p \, V^2 \, C_l \, S$$

$$D = \text{Drag} = 1/2 \, p \, V^2 \, C_d \, S$$

$$T = \text{Thrust} = (P \, n)/V$$

$$W = \text{Weight} = \text{Mass } G_{mars}$$

Where :
- p = atmospheric density
- C_l = Coefficient of lift
- C_d = Coefficient of Drag
- S = Wing area
- V = flight velocity
- P = power required
- n = propeller efficiency
- G_{mars} = Mars gravitational acceleration (3.76 m/sec^2)

For a steady state, we have :

Lift = Weight $\Rightarrow$ $\text{Mass } G_{mars} = 1/2 \, p \, V^2 \, C_l \, S$

Drag = Thrust $\Rightarrow$ $(P \, n)/V = 1/2 \, p \, V^2 \, C_d \, S$

<u>Estimation of the aerodynamic coefficients</u>

- Coefficient of lift: as advised in ref. (1), we will consider that :
$$(C_l)_{aircraft} = (C_l)_{wing}$$

- Coefficient of Drag:

For a cambered airfoil as the Eppler E61 , the coefficient of drag is expressed as:

$$C_d = C_{d_{min}} + K' \, C_l^2 + K'' \, (C_l - C_{l_{min}})^2$$

with K′ = inviscid drag due to the lift or induced drag
K″ = viscous drag due to the lift.

In order to minimize Cdmin, we will use cruise coefficient of lift very close to Clmin and then we can approximate the previous equation as :

$$C_{d_{wing}} = C_{d_{min}} + K' C_l^2$$

With K′ = 1/(pi A e)

A = wing aspect ratio = (wingspan)^2/wing surface
e = wing efficiency factor

We thus see that a higher aspect ratio wing will allow a smaller induced-drag coefficient.

Since we have a wing without sweep, with a taper ratio equal to 1 and a small body effect, we can approximate the wing efficiency factor to be equal to 1.

Considering that the drag-due-to-lift is primarily due to the wing, we can express the total aircraft drag coefficient as :

$$C_d = (C_{d0})_{wing} + (C_{d0})_{body} + K' C_l^2$$

1. (C$_{d0}$)wing:
        It is found directly on the C$_l$-C$_d$ diagram of the Eppler E61 airfoil, according to the current Reynolds number

2. (C$_{d0}$)body

$$(C_{d0})_{body} = (C_{d0})_{fuselage} + (C_{d0})_{tail} + (C_{d0})_{boom(s)} + (C_{d0})_{misc}$$

As a rule of thumb, we will approximate the drag of the fuselage+ boom + miscellaneous to be approximately equal to 1.1 (C$_{d0}$)fuselage.
Assuming we are using the same kind of profile for the tail as for the wing, we can approximate: (C$_{d0}$)tail = (C$_{d0}$)wing (S$_{tail}$/S$_{ref}$)

Thus,

$$(C_{d0})_{a/c} = 1.1(C_{d0})_{fuselage} + ((S_{wing} + S_{tail})/S_{ref})(C_{d0})_{wing}$$

We estimate the drag of the fuselage by using a calculated flat-plate skin-friction drag coefficient(Cf) and a component "form factor" (FF)

Thus $(C_{d0})_{body} = Cf\ FF\ S_{wet}/S_{ref}$

and As an approximation, we consider that the flow is laminar (low Reynolds numbers) thus:

$$Cf = 1.328/Re^{0.5}$$

where Reynolds number is

$$R = pVl/u$$

l: characteristic length
V: speed
p: atmospheric pressure
u: viscosity

-The form factor for the fuselage is given by

$$FF = (1 + 60/f^3 + f/400)$$

where $f = l/d = 1/((4/pi)\ A_{max})^{0.5}$ (Cf D. Raymer: "aircraft design, a conceptual approach", p 281)

Computation of power required

$$P_{required} = D\ V\ /\ n$$

V: airspeed

F-3

D: drag

n : propeller efficiency

Computation of rate of climb

$$dhe/dt = V(T_{available} - Drag)Weight$$

Computation of range

The range is given by the breguet equation

$$R = (L/D)\ ln(Wi/Wf)\ (3600\ n)/\ (g\ c)$$

<div style="margin-left: 2em">

with L/D: lift/drag ratio

Wi: initial weight of the aircraft

Wf: final weight of the aircraft

n: propeller efficiency (0.88)

c: specific cruise consumption (0.8 kg/(kW hr))

</div>

Results

The results of the computations are given as charts displaying the aircraft parameters(speed, Reynolds number, L/D, Power, Rate of climb) versus the altitude, for different aircraft total weight (in order to take into account the decrease of aircraft's weight during the mission due to the fuel burning).

It should be noted that since we didn't take into account the effect of mach, results presented are not very accurate if the aircraft airspeed is high (>130 m/s), i.e. if the aircraft is heavy and/or flies at high altitudes.

L/D large aircraf

Legend:
- M= 600 kg
- M=800kg
- M=1000kg
- M=1200 kg

Y-axis: L/D
X-axis: H (KM)

L/D small aircraf

Legend:
- M = 450 kg
- M= 400 kg
- M= 350 kg

Y-axis: L/D
X-axis: H (KM)
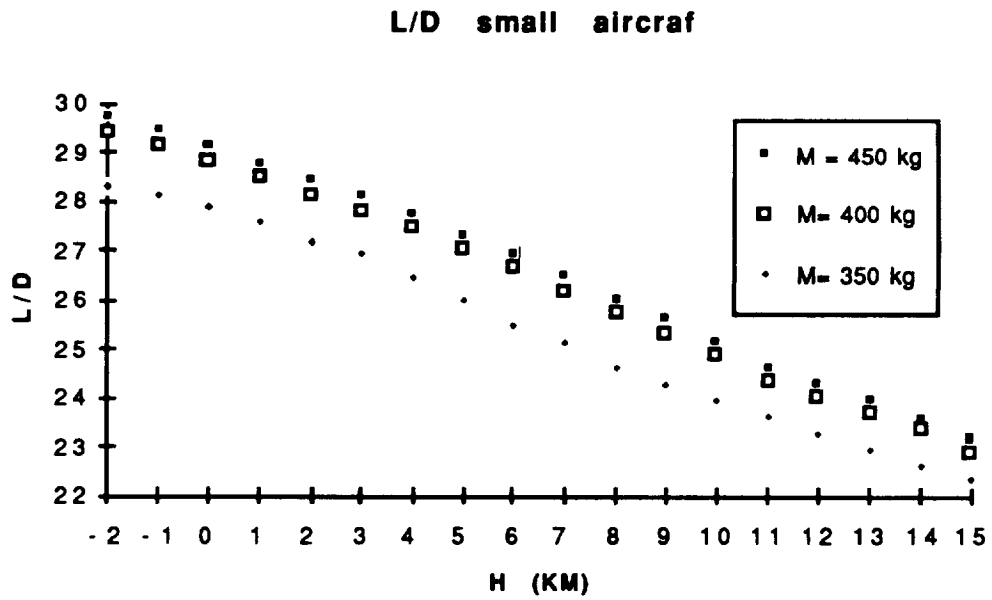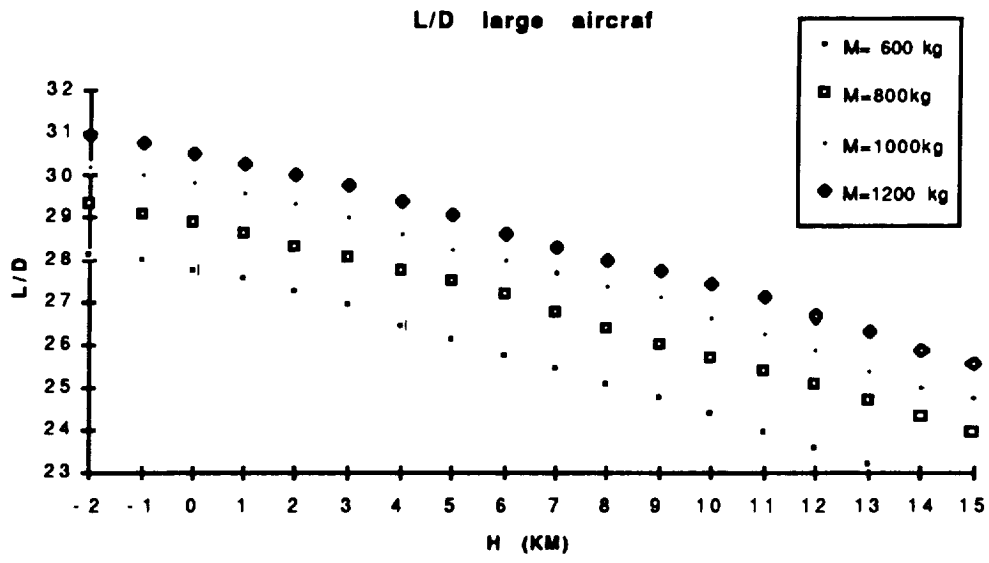
Large aircraft Mach number
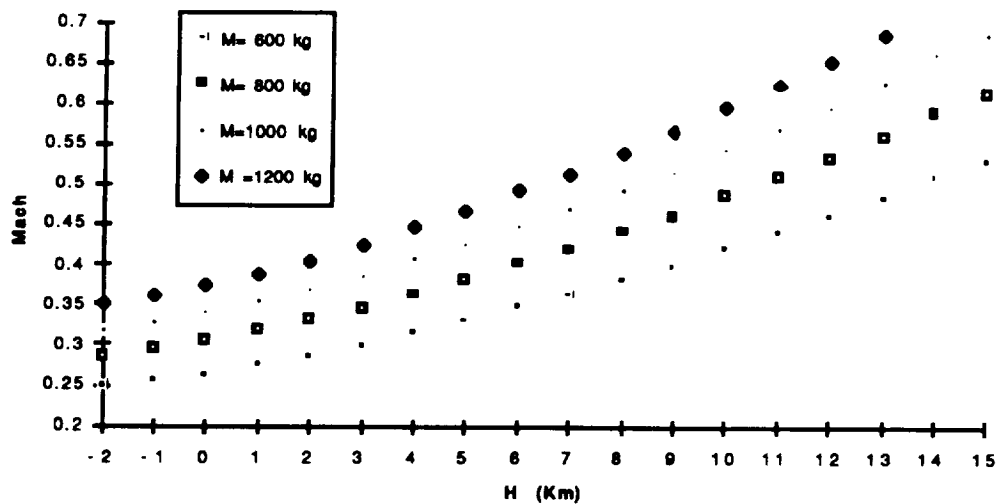
Mach number small aircraft

F-6

POWER LARGE AIRCRAFT (W)

Legend:
- M= 600 kg
- M =800 kg
- M=1000 kg
- M=1200 kg

Y-axis: Power required (W) — 5000, 10000, 15000, 20000, 25000, 30000

X-axis: H (KM) — -2 -1 0 1 2 3 4 5 6 7 8 9 10 11 12 13 14 15

Power small aircraf

Legend:
- M= 450 kg
- M= 400 kg
- M= 350 kg

Y-axis: Power (W) — 4000, 5000, 6000, 7000, 8000, 9000, 10000, 11000, 12000, 13000, 14000

X-axis: H (KM) — -2 -1 0 1 2 3 4 5 6 7 8 9 10 11 12 13 14 15
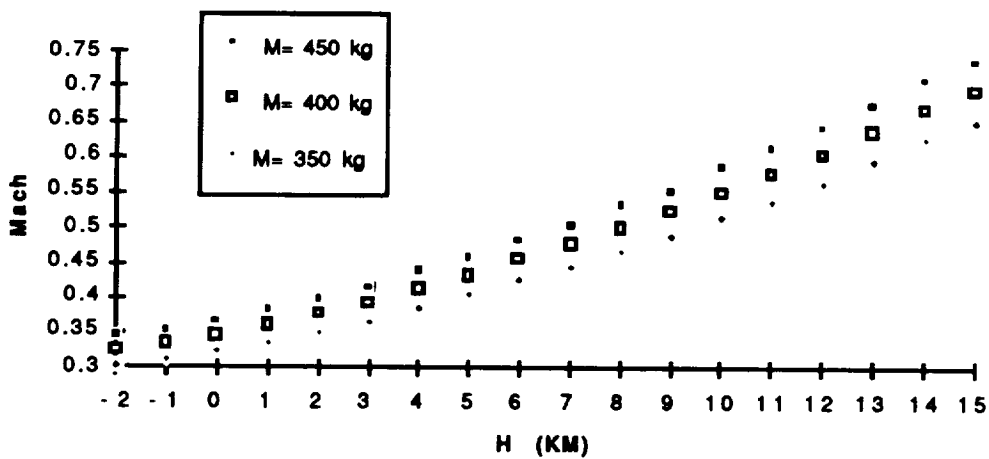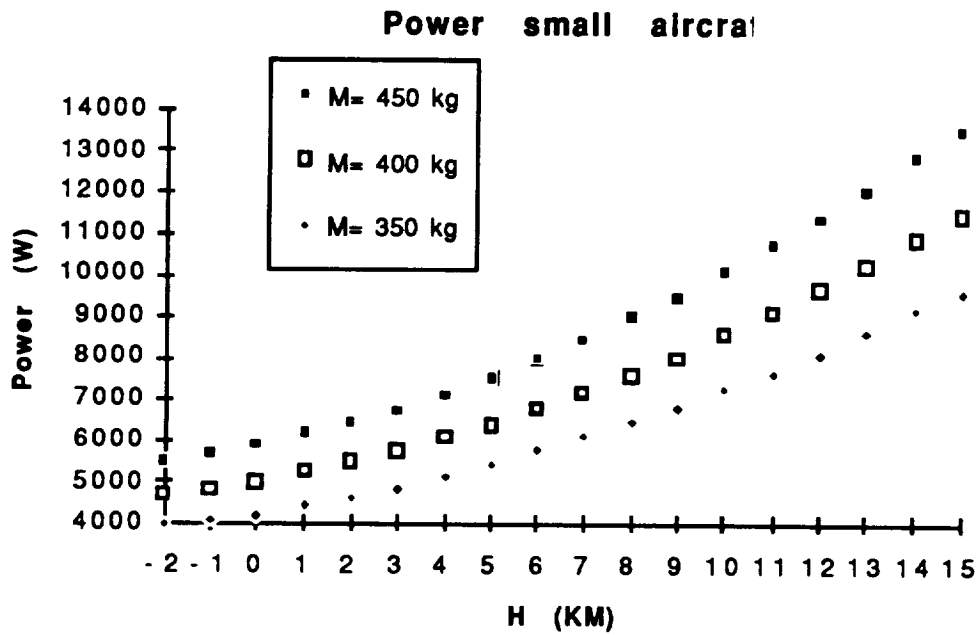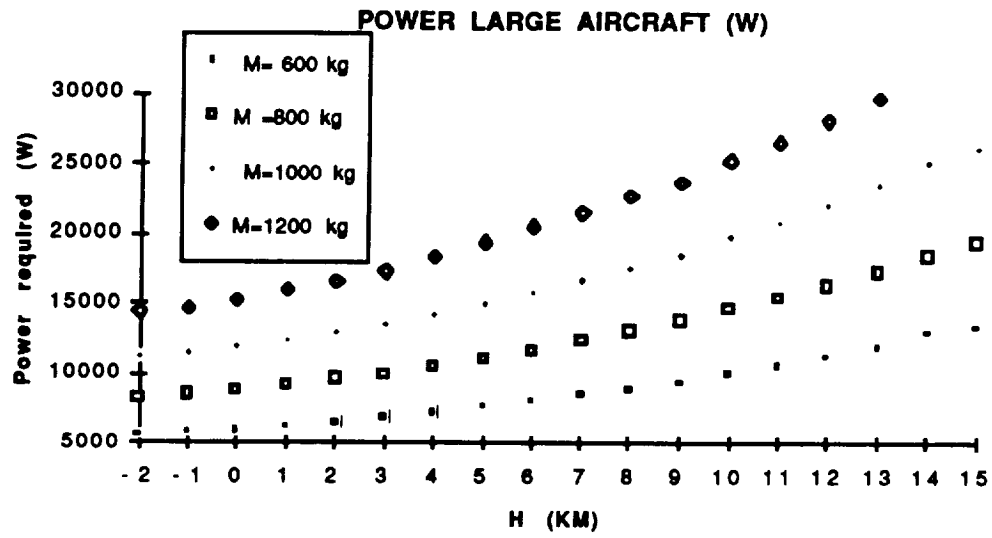
Rate of climb small aircra
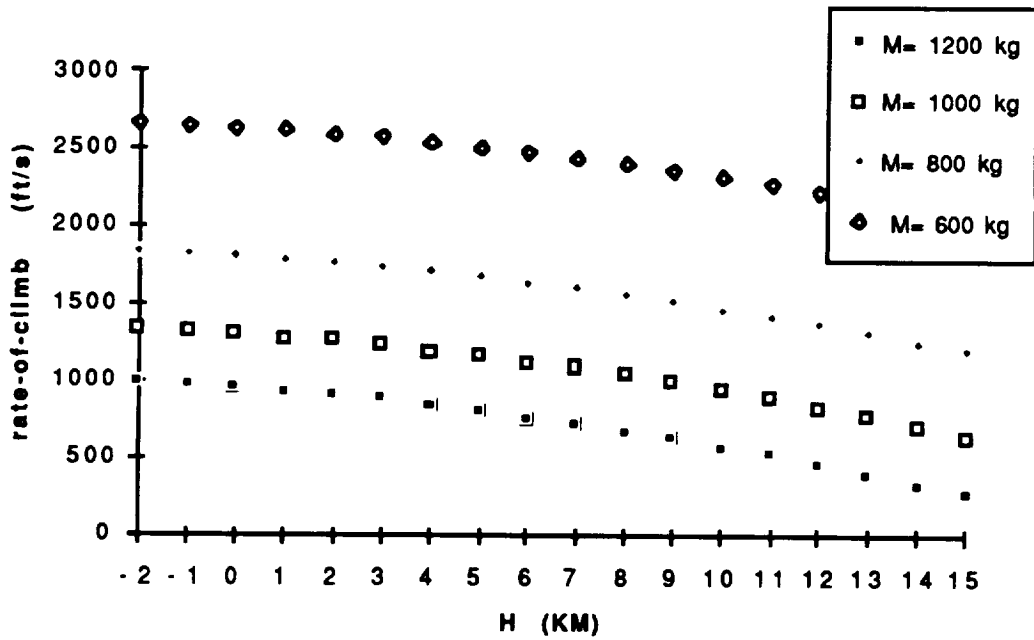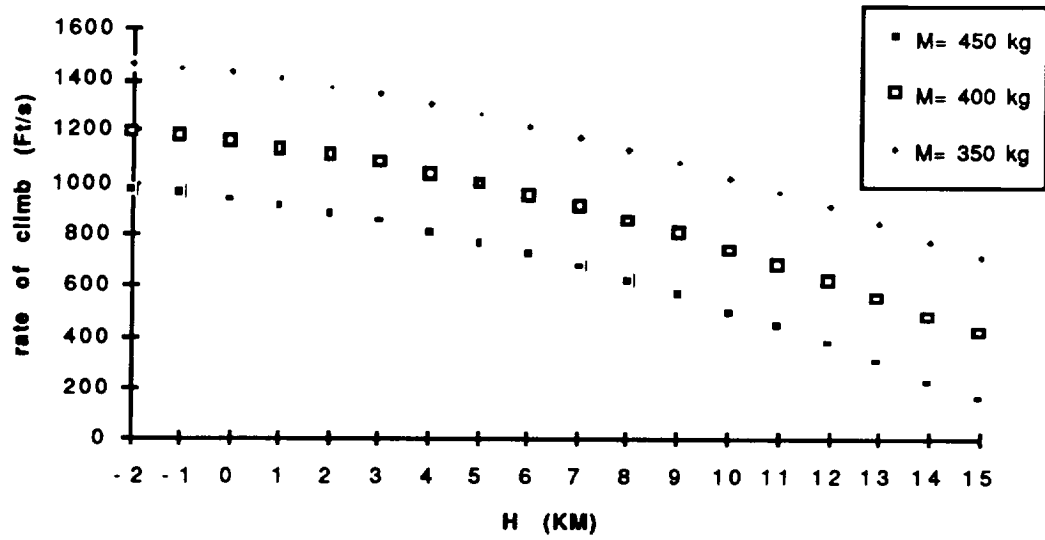
Large aircraft reynolds numbe

Legend:
- M= 1200 kg
- M= 1000 kg
- M = 800 kg
- M= 600 kg

Small aircraft Reynolds numb

Legend:
- M= 450 kg
- M= 400 kg
- M= 350 kg
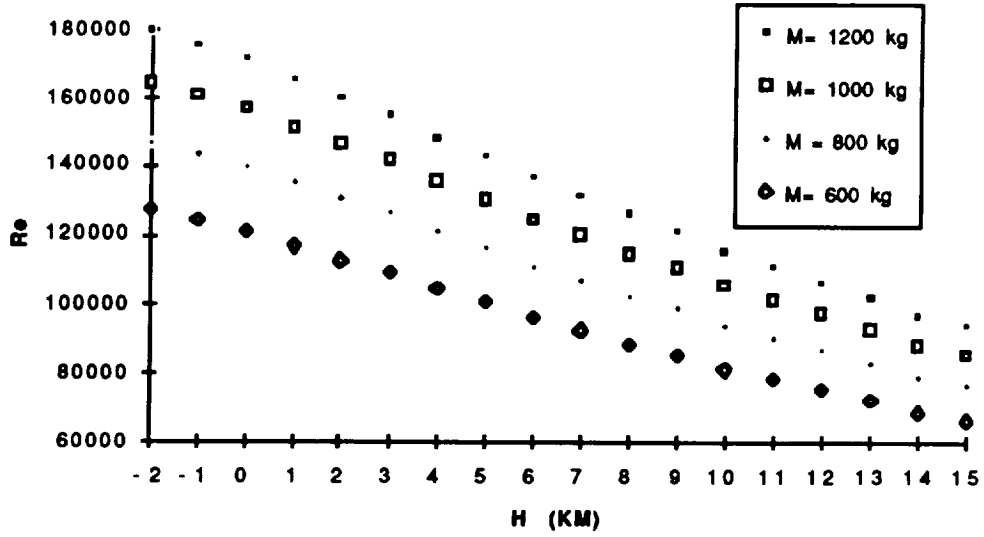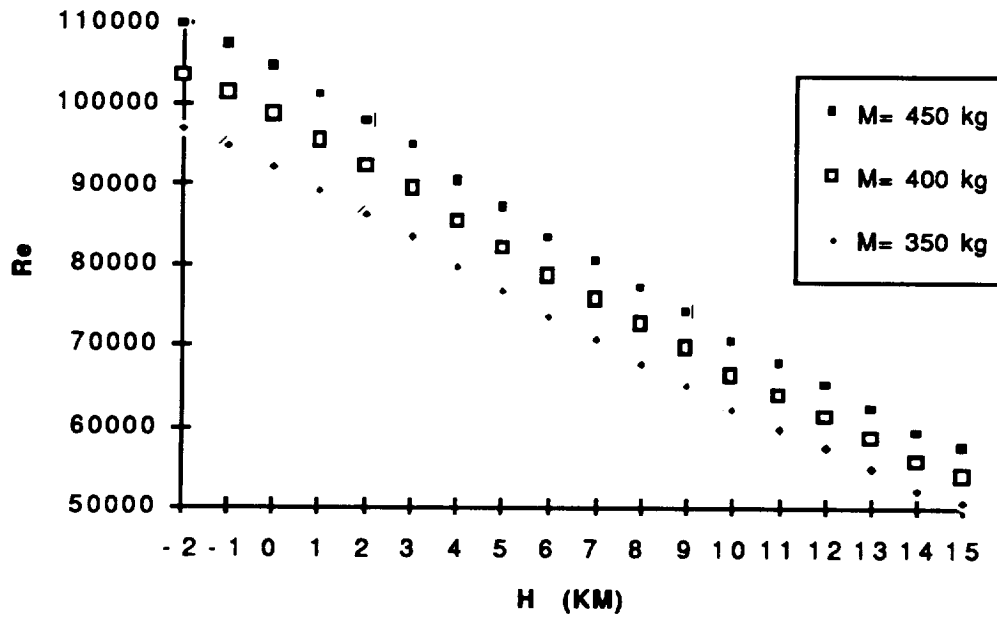
Speed large aircraf
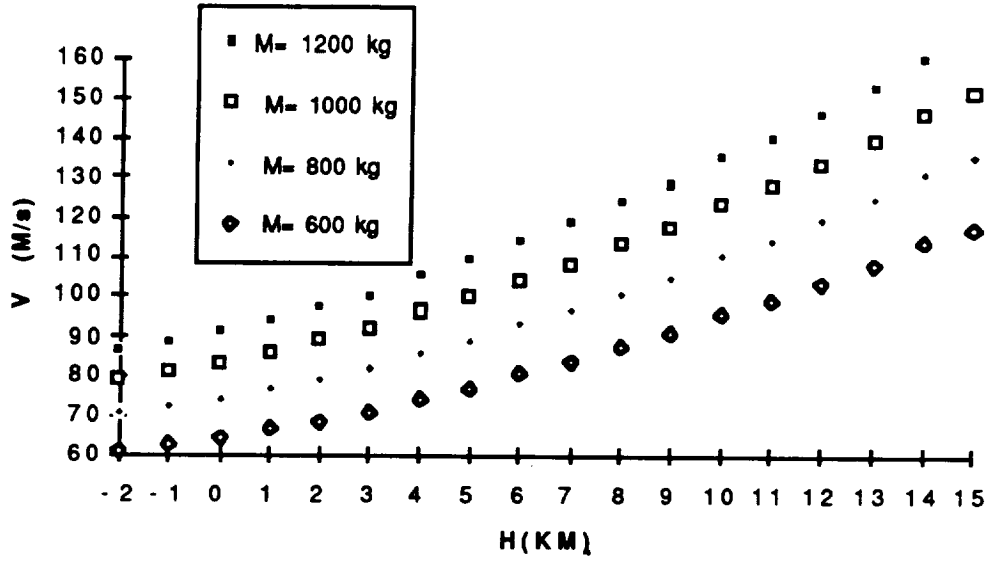
Speed small aircraf

F-10
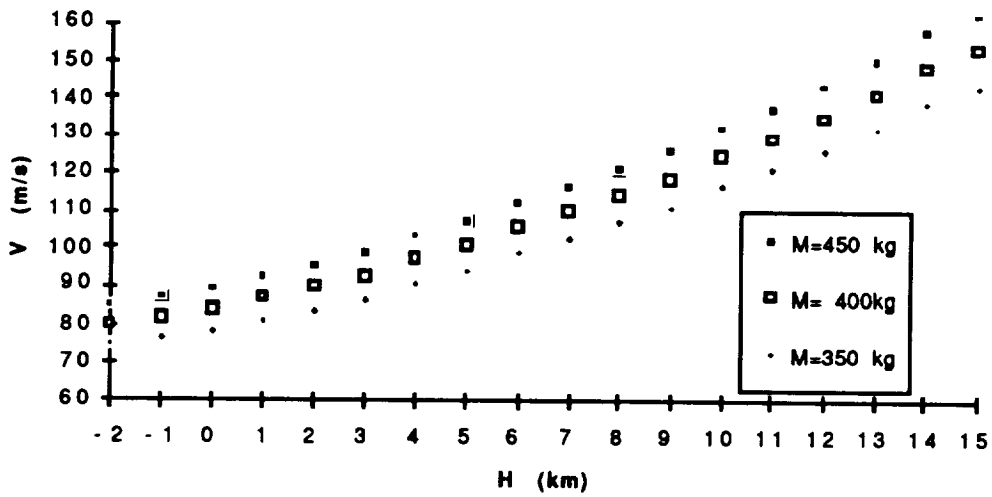
Appendix G
NASTRAN Analysis for Heavy and Light Chassis Design

Light Chassis NASTRAN Analysis

Since the light chassis, had a front and a back portion, both of which are symmetric about two axes, the chassis' loading can be analyzed by evaluating a finite element model of one half of each structure cut along an axis of symmetry. For example, a cut along the x axis in Figure E.1 would give the user information about deformations along the y axis. The axes of symmetry in Figure E.1 below are the x axis and the axes parallel to the y axis at y = .7 cm and y = 3.1 m for the front and back portions of the chassis, respectively.
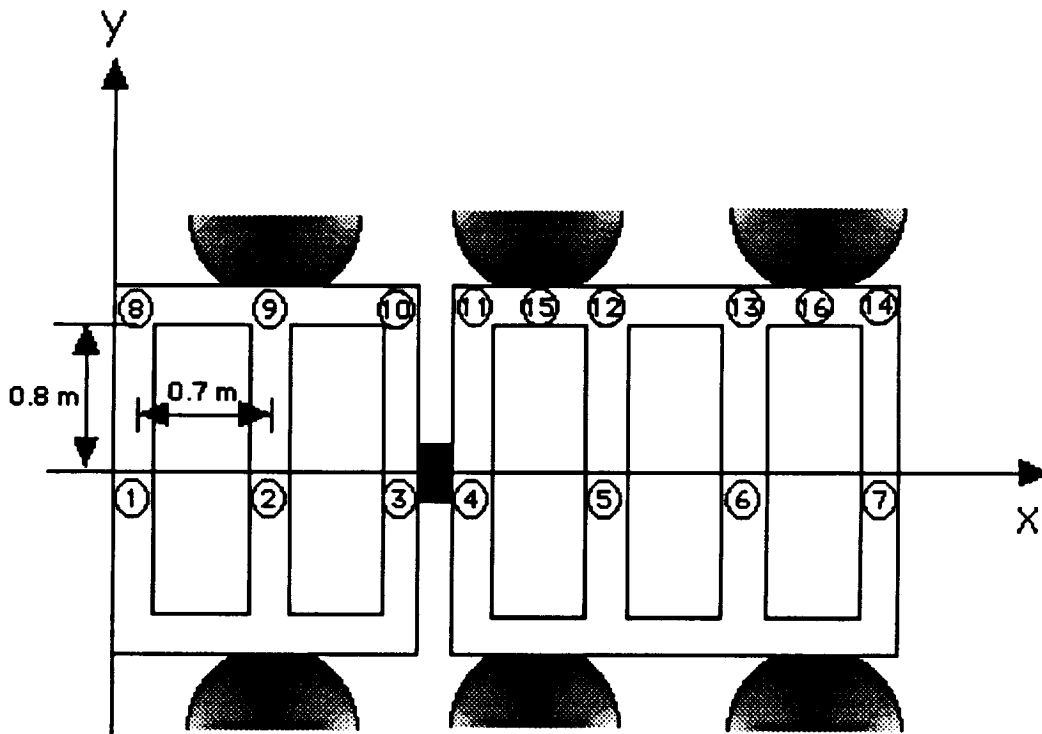
Figure E.1. Light Rover Chassis with NASTRAN Grid Points Labeled

The input decks for the analysis of these axes were entitled par.dat (indicating a lengthwise, i.e.. parallel cut along the axis). Input decks for the analysis of half of the structure divided along an axis parallel to the y axis were entitled perp.dat. The results will be symmetric since the loading is symmetric as well as the structure.
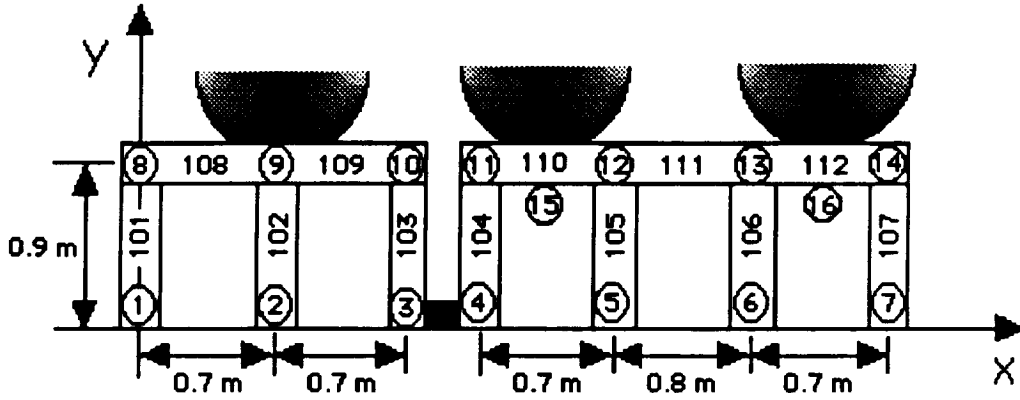
Figure E.2. Parallel FE Model of Light Chassis Loading from Suspension
System at Nodes 9, 15, and 16
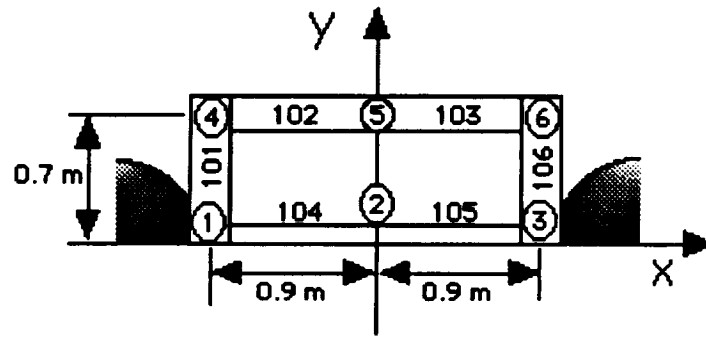
Figure E.3. Perpendicular FE Model of Front Section of Light Chassis with
Loading from Suspension System at Nodes 1 and 3
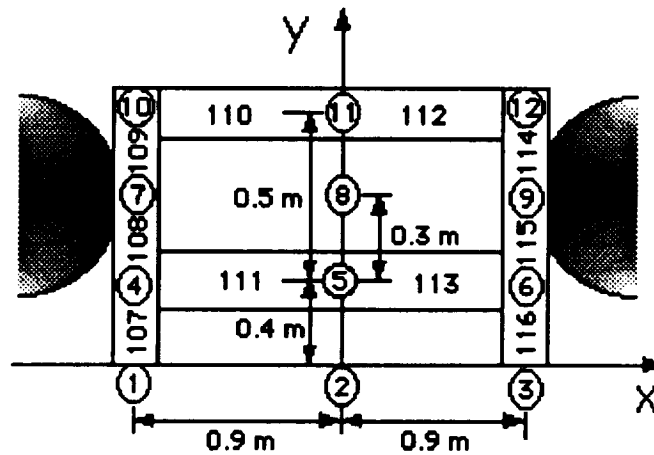
Figure E.4. Perpendicular FE Model of Back Section of Light Chassis with
Loading from Suspension System at Nodes 7 and 9

The following NASTRAN input decks were used for analyzing the stresses in the light chassis. Figures E.2 - E.4 indicate the finite element models used to analyze the four different cuts of the light chassis. Figure E.5 is the finite element model used to analyze the heavy chassis.
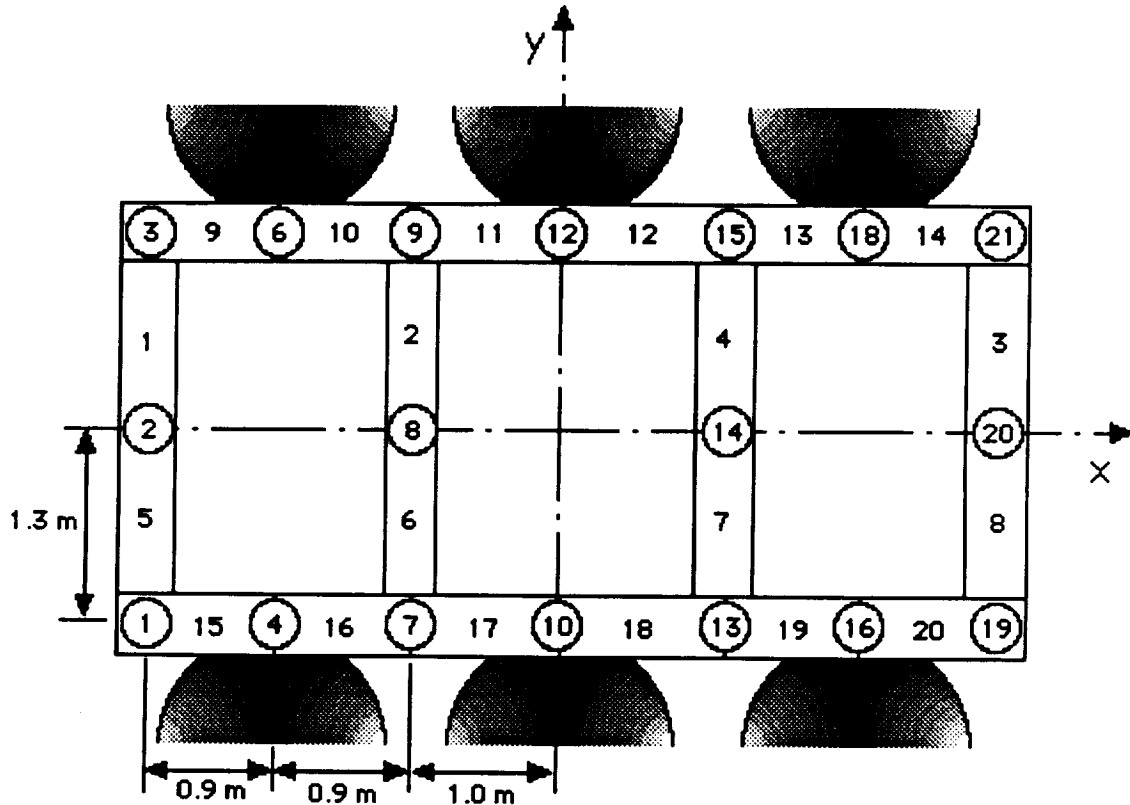
Figure E.5. Finite Element Model of Heavy Chassis with Loadings from Suspension System at Nodes 4, 6, 16, and 18

Three different configurations were analyzed. First the model was bisected along the x axis (a parallel cut) to determine deflections along the y axis. The second and third NASTRAN runs were performed for the front and back halves of the heavy chassis cut along the y axis to determine the deflections in the z direction along the x axis. Even though the chassis is symmetric, it was necessary to analyze the front and the back deflections due to the large load of the radiator at the rear of the chassis. The node points that are located at the axes that are cut are fixed in all degrees of freedom to assure symmetry. All of the elements are subjected to a distributed load corresponding to the fully loaded capacity of the heaviest rover for each chassis type. Point loads were

added at the locations of the suspension system in order to support the structure in the z direction.

Input deck for the small section of light chassis:

```
For parallel cut:
ID MSC, MTI01
SOL 24
APP DISP
CEND
TITLE=Static analysis of MARGE load to chassis
SUBTITLE=FTS
ECHO=SORT
DISPLACEMENT=ALL
ELFORCE=ALL
ELSTRESS=ALL
ESE=ALL
LOAD=500
OLOAD=ALL
BEGIN BULK
$
$
$ ************************************************************
$            Loading from Suspension System
$ ************************************************************
$
FORCE   500     9               4019.0 0.    0.    1.
$
$ ************************************************************
$            Distributed Load from MARGE
$ ************************************************************
$
PLOAD1  500     101     FZ      FR      0.0    -5.002+3    1.0    -5.002+$
$
$ ************************************************************
$            Material Properties for Everything
$ ************************************************************
$
$       Material properties for titanium
$MAT1   31      120.+9 44.+9            4500.0
$
$       Material properties for aluminum
MAT1    31      72.+9  27.+9            2800.0
$
$ ************************************************************
$
$                Chassis Structure
$
$ ************************************************************
$
$ Chassis Grid Points
$
$ *****************
$                     X      Y      Z
GRID    1            0.0    0.0    0.0        123456
GRID    2            0.7    0.0    0.0        123456
GRID    3            1.4    0.0    0.0        123456
GRID    8            0.0    0.9    0.0
GRID    9            0.7    0.9    0.0
GRID    10           1.4    0.9    0.0
$
$
```

```
$  ****************************************************************
$
$ Define Beam Elements
$
$  *****************
$
CBAR   101   21   1    8    0.0   0.0   1.0
CBAR   102   21   2    9    0.0   0.0   1.0
CBAR   103   21   3    10   0.0   0.0   1.0
CBAR   108   21   8    9    0.0   0.0   1.0
CBAR   109   21   9    10   0.0   0.0   1.0
$
$  ****************************************************************
$
$ Define Beam Properties
$
$  *****************
$
$ PBAR stuff
$PBAR   pid   mid   A    I1   I2    J     NSM   ____
$      C1    C2
$
$PBAR   21    31      0.00485 2.759-5 2.473-5 5.2324-5
$      0.1   0.0
$PBAR   21    31      0.0594 5.071-5 4.587-5 9.6581-5
$      0.1   0.0
$PBAR   21    31      0.01365 6.987-5 6.378-5 1.3365-4
$      0.1   0.0
PBAR    21    31      0.0176 8.555-5 7.883-5 1.6437-4
        0.1   0.0
$
$
$  ****************************************************************
$
$ Constrain DOF's Accordingly
$
$  *****************
$
PARAM  AUTOSPC YES
$
$MPCADD 101   1     2     4     5     6     8     9
$      10    30    40    50    60
$MPC    1     1040  1     1.0   2010  1     -1.0
$MPC    1     1040  2     1.0   2010  2     -1.0
$MPC    1     1040  3     1.0   2010  3     -1.0
$MPC    1     1040  4     1.0   2010  4     -1.0
$MPC    1     1040  5     1.0   2010  5     -1.0
$MPC    1     1040  6     1.0   2010  6     -1.0
$
$MPC    2     1030  1     1.0   2020  1     -1.0
$MPC    2     1030  2     1.0   2020  2     -1.0
$MPC    2     1030  3     1.0   2020  3     -1.0
$MPC    2     1030  4     1.0   2020  4     -1.0
$MPC    2     1030  5     1.0   2020  5     -1.0
$

ENDDATA


For perpendicular cut:
ID MARGE, Perpendicular front
SOL 24
APP DISP
TIME 40
```

```
CEND
TITLE=Static analysis of MARGE load to chassis
SUBTITLE=FTS
ECHO=SORT
DISPLACEMENT=ALL
ELFORCE=ALL
ELSTRESS=ALL
ESE=ALL
LOAD=500
OLOAD=ALL
BEGIN BULK
$
$
$ ********************************************************************
$           Loading from Suspension System
$ ********************************************************************
$
FORCE   500    1             4019.0 0.    0.    1.
FORCE   500    3             4019.0 0.    0.    1.
$
$ ********************************************************************
$           Loading from Radiator
$ ********************************************************************
$
FORCE   500    5             -1118.34 0.   0.    1.
$
$ ********************************************************************
$           Distributed Load from MARGE
$ ********************************************************************
$
PLOAD1 500    101    FZ     FR     0.0    -5.002+3     1.0     -5.002+$
$
$ ********************************************************************
$           Material Properties for Everything
$ ********************************************************************
$
$     Material properties for titanium
$MAT1   31      120.+9  44.+9           4500.0
$
$     Material properties for aluminum
MAT1    31      72.+9   27.+9           2800.0
$
$
$ ********************************************************************
$
$           Chassis Structure
$
$ ********************************************************************
$
$ Chassis Grid Points
$
$ ******************
$                   X      Y      Z
GRID   1             -.9    0.0    0.0      123456
GRID   2             0.0    0.0    0.0      123456
GRID   3             0.9    0.0    0.0      123456
GRID   4             -.9    0.7    0.0
GRID   5             0.0    0.7    0.0
GRID   6             0.9    0.7    0.0
$
$
$ ********************************************************************
$
$ Define Beam Elements
```

```
$
$ ****************
$
CBAR     101     21      1       4       0.0     0.0     1.0
CBAR     102     21      4       5       0.0     0.0     1.0
CBAR     103     21      5       6       0.0     0.0     1.0
CBAR     104     21      1       2       0.0     0.0     1.0
CBAR     105     21      2       3       0.0     0.0     1.0
CBAR     106     21      3       6       0.0     0.0     1.0
$
$ ***************************************************************
$
$ Define Beam Properties
$
$ *****************
$
PBAR     21      31      0.00485 2.759-5 2.473-5 0.      5.2324-5
         0.1     0.0
$PBAR    21      31      0.0594  5.071-5 4.587-5 0.      9.6581-5
$        0.1     0.0
$PBAR    21      31      0.01365 6.987-5 6.378-5 0.      1.3365-4
$        0.1     0.0
$PBAR    21      31      0.0176  8.555-5 7.883-5 0.      1.6437-4
$        0.1     0.0
$
$
$ ***************************************************************
$
$ Constrain DOF's Accordingly
$
$ *****************
$
PARAM   AUTOSPC YES
$
$MPCADD 101     1       2       4       5       6       8       9
$       10      30      40      50      60
$MPC    1       1040    1       1.0     2010    1       -1.0
$MPC    1       1040    2       1.0     2010    2       -1.0
$MPC    1       1040    3       1.0     2010    3       -1.0
$MPC    1       1040    4       1.0     2010    4       -1.0
$MPC    1       1040    5       1.0     2010    5       -1.0
$MPC    1       1040    6       1.0     2010    6       -1.0
$
$MPC    2       1030    1       1.0     2020    1       -1.0
$MPC    2       1030    2       1.0     2020    2       -1.0
$MPC    2       1030    3       1.0     2020    3       -1.0
$MPC    2       1030    4       1.0     2020    4       -1.0
$MPC    2       1030    5       1.0     2020    5       -1.0
$

ENDDATA
```

For larger section of light chassis:

For parallel cuts:
```
ID MSC, MT101
SOL 24
APP DISP
CEND
TITLE=Static analysis of MARGE load to chassis
SUBTITLE=FTS
ECHO=SORT
DISPLACEMENT=ALL
```

```
ELFORCE=ALL
STRESS=ALL
ESE=ALL
LOAD=500
OLOAD=ALL
BEGIN BULK
$
$
$  ***********************************************************
$            Loading from Suspension System
$  ***********************************************************
$
FORCE   500    15              4019.0 0.    0.    1.
FORCE   500    16              4019.0 0.    0.    1.
$
$  ***********************************************************
$            Distributed Load from MARGE
$  ***********************************************************
$
PLOAD1  500    104    FZ     FR     0.0     -5.002+3     1.0     -5.002+$
$
$  ***********************************************************
$            Material Properties for Everything
$  ***********************************************************
$
$      Material properties for titanium
$MAT1   31     120.+9 44.+9           4500.0
$
$      Material properties for aluminum
MAT1    31     72.+9  27.+9           2800.0
$
$
$  ***********************************************************
$
$
$                 Chassis Structure
$
$
$  ***********************************************************
$
$ Chassis Grid Points
$
$ ****************
$                   X     Y     Z
GRID    4          1.8   0.0   0.0       123456
GRID    5          2.5   0.0   0.0       123456
GRID    6          3.3   0.0   0.0       123456
GRID    7          4.0   0.0   0.0       123456
GRID    11         1.8   0.9   0.0
GRID    12         2.5   0.9   0.0
GRID    13         3.3   0.9   0.0
GRID    14         4.0   0.9   0.0
GRID    15         2.2   0.9   0.0
GRID    16         3.6   0.9   0.0
$
$
$  ***********************************************************
$
$ Define Beam Elements
$
$ ****************
$
CBAR    104    21    4     11    0.0   0.0   1.0
CBAR    105    21    5     12    0.0   0.0   1.0
CBAR    106    21    6     13    0.0   0.0   1.0
CBAR    107    21    7     14    0.0   0.0   1.0
```

```
CBAR   110   21    11    15    0.0    0.0    1.0
CBAR   111   21    15    16    0.0    0.0    1.0
CBAR   112   21    16    14    0.0    0.0    1.0
$
$  *************************************************************
$
$ Define Beam Properties
$
$  ******************
$
PBAR   21    31       0.00485 2.759-5 2.473-5 0.    5.2324-5
       0.1   0.0
$PBAR  21    31       0.0594  5.071-5 4.587-5 0.    9.6581-5
$PBAR  21    31       0.01365 6.987-5 6.378-5 0.    1.3365-4
$PBAR  21    31       0.0176  8.555-5 7.883-5 0.    1.6437-4
$
$
$  *************************************************************
$
$ Constrain DOF's Accordingly
$
$  ******************
$
PARAM  AUTOSPC YES
$
$MPCADD 101   1     2     4     5     6     8     9
$      10    30    40    50    60
$MPC   1     1040  1     1.0   2010  1     -1.0
$MPC   1     1040  2     1.0   2010  2     -1.0
$MPC   1     1040  3     1.0   2010  3     -1.0
$MPC   1     1040  4     1.0   2010  4     -1.0
$MPC   1     1040  5     1.0   2010  5     -1.0
$MPC   1     1040  6     1.0   2010  6     -1.0
$
$MPC   2     1030  1     1.0   2020  1     -1.0
$MPC   2     1030  2     1.0   2020  2     -1.0
$MPC   2     1030  3     1.0   2020  3     -1.0
$MPC   2     1030  4     1.0   2020  4     -1.0
$MPC   2     1030  5     1.0   2020  5     -1.0
$

ENDDATA


For perpendicular cuts:
ID, Perpendicular back
SOL 24
APP DISP
TIME 40
CEND
TITLE=Static analysis of MARGE load to chassis
SUBTITLE=FTS
ECHO=SORT
DISPLACEMENT=ALL
ELFORCE=ALL
ELSTRESS=ALL
ESE=ALL
LOAD=500
OLOAD=ALL
BEGIN BULK
$
$
$  *************************************************************
$           Loading from Suspension System
```

```
$  ************************************************************
$
FORCE  500   9              4019.0  0.    0.    1.
FORCE  500   7              4019.0  0.    0.    1.
$
$  ************************************************************
$            Distributed Load from MARGE
$  ************************************************************
$
PLOAD1 500   107   FZ   FR    0.0    -5.002+3    1.0    -5.002+$
$
$  ************************************************************
$            Material Properties for Everything
$  ************************************************************
$
$       Material properties for titanium
MAT1   31    120.+9 44.+9        4500.0
$
$       Material properties for aluminum
$MAT1   31    72.+9  27.+9        2800.0
$
$
$  ************************************************************
$
$                  Chassis Structure
$
$  ************************************************************
$
$ Chassis Grid Points
$
$  *****************
$                    X     Y     Z
GRID   1            -.9    0.0    0.0      123456
$GRID  2             0.0    0.0    0.0
GRID   3             0.9    0.0    0.0      123456
GRID   4            -.9    0.4    0.0
GRID   5             0.0    0.4    0.0
GRID   6             0.9    0.4    0.0
GRID   7            -.9    0.7    0.0
$GRID  8             0.0    0.7    0.0
GRID   9             0.9    0.7    0.0
GRID   10           -.9    0.9    0.0
GRID   11            0.0    0.9    0.0
GRID   12            0.9    0.9    0.0
$
$
$  ************************************************************
$
$ Define Beam Elements
$
$  *****************
$
CBAR   107   21   1    4    0.0    0.0    1.0
CBAR   108   21   4    7    0.0    0.0    1.0
CBAR   109   21   7    10   0.0    0.0    1.0
CBAR   110   21   10   11   0.0    0.0    1.0
CBAR   111   21   4    5    0.0    0.0    1.0
CBAR   112   21   11   12   0.0    0.0    1.0
CBAR   113   21   5    6    0.0    0.0    1.0
CBAR   114   21   9    12   0.0    0.0    1.0
CBAR   115   21   6    9    0.0    0.0    1.0
CBAR   116   21   3    6    0.0    0.0    1.0
$
$  ************************************************************
```

G-10

```
$
$ Define Beam Properties
$
$ *****************
$
PBAR    21      31      0.00485 2.759-5 2.473-5 0.      5.2324-5
        0.1     0.0
$PBAR   21      31      0.0594  5.071-5 4.587-5 0.      9.6581-5
$PBAR   21      31      0.01365 6.987-5 6.378-5 0.      1.3365-4
$PBAR   21      31      0.0176  8.555-5 7.883-5 0.      1.6437-4
$
$
$ ****************************************************************
$
$ Constrain DOF's Accordingly
$
$ ******************
$
PARAM   AUTOSPC YES
$
$MPCADD 101     1       2       4       5       6       8       9
$       10      30      40      50      60
$MPC    1       1040    1       1.0     2010    1       -1.0
$MPC    1       1040    2       1.0     2010    2       -1.0
$MPC    1       1040    3       1.0     2010    3       -1.0
$MPC    1       1040    4       1.0     2010    4       -1.0
$MPC    1       1040    5       1.0     2010    5       -1.0
$MPC    1       1040    6       1.0     2010    6       -1.0
$
$MPC    2       1030    1       1.0     2020    1       -1.0
$MPC    2       1030    2       1.0     2020    2       -1.0
$MPC    2       1030    3       1.0     2020    3       -1.0
$MPC    2       1030    4       1.0     2020    4       -1.0
$MPC    2       1030    5       1.0     2020    5       -1.0
$

ENDDATA


For perpendicular cuts with radiator:
ID, Perpendicular back
SOL 24
APP DISP
TIME 40
CEND
TITLE=Static analysis of MARGE load to chassis
SUBTITLE=FTS
ECHO=SORT
DISPLACEMENT=ALL
ELFORCE=ALL
ELSTRESS=ALL
ESE=ALL
LOAD=500
OLOAD=ALL
BEGIN BULK
$
$
$ ****************************************************************
$           Loading from Suspension System
$ ****************************************************************
$
FORCE   500     9               4019.0  0.      0.      1.
FORCE   500     7               4019.0  0.      0.      1.
$
```

```
$ ************************************************************
$               Loading from Radiator
$ ************************************************************
$
FORCE   500   11           -1118.34 0.    0.    1.
$
$ ************************************************************
$            Distributed Load from MARGE
$ ************************************************************
$
$
$
$ ************************************************************
$            Material Properties for Everything
$ ************************************************************
$
$       Material properties for titanium
$MAT1   31     120.+9 44.+9          4500.0
$
$       Material properties for aluminum
MAT1    31     72.+9  27.+9          2800.0
$
$
$ ************************************************************
$
$                  Chassis Structure
$
$ ************************************************************
$
$ Chassis Grid Points
$
$ *****************
$                    X     Y     Z
GRID    1           -.9    0.0   0.0      123456
$GRID   2            0.0   0.0   0.0
GRID    3            0.9   0.0   0.0      123456
GRID    4           -.9    0.4   0.0
GRID    5            0.0   0.4   0.0
GRID    6            0.9   0.4   0.0
GRID    7           -.9    0.7   0.0
$GRID   8            0.0   0.7   0.0
GRID    9            0.9   0.7   0.0
GRID    10          -.9    0.9   0.0
GRID    11           0.0   0.9   0.0
GRID    12           0.9   0.9   0.0
$
$
$ ************************************************************
$
$ Define Beam Elements
$
$ *****************
$
CBAR    107   21   1     4     0.0   0.0   1.0
CBAR    108   21   4     7     0.0   0.0   1.0
CBAR    109   21   7     10    0.0   0.0   1.0
CBAR    110   21   10    11    0.0   0.0   1.0
CBAR    111   21   4     5     0.0   0.0   1.0
CBAR    112   21   11    12    0.0   0.0   1.0
CBAR    113   21   5     6     0.0   0.0   1.0
CBAR    114   21   9     12    0.0   0.0   1.0
CBAR    115   21   6     9     0.0   0.0   1.0
CBAR    116   21   3     6     0.0   0.0   1.0
$
```

```
$ *******************************************************************
$
$ Define Beam Properties
$
$ ******************
$
PBAR    21      31      0.00485 2.759-5 2.473-5 0.      5.2324-5
        0.1     0.0
$PBAR   21      31      0.0594  5.071-5 4.587-5 0.      9.6581-5
$PBAR   21      31      0.01365 6.987-5 6.378-5 0.      1.3365-4
$PBAR   21      31      0.0176  8.555-5 7.883-5 0.      1.6437-4
$
$
$ *******************************************************************
$
$ Constrain DOF's Accordingly
$
$ ******************
$
PARAM   AUTOSPC YES
$
$MPCADD 101     1       2       4       5       6       8       9
$       10      30      40      50      60
$MPC    1       1040    1       1.0     2010    1       -1.0
$MPC    1       1040    2       1.0     2010    2       -1.0
$MPC    1       1040    3       1.0     2010    3       -1.0
$MPC    1       1040    4       1.0     2010    4       -1.0
$MPC    1       1040    5       1.0     2010    5       -1.0
$MPC    1       1040    6       1.0     2010    6       -1.0
$
$MPC    2       1030    1       1.0     2020    1       -1.0
$MPC    2       1030    2       1.0     2020    2       -1.0
$MPC    2       1030    3       1.0     2020    3       -1.0
$MPC    2       1030    4       1.0     2020    4       -1.0
$MPC    2       1030    5       1.0     2020    5       -1.0
$

ENDDATA
```

Results:

Front Chassis Data
Aluminum
Parallel analysis

Skin Thickness (m)	Max Displacement (m)	Max Bending Moment (N-m)	Max Stress (Pa)
0.005	-6.10E-04	-3.13E+03	6.08E+06
0.01	-2.15E-04	-3.12E+03	6.16E+06
0.015	-1.56E-04	-3.12E+03	4.47E+06
0.02	-1.27E-04	-3.12E+03	3.65E+06

Front perpendicular analysis

Skin Thickness (m)	Max Displacement (m)	Max Bending Moment (N-m)	Max Stress (Pa)
0.005	-6.94E-04	-5.64E+03	2.05E+07
0.01	-3.78E-04	-5.64E+03	1.11E+07
0.015	-2.74E-04	-5.64E+03	8.08E+06
0.02	-2.24E-04	-5.64E+03	6.60E+06

Titanium
Parallel Analysis

Skin Thickness (m)	Max Displacement (m)	Max Bending Moment (N-m)	Max Stress (Pa)
0.005	-2.38E-04	-3.14E+03	1.14E+07
0.01	-1.30E-04	-3.13E+03	6.18E+06
0.015	-9.39E-05	-3.13E+00	4.48E+06
0.02	-7.67E-05	-3.13E+03	3.66E+06

Perpendicular Analysis

Skin Thickness (m)	Max Displacement (m)	Max Bending Moment (N-m)	Max Stress (Pa)
0.005	-4.17E-04	-5.64E+03	2.05E+07
0.01	-2.27E-04	-5.64E+03	1.11E+07
0.015	-1.65E-04	-5.64E+03	8.08E+06
0.02	-1.34E-04	-5.64E+03	6.60E+06

Back Chassis Data
Aluminum
Parallel Analysis

Skin Thickness (m)	Max Displacement (m)	Max Bending Moment (N-m)	Max Stress (Pa)
0.005	-7.32E-04	-5.39E+03	1.95E+07
0.01	-3.98E-04	-5.39E+03	1.06E+07
0.015	-2.89E-04	-5.39E+03	7.71E+06
0.02	-2.36E-04	-5.39E+03	6.30E+06

Perpendicular Analysis

Skin Thickness (m)	Max Displacement (m)	Max Bending Moment (N-m)	Max Stress (Pa)
0.005	-1.38E-03	-1.24E+04	4.51E+07
0.01	-7.53E-04	-1.24E+04	2.45E+07
0.015	-5.47E-04	-1.24E+04	1.78E+07
0.02	-4.47E-04	-1.24E+04	1.45E+07

Back Chassis w/ Radiator Data

Skin Thickness (m)	Max Displacement (m)	Max Bending Moment (N-m)	Max Stress (Pa)
0.005	-1.45E-03	-1.29E+04	4.69E+07
0.01	-7.91E-04	-1.29E+04	2.55E+07
0.015	-5.74E-04	-1.29E+04	1.85E+07
0.02	-4.69E-04	-1.29E+04	1.51E+07

Titanium
Parallel Analysis

Skin Thickness (m)	Max Displacement (m)	Max Bending Moment (N-m)	Max Stress (Pa)
0.005	-4.39E-04	-5.39E+03	1.95E+07
0.01	-2.39E-04	-5.39E+03	1.06E+07
0.015	-1.73E-04	-5.39E+03	7.71E+06
0.02	-1.42E-04	-5.39E+03	6.30E+06

Perpendicular Analysis

Skin Thickness (m)	Max Displacement (m)	Max Bending Moment (N-m)	Max Stress (Pa)
0.005	-8.31E-04	-1.24E+04	4.51E+07
0.01	-4.52E-04	-1.24E+04	2.45E+07
0.015	-3.28E-04	-1.24E+04	1.78E+07
0.02	-2.68E-04	-1.24E+04	1.45E+07

Perpendicular Analysis with Radiator

Skin Thickness (m)	Max Displacement (m)	Max Bending Moment (N-m)	Max Stress (Pa)
0.005	-8.72E-04	-1.29E+04	4.69E+07
0.01	-4.74E-04	-1.29E+04	2.55E+07
0.015	-3.44E-04	-1.29E+04	1.85E+07
0.02	-2.81E-04	-1.29E+04	1.51E+07

Heavy Chassis NASTRAN Analysis

For all parallel cuts:

ID MSC, MTI01

SOL 24

APP DISP

CEND

TITLE=Static analysis of Homer load to chassis

SUBTITLE=FTS

```
ECHO=SORT

DISPLACEMENT=ALL

ELFORCE=ALL

ELSTRESS=ALL

ESE=ALL

LOAD=500

OLOAD=ALL

BEGIN BULK

$

$

$  ****************************************************************

$          Loading from Suspension System

$  ****************************************************************

$

FORCE   500    6              13.91+3 0.     0.    1.

FORCE   500    18             13.91+3 0.     0.    1.

$

$  ****************************************************************

$          Distributed Load from HOMER

$  ****************************************************************

$

PLOAD1  500    101    FZ     FR     0.0     -6688.7      1.0    -6688.7

PLOAD1  500    102    FZ     FR     0.0     -6688.7      1.0    -6688.7

$

$

$  ****************************************************************

$          Material Properties for Everything

$  ****************************************************************

$

$

$  ****************************************************************

$

$              Chassis Structure

$

$  ****************************************************************

$
```

$ Chassis Grid Points

$

$ ******************

$ X   Y   Z

GRID   2   -2.8 0.0 0.0   123456

GRID   3   -2.8 -1.3 0.0

$GRID   5   -1.9 0.0 0.0

GRID   6   -1.9 1.3 0.0   3

GRID   8   -1.0 0.0 0.0   123456

GRID   9   -1.0 1.3 0.0

$GRID   11   0.0 0.0 0.0

GRID   12   0.0 1.3 0.0

GRID   14   1.0 0.0 0.0   123456

GRID   15   1.0 1.3 0.0

$GRID   17   1.9 0.0 0.0

GRID   18   1.9 1.9 0.0   3

GRID   20   2.8 0.0 0.0   123456

GRID   21   2.8 1.3 0.0

$

$

$ **

$

$ Define Beam Elements

$

$ ******************

$

CBAR   101   21   2   3   0.0   0.0   1.0

CBAR   102   21   8   9   0.0   0.0   1.0

CBAR   103   21   14   15   0.0   0.0   1.0

CBAR   104   21   20   21   0.0   0.0   1.0

CBAR   109   21   3   6   0.0   0.0   1.0

CBAR   110   21   6   9   0.0   0.0   1.0

CBAR   111   21   9   12   0.0   0.0   1.0

CBAR   112   21   12   15   0.0   0.0   1.0

CBAR   113   21   15   18   0.0   0.0   1.0

CBAR   114   21   18   21   0.0   0.0   1.0

G-17

```
$
$ *************************************************************
$
$ Define Beam Properties
$
$ ******************
$
$ *************************************************************
$
$ Constrain DOF's Accordingly
$
$ ******************
$
PARAM  AUTOSPC YES

For all perpendicular cuts:
ID MSC, MTI01
SOL 24
APP DISP
CEND
TITLE=Static analysis of Homer load to chassis
SUBTITLE=FTS
ECHO=SORT
DISPLACEMENT=ALL
ELFORCE=ALL
ELSTRESS=ALL
ESE=ALL
LOAD=500
OLOAD=ALL
BEGIN BULK
$
$
$ *************************************************************
$            Loading from Suspension System
$ *************************************************************
$
```

```
FORCE   500   4              13.91+3 0.    0.    1.
FORCE   500   6              13.91+3 0.    0.    1.
$
$  ***********************************************************
$          Distributed Load from HOMER
$  ***********************************************************
$
$    1              2         3         4              5    101
*LD1    0.0           -6.6887+3   1.0           -6.6887+3
PLOAD1* 500           102         FZ            FR            PLD2
*LD2    0.0           -6.6887+3   1.0           -6.6887+3
PLOAD1* 500           105         FZ            FR            PLD3
*LD3    0.0           -6.6887+3   1.0           -6.6887+3
PLOAD1* 500           106         FZ          • FR            PLD4
*LD4    0.0           -6.6887+3   1.0           -6.6887+3
PLOAD1* 500           109         FZ            FR            PLD5
*LD5    0.0           -6.6887+3   1.0           -6.6887+3
PLOAD1* 500           110         FZ            FR            PLD6
*LD6    0.0           -6.6887+3   1.0           -6.6887+3
PLOAD1* 500           111         FZ            FR            PLD7
*LD7    0.0           -6.6887+3   1.0           -6.6887+3
PLOAD1* 500           115         FZ            FR            PLD8
*LD8    0.0           -6.6887+3   1.0           -6.6887+3
PLOAD1* 500           116         FZ            FR            PLD9
*LD9    0.0           -6.6887+3   1.0           -6.6887+3
PLOAD1* 500           117         FZ            FR            PLD10
*LD10   0.0           -6.6887+3   1.0           -6.6887+3
$
$
$  ***********************************************************
$          Material Properties for Everything
$  ***********************************************************
$
$  ***********************************************************
$
```

G-19

```
$                    Chassis Structure
$
$ *********************************************************
$
$ Chassis Grid Points
$
$ *****************
$                    X    Y    Z
GRID    1            -2.8  -1.3  0.0
GRID    2            -2.8  0.0   0.0
GRID    3            -2.8  -1.3  0.0
GRID    4            -1.9  -1.3  0.0      3
$GRID   5            -1.9  0.0   0.0
GRID    6            -1.9  1.3   0.0      3
GRID    7            -1.0  1.3   0.0
GRID    8            -1.0  0.0   0.0
GRID    9            -1.0  1.3   0.0
GRID    10           0.0   -1.3  0.0      123456
$GRID   11           0.0   0.0   0.0
GRID    12           0.0   1.3   0.0      123456
$
$
$ *********************************************************
$
$ Define Beam Elements
$
$ *****************
$
CBAR   101  21   2    3    0.0   0.0   1.0
CBAR   102  21   8    9    0.0   0.0   1.0
CBAR   105  21   1    2    0.0   0.0   1.0
CBAR   106  21   7    8    0.0   0.0   1.0
CBAR   109  21   3    6    0.0   0.0   1.0
CBAR   110  21   6    9    0.0   0.0   1.0
CBAR   111  21   9    12   0.0   0.0   1.0
CBAR   115  21   1    4    0.0   0.0   1.0
```

G-20

```
CBAR   116   21   4   7   0.0   0.0   1.0
CBAR   117   21   7   10  0.0   0.0   1.0
$
$ *************************************************************
$
$ Define Beam Properties
$
$ ******************
$
$
$ *************************************************************
$
$ Constrain DOF's Accordingly
$
$ ******************
$
PARAM   AUTOSPC YES
```

For all perpendicular cuts which include the radiator:

```
ID MSC, MTI01
SOL 24
APP DISP
CEND
TITLE=Static analysis of Homer load to chassis
SUBTITLE=FTS
ECHO=SORT
DISPLACEMENT=ALL
ELFORCE=ALL
ELSTRESS=ALL
ESE=ALL
LOAD=500
OLOAD=ALL
BEGIN BULK
$
$
$ *************************************************************
```

```
$              Loading from Suspension System
$ ***********************************************************
$
FORCE   500    16            13.91+3 0.    0.    1.
FORCE   500    18            13.91+3 0.    0.    1.
FORCE   500    19            1471.5  0.    0.    -1.
FORCE   500    20            1471.5  0.    0.    -1.
$
$ ***********************************************************
$          Distributed Load from HOMER
$ ***********************************************************
$
PLOAD1* 500           103         FZ          FR          PLD1
*LD1    0.0           -6.6887+3   1.0         -6.6887+3
PLOAD1* 500           104         FZ          FR          PLD2
*LD2    0.0           -6.6887+3   1.0         -6.6887+3
PLOAD1* 500           107         FZ          FR          PLD3
*LD3    0.0           -6.6887+3   1.0         -6.6887+3
PLOAD1* 500           108         FZ          FR          PLD4
*LD4    0.0           -6.6887+3   1.0         -6.6887+3
PLOAD1* 500           112         FZ          FR          PLD5
*LD5    0.0           -6.6887+3   1.0         -6.6887+3
PLOAD1* 500           113         FZ          FR          PLD6
*LD6    0.0           -6.6887+3   1.0         -6.6887+3
PLOAD1* 500           114         FZ          FR          PLD7
*LD7    0.0           -6.6887+3   1.0         -6.6887+3
PLOAD1* 500           118         FZ          FR          PLD8
*LD8    0.0           -6.6887+3   1.0         -6.6887+3
PLOAD1* 500           119         FZ          FR          PLD9
*LD9    0.0           -6.6887+3   1.0         -6.6887+3
PLOAD1* 500           120         FZ          FR          PLD10
*LD10   0.0           -6.6887+3   1.0         -6.6887+3
$
$
$ ***********************************************************
$          Material Properties for Everything
```

```
$ **********************************************************

$

$

$ **********************************************************

$

$                    Chassis Structure

$

$ **********************************************************

$

$ Chassis Grid Points

$

$ *****************

$                   X     Y     Z
GRID   10          0.0   -1.3   0.0        123456
$GRID  11          0.0    0.0   0.0
GRID   12          0.0    1.3   0.0        123456
GRID   13          1.0   -1.3   0.0
GRID   14          1.0    0.0   0.0
GRID   15          1.0    1.3   0.0
GRID   16          1.9   -1.9   0.0          3
$GRID  17          1.9    0.0   0.0
GRID   18          1.9    1.9   0.0          3
GRID   19          2.8   -1.3   0.0
GRID   20          2.8    0.0   0.0
GRID   21          2.8    1.3   0.0

$

$

$ **********************************************************

$

$ Define Beam Elements

$

$ *****************

$

CBAR   103   21   14   15   0.0   0.0   1.0
CBAR   104   21   20   21   0.0   0.0   1.0
CBAR   107   21   13   14   0.0   0.0   1.0
```

```
CBAR    108    21    19    20    0.0    0.0    1.0
CBAR    112    21    12    15    0.0    0.0    1.0
CBAR    113    21    15    18    0.0    0.0    1.0
CBAR    114    21    18    21    0.0    0.0    1.0
CBAR    118    21    10    13    0.0    0.0    1.0
CBAR    119    21    13    16    0.0    0.0    1.0
CBAR    120    21    16    19    0.0    0.0    1.0
$
$ ***********************************************************
$
$ Define Beam Properties
$
$ ******************
$
$
$ ***********************************************************
$
$ Constrain DOF's Accordingly
$
$ ******************
$
PARAM  AUTOSPC YES

PBAR cards for different skin thicknesses (t):
$ t= .005
PBAR*   21          31            .00685        .000046607    QED001
*ED001 .000127451    .000174058                              +PB2
+PB2    0.1    0.0
$
$ t=.0075
PBAR*   21          31            .0101625      .000067484    QED001
*ED001 .000186896    .00025438                               +PB2
+PB2    0.1    0.0
$ t= .01
PBAR*   21          31            .0134         .000086847    QED001
*ED001 .00024360     .000330448                              +PB2
```

```
+PB2    0.1     0.0

$ t= .0125

PBAR*   21              31              .0165625        .000104769  QED001
*ED001 .00029765    .000402421                          +PB2

+PB2    0.1     0.0

$ t= .015

PBAR*   21              31              .01965          .000121324  QED001
*ED001 .00034913    .000470454                          +PB2

+PB2    0.1     0.0

$ t= .0175

PBAR*   21              31              .0226625        .000136582  QED001
*ED001 .00039812    .0005346996                         +PB2

+PB2    0.1     0.0

$ t= .02

PBAR*   21              31              .0256           .000150613  QED001
*ED001 .00044469    .000595307                          +PB2

+PB2    0.1     0.0


Material property card for runs with aluminum:
MAT1    31      72.+9   27.+9           2800.0


Material property card for runs with titanium:

MAT1    31      120.+9  44.+9           4500.0
```

Parallel Analysis Chassis Data
Aluminum

Skin Thickness (m)	Max Displacement (m)	Max Bending Moment (N-m)	Max Stress (Pa)
0.005	-1.10E-03	-7.12E+03	1.53E+07
0.0075	-7.62E-04	-7.12E+03	1.05E+07
0.01	-5.92E-04	-7.12E+03	8.19E+06
0.0125	-4.91E-04	-7.12E+03	6.79E+06
0.015	-4.24E+00	-7.12E+03	5.86E+06
0.0175	-3.76E-04	-7.11E+03	5.21E+06
0.02	-3.41E-04	-7.11E+03	4.72E+06

Titanium

Skin Thickness (m)	Max Displacement (m)	Max Bending Moment (N-m)	Max Stress (Pa)
0.005	-6.62E-04	-7.12E+03	1.53E+07
0.0075	-4.57E-04	-7.12E+03	1.05E+07
0.01	-3.55E-04	-7.12E+03	8.20E+06
0.0125	-2.95E+00 ·	-7.12E+03	6.79E+06
0.015	-2.54E-04	-7.12E+03	5.87E+06
0.0175	-2.26E+00	-7.12E+03	5.21E+06
0.02	-2.05E-04	-7.12E+03	4.72E+06

Perpendicular Analysis Chassis Data
Aluminum

Skin Thickness (m)	Max Displacement (m)	Max Bending Moment (N-m)	Max Stress (Pa)
0.005	-1.69E-02	2.43E+04	-5.22E+07
0.0075	-1.16E-02	2.43E+04	-3.60E+07
0.01	-8.98E-03	2.43E+04	-2.80E+07
0.0125	-7.41E-03	2.43E+04	-2.32E+07
0.015	-6.36E-03	2.43E+04	-2.00E+07
0.0175	-5.62E-03	2.43E+04	-1.78E+07
0.02	-5.07E-03	2.43E+04	-1.61E+07

Titanium

Skin Thickness (m)	Max Displacement (m)	Max Bending Moment (N-m)	Max Stress (Pa)
0.005	-1.03E-02	2.43E+04	-5.22E+07
0.0075	-7.06E-03	2.43E+04	-3.60E+07
0.01	-5.46E-03	2.43E+04	-2.80E+07
0.0125	-4.50E-03	2.43E+04	-2.32E+07
0.015	-3.87E-03	2.43E+04	-2.00E+07
0.0175	-3.42E-03	2.43E+04	-1.78E+07
0.02	-3.08E-03	2.43E+04	-1.61E+07

Chassis (w/ Radiator) Data
Aluminum

Skin Thickness (m)	Max Displacement (m)	Max Bending Moment (N-m)	Max Stress (Pa)
0.005	-8.10E-03	-1.24E+04	2.67E+07
0.0075	-5.58E-03	-1.24E+04	1.84E+07
0.01	-4.32E-03	-1.24E+04	1.43E+07
0.0125	-3.57E-03	-1.25E+04	1.19E+07
0.015	-3.07E-03	-1.25E+04	1.03E+07
0.0175	-2.72E-03	-1.25E+04	9.14E+06
0.02	-2.45E-03	-1.25E+04	8.30E+06

Titanium

Skin Thickness (m)	Max Displacement (m)	Max Bending Moment (N-m)	Max Stress (Pa)
0.005	-4.90E-03	-1.24E+04	2.66E+07
0.0075	-3.37E-03	-1.24E+04	1.84E+07
0.01	-2.61E-03	-1.24E+04	1.43E+07
0.0125	-2.16E-03	-1.24E+04	1.19E+07
0.015	-1.86E-03	-1.24E+04	1.03E+07
0.0175	-1.64E-03	-1.25E+04	9.12E+06
0.02	-1.48E-03	-1.25E+04	8.28E+06

Appendix H
Rover Configurations

Vehicle Configurations

Though many rover configurations are possible within the lego concept, the following seven configurations were selected to support the activities of an advanced base.

Human-Operated Mars Exploration Rover

HOMER, shown in Figure H.1, is a manned, mobile laboratory which consists of the following legoble blocks connected to a heavy chassis.

Communications
Command and Data Handling
GNC (several separate blocks)
HOMER module
Scientific Equipment or Supplies

A mass and power breakdown for this configuration appear in Table H.1.
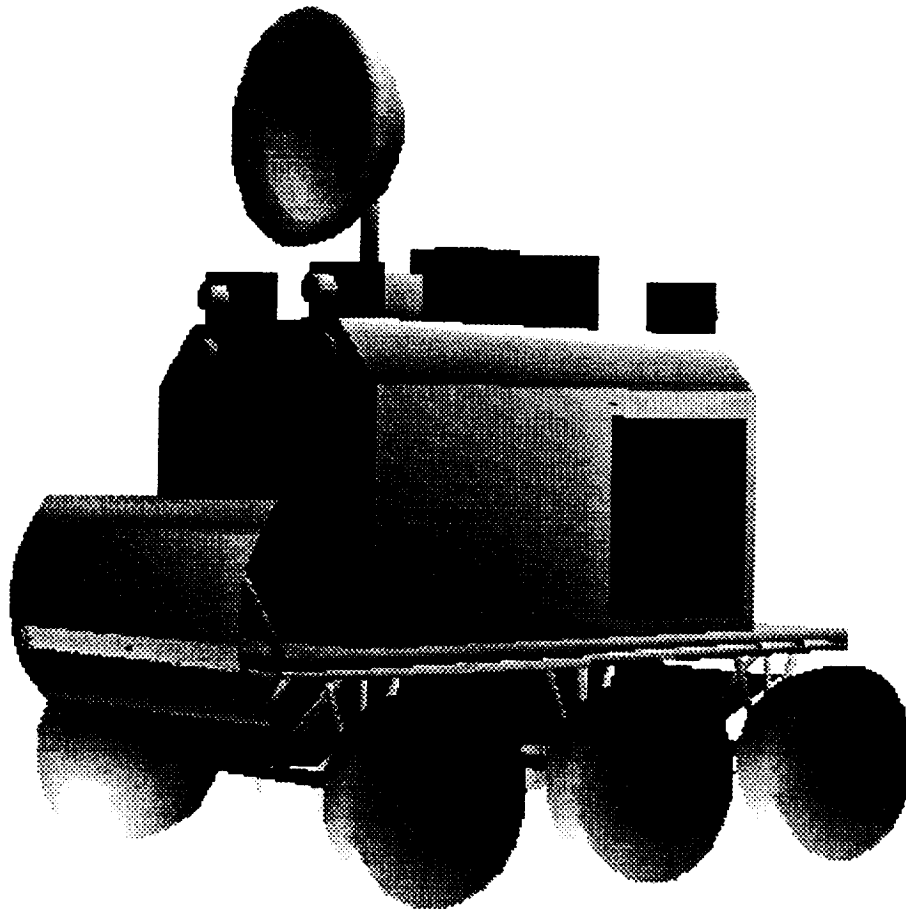
Figure H.1. HOMER Configuration

Table H.1. Mass and Power Breakdown for HOMER Configuration

Subsystem	Mass (kg)	Power Req.(kw)
GNC	200.000	0.200
Chassis	395.110	N/A
Power	800.000	N/A
Communications	30.000	1.000
C & DH	50.000	0.200
Crew compartment	500.000	15.000
Life Support	236.968	0.400
Thermal Systems	900.000	2.000
Homer Module	1616.240	N/A
Fuel & tanks	2653.5	2.000
Air Lock	225.000	5.000
Wheels	1000.000	110.000
Payload	3000.000	14.200
Total	11606.818	150.000

Fuel Transport Vehicle

FTV, shown in Figure H.2, consists of the following legoble blocks connected to a heavy chassis.

Communications
Command and Data Handling
GNC (several separate blocks)
FTV module

A mass and power breakdown for this configuration appear in Table H.2.
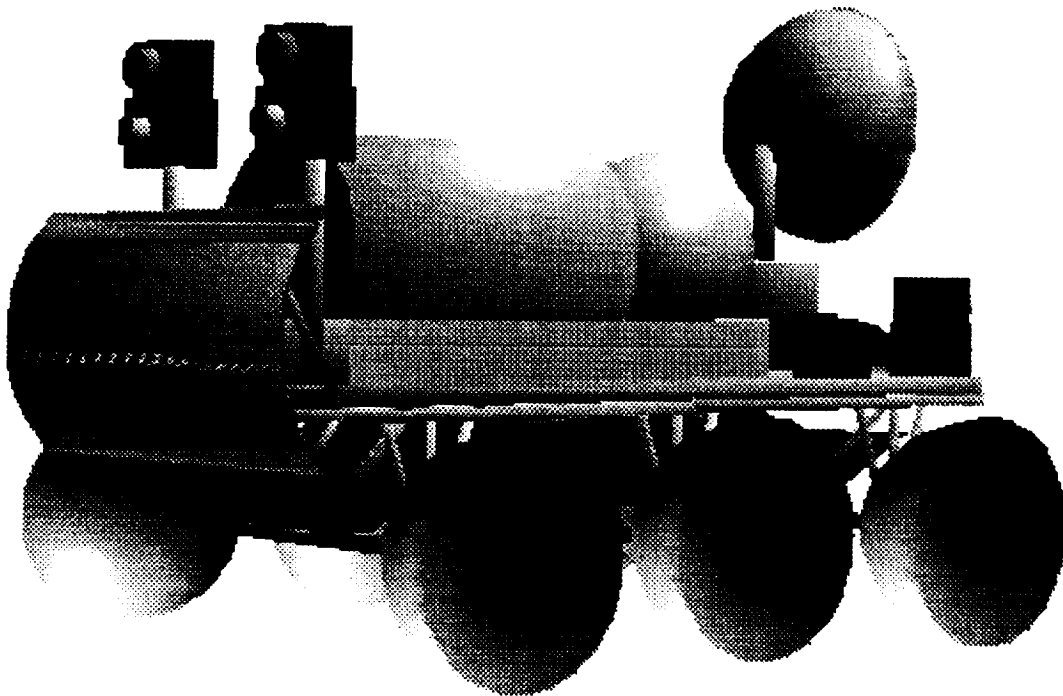

Figure H.2. FTV Configuration

Table H.2. Mass and Power Breakdown for FTV Configuration

Subsystem	Mass (kg)	Power Req.(kw)
Power	800.0	N/A
Chassis	395.1	N/A
Cargo Tank (empty)	1389.5	2.0
Cargo (fuel)	7000.0	N/A
C & DH	50.0	0.2
Communications	30.0	1.0
GNC	200.0	0.2
Wheels	1000.0	110.0
Thermal Systems	900.0	2.0
Fuel & Tanks	2653.5	2.0
Total	14418.1	117.4

Heavy Cargo Vehicle

HCV, shown in Figure H.3, consists of the following legoble blocks connected to a heavy chassis.

> Communications
> Command and Data Handling
> GNC (several separate blocks)
> Heavy Cargo module

A mass and power breakdown for this configuration appear in Table H.3.
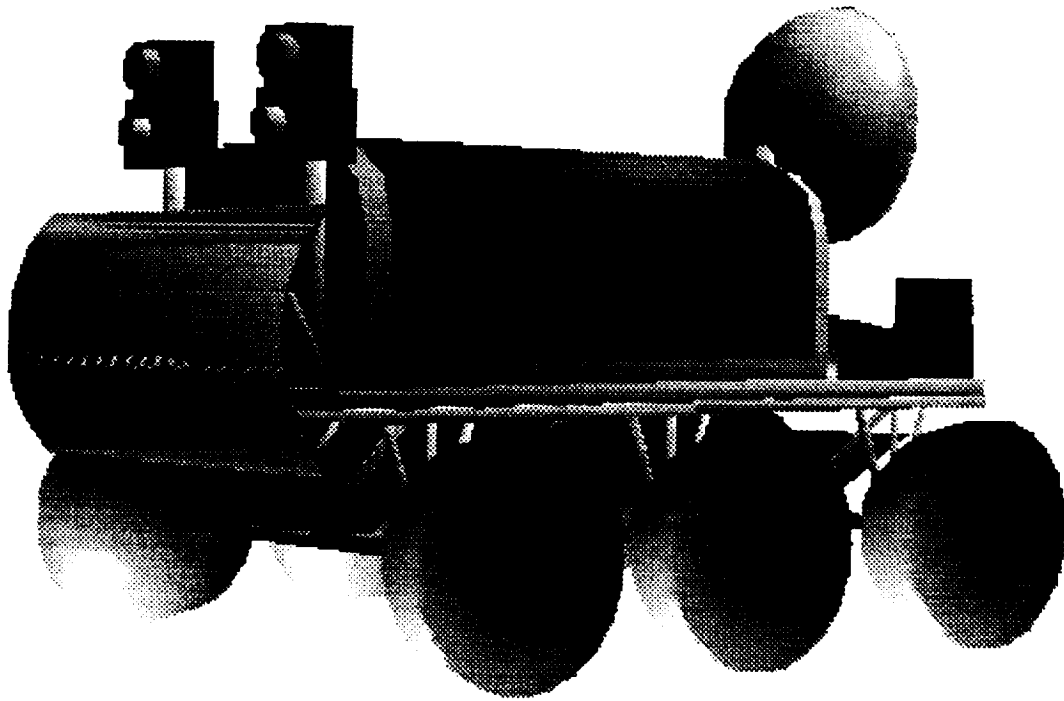
Figure H.3. HCV Configuration

Table H.3. Mass and Power Breakdown for HCV Configuration

Subsystem	Mass (kg)	Power Req.(kw)
Chassis	395.1	N/A
C &DH	50.0	0.2
Power	800.0	N/A
Communications	30.0	1.0
GNC	200.0	0.2
Wheels	1000.0	110.0
Thermal Systems	900.0	2.0
Fuel & Tanks	2653.5	2.0
Payload	8000.0	34.6
Cargo Modules	200	N/A
Total	14228.6	150.0

Materials Transport Vehicle

HCV, shown in Figure H.4, consists of the following legoble blocks connected to a heavy chassis.

Communications

Command and Data Handling

GNC (several separate blocks)
MTV module

A mass and power breakdown for this configuration appear in Table H.4.
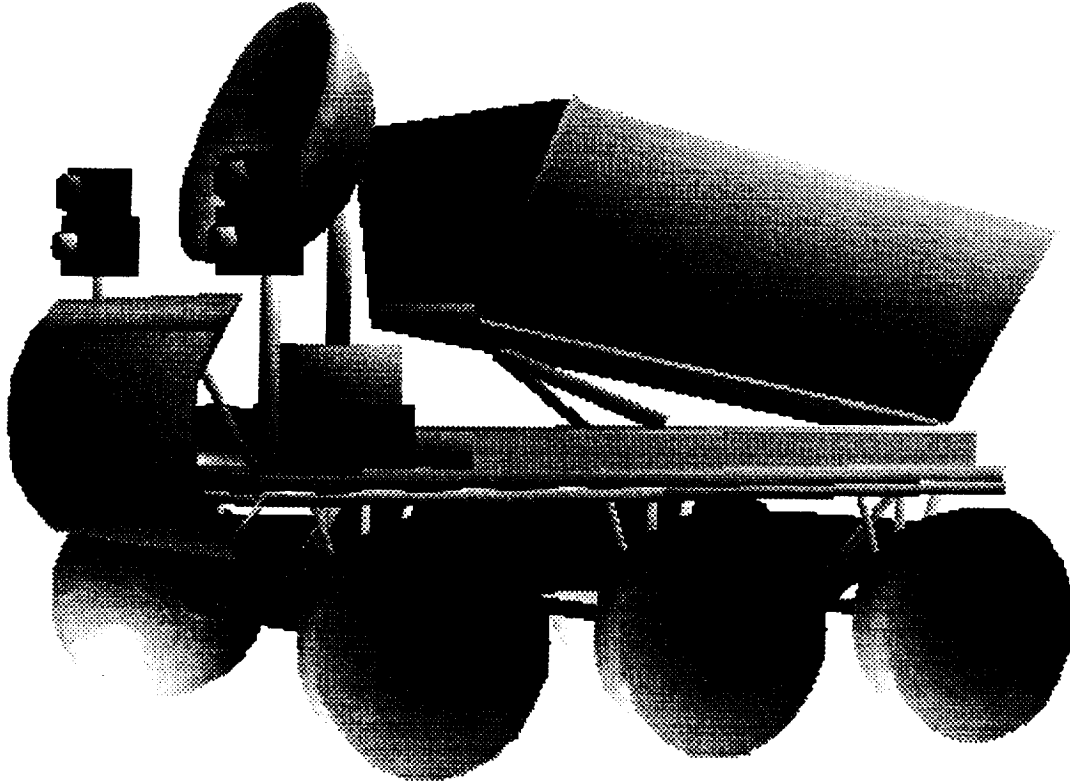
Figure H.4. MTV Configuration

Table H.4. Mass and Power Breakdown for MTV Configuration

Subsystem	Mass (kg)	Power Req.(kw)
Chassis	395.1	N/A
Power	3400.0	N/A
C & DH	50.0	0.2
GNC	200.0	0.2
Communications	30.0	1.0
Mined Materials Module	1246.0	N/A
Wheels	2500.0	110.0
Fuels & Tanks	3107.0	2.0
Regolith	8000.0	N/A
Thermal Systems	900.0	2.0
Total	19828.1	116.4

Light Cargo Vehicle

LCV, shown in Figure H.5, consists of the following legoble blocks connected to a heavy chassis.

Communications
Command and Data Handling
GNC (several separate blocks)
Light Cargo Module

A mass and power breakdown for this configuration appear in Table H.5.
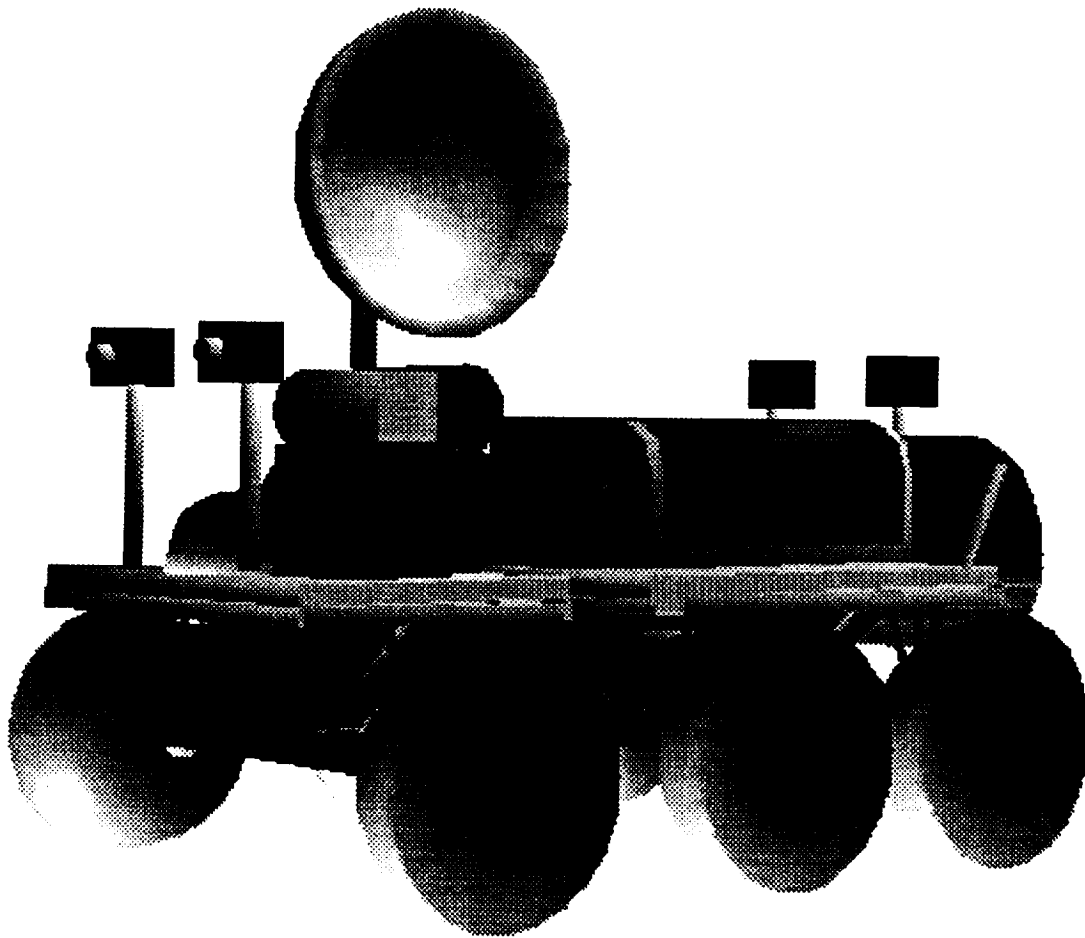
Figure H.5. LCV Configuration

Table H.5 Mass and Power Breakdown for LCV Configuration

Subsystem	Mass (kg)	Power Req.(kw)
Chassis	260.7	N/A
Wheels	600.0	42.0
Power	110.0	N/A
C & DH	50.0	0.2
Cargo Module	120.0	N/A
Communications	30.0	0.1
GNC	200.0	0.2
Fuel & Tankage	1296.0	2.0
Payload	2500.0	N/A
Thermal Systems	300.0	2.0
Total	5466.7	46.5

Mars Autonomous Rover for Ground Exploration (MARGE)

MARGE, shown in Figure H.6, consists of the following legoble blocks connected to a heavy chassis.

Communications

Command and Data Handling

GNC (several separate blocks)

Scientific Equipment or Supplies

A mass and power breakdown for this configuration appear in Table H.6.
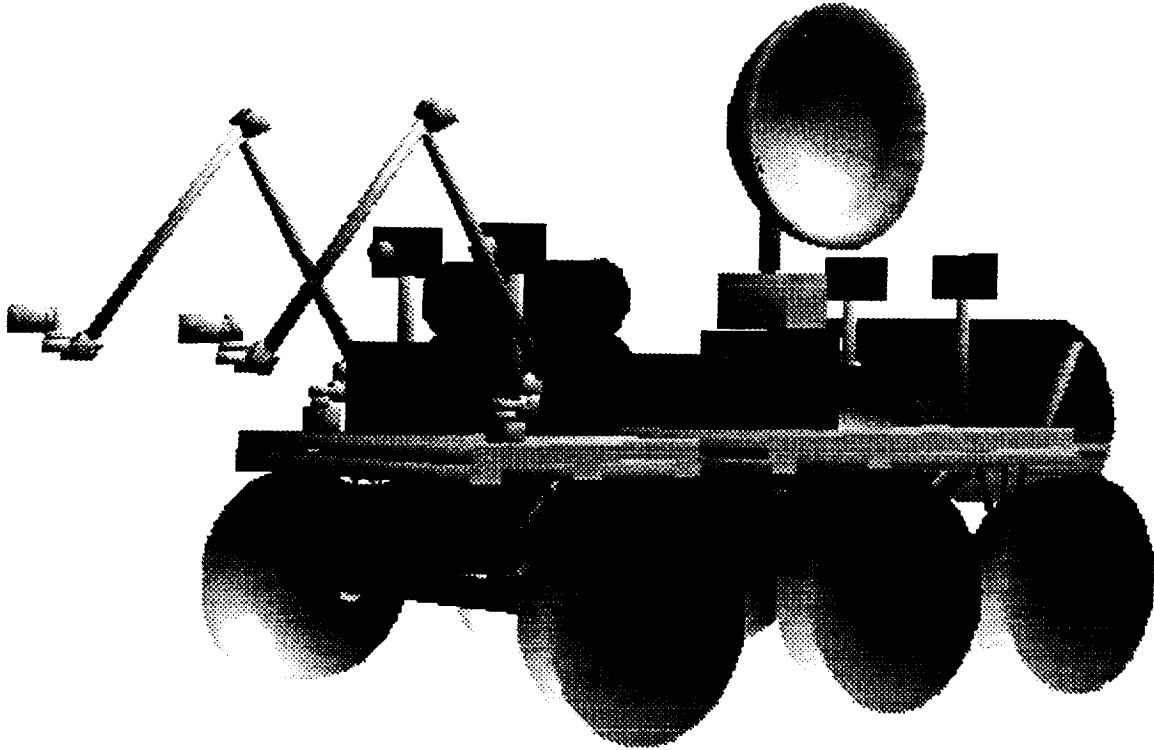
Figure H.6. MARGE Configuration

Table H.6 Mass and Power Breakdown for MARGE Configuration

Subsystem	Mass (kg)	Power Req.(kw)
Power	110.0	N/A
Chassis	260.7	N/A
Wheels	600.0	42.0
Communications	30.0	1.0
C & DH	50.0	0.2
GNC	200.0	0.2
Payload	2500.0	42.6
Fuel & Tankage	1296.0	2.0
Batteries	617.0	N/A
Thermal Systems	300.0	2.0
Total	5963.7	90.0

Manned, Short-Range Vehicle (MSRV)

MSRV, shown in Figure H.7, consists of the following legoble blocks connected to a heavy chassis.

Communications

Command and Data Handling
GNC (several separate blocks)
MSRV Module
2 Small Cargo Modules
Scientific Equipment or Supplies

A mass and power breakdown for this configuration appear in Table H.7.
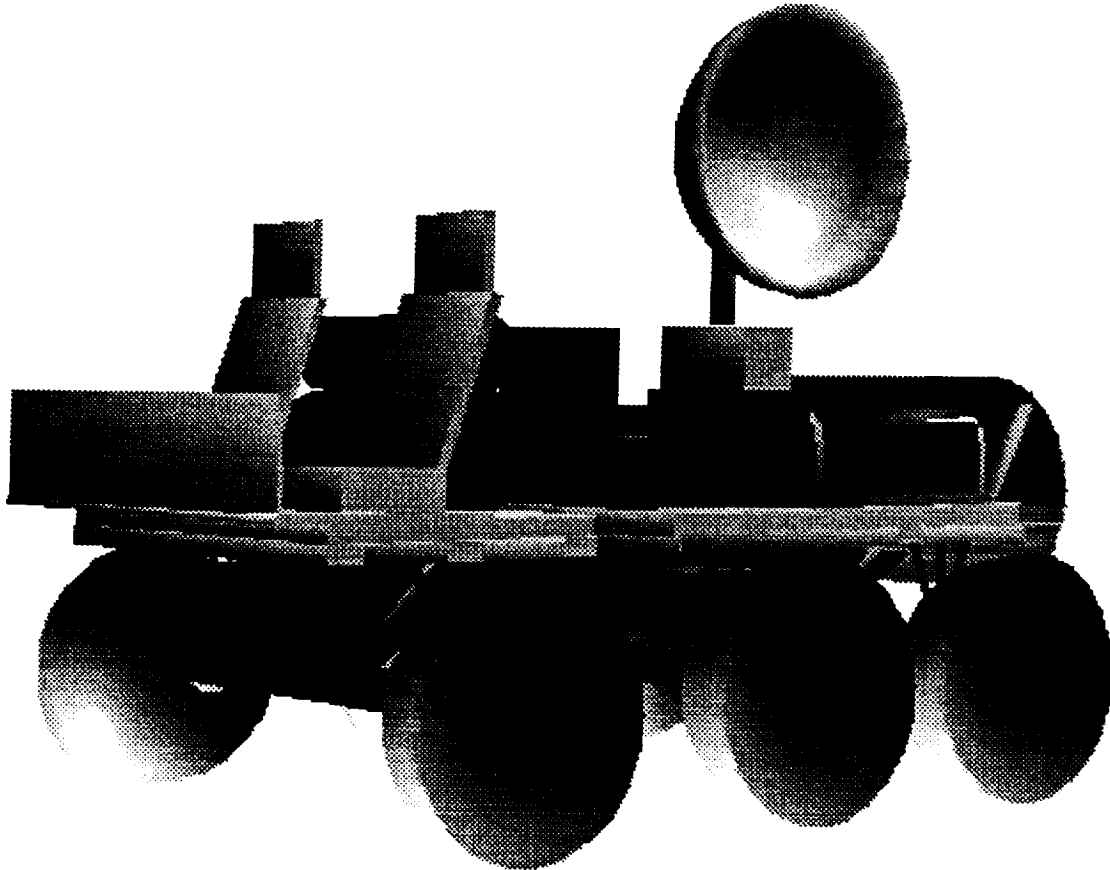
Figure H.7. MSRV Configuration

Table H.7. Mass and Power Breakdown for MSRV Vehicle

Subsystem	Mass (kg)	Power Req.(kw)
Chassis	260.7	N/A
Wheels	600.0	42.0
Power	110.0	N/A
Manned Module	150.0	1.0
C & DH	50.0	0.2
GNC	200.0	0.2
Communications	30.0	1.0
Fuel & Tankage	1296.0	2.0
Payload	2000.0	41.6
Batteries	617.0	N/A
Thermal Systems	300.0	2.0
Cargo Modules	60.0	N/A
Total	5673.7	90.0

Appendix I
TK Model for Sizing of Structural Interface

The load-carrying section of the structural interface is the base section. As seen in Figure I.1, this base is a cylinder with a hollow tube in the center. The base of the structural interface was sized using TK solver based on a model created with the following assumptions.

- Maximum payload on any vehicle will not exceed 20,000 kg.
- At least four interfaces will be available to support maximum loads.
- Payloads weight is supported by chassis frame only (not interfaces).
- Only force on interface will be weight of payload acting parallel to the chassis frame when vehicle is on a slope (see Figure I.1).
- Dynamic loads and response are much smaller than static loads and response.
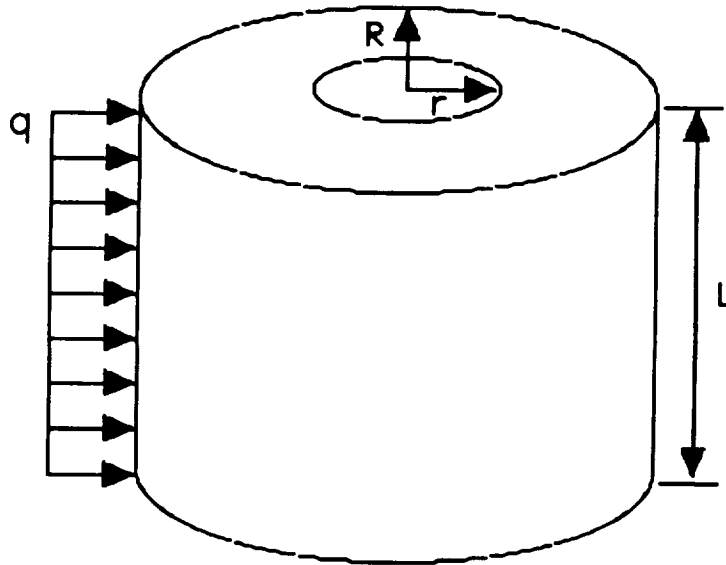
Figure I.1. Diagram of Base of Structural Interface

The following criteria were considered in sizing the interface.

- Tip Displacement
- Shear Stress
- Tensile Stress

Tip displacement for a given distributed load is given by [I1]

$$\delta = \frac{qL^4}{8EI} \qquad (1)$$

where q is the distributed load in N/m, L is the interface length in m, I is the area moment of inertia of a cross-section in m^4, and E is the modulus of elasticity in Pa. The shear stress at the base of the interface is given by

$$\tau = \frac{qL}{nA} \qquad (2)$$

where n is the number of interfaces and A is the cross-sectional area in m^2. The maximum tensile stress in the interface is given by

$$\sigma = \frac{qLR}{2I} \qquad (3)$$

The cross-sectional area is given by

$$A = \pi R^2(1-c^2) \qquad (4)$$

where R is the outer radius in m and c is the ratio of the inner radius to the outer radius. The area moment of inertial of a cross-section is given by

$$I = \frac{\pi}{4}R^4 (1-c^4) \qquad (5)$$

Substituting equations 4 and 5 into 1, 2 and 3, the following equations were obtained which were used in the TK model.

$$\delta = \frac{qL^4}{4n\pi ER^4 (1-c^4)} \qquad (6)$$

$$\tau = \frac{qL}{2\pi nR^2 (1-c^2)} \qquad (7)$$

$$\sigma = \frac{qL^2}{\pi nR^3 (1-c^4)} \qquad (8)$$

In the Tk model, the effects of the following variables within the listed ranges on the stresses and displacement were used to size the interface.

R   (0.05 m - 0.30 m)

c   (0.01 - 0.30)

L   (0.05 m - 0.30 m)

TK Model

Rule List
F=m*gmars
delta = 1/4*F*L^3/n/(E*R^4*(1-c^4))*1000
sigma = F*L/n/(pi*R^3*(1-c^4))/1000
tau = F/(2*pi*n*R^2*(1-c^2))/1000
mmax=F/n/gmars
fmax=F/n/2

Variable List

Input	Name	Output	Unit	Comment
3.14159	pi			
.03	R		m	Outer Radius
.33333	c			Ratio of Radii
	delta	.002484	m m	Tip Displacement
	F	74200	N	Weight of Max Payload
4	n			Number of Interfaces Supporting Load
3.5E10	E		Pa	Modulus of Elasticity
	sigma	6521.48	kPa	Maximum Tensile Stress (bending)
.04	L		m	Interface Length
	tau	3690.41	kPa	Maximum Shear Stress
20000	m		kg	Mass of Max Payload
3.71	gmars		m/s^2	Surface gravitational acceleration
	mmax	5000	kg	Mass of Max Payload on One Interface
	fmax	9275	N	Weight of Max Payload on One Interface

TK Results

Figures I.2 - I.10 show the sensitivity of the stresses and displacement to changes in outer radius, radii ratio, and length.
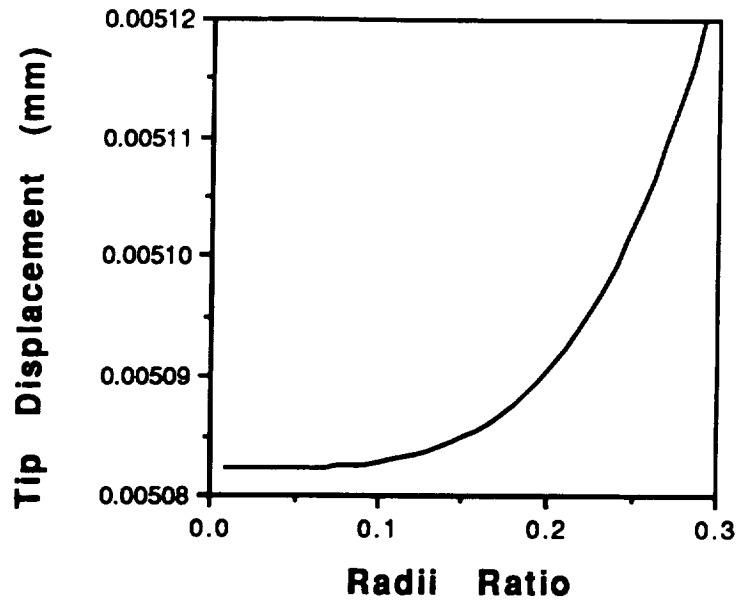
Figure I.2. Tip Displacement as a Function of Radii Ratio
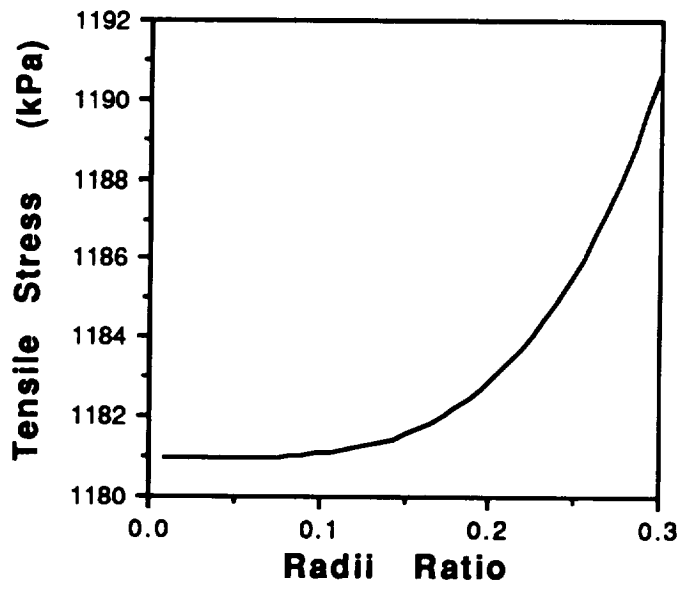
Figure I.3. Tensile Stress as a Function of Radii Ratio
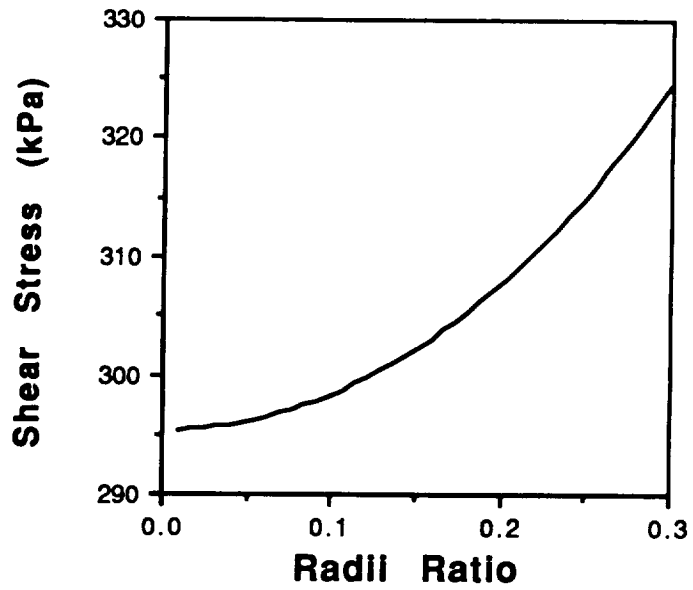
Figure I.4. Shear Stress as a Function of Radii Ratio
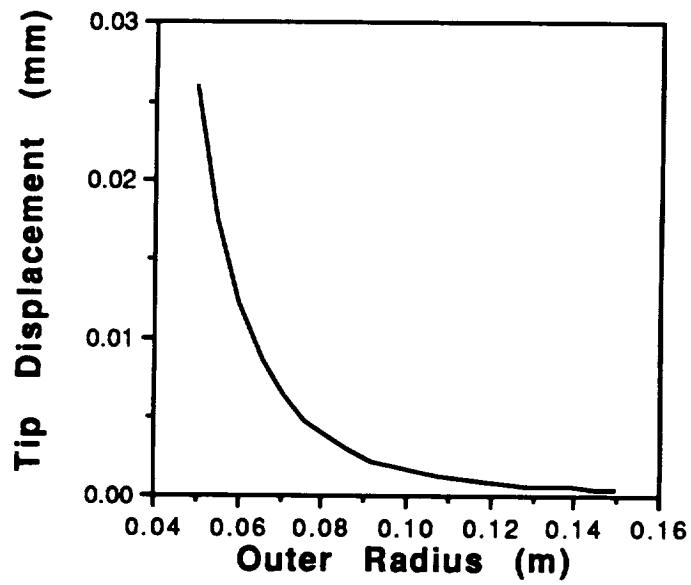
Figure I.5. Tip Displacement as a Function of Outer Radius
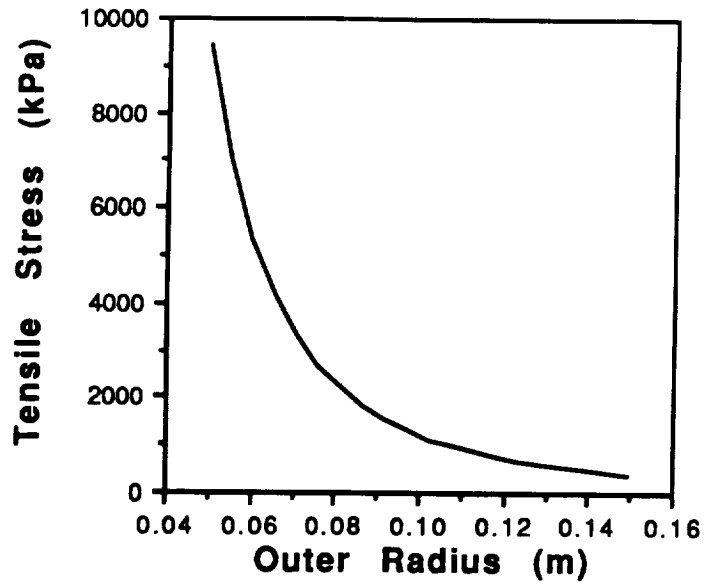
Figure I.6. Tensile Stress as a Function of Outer Radius
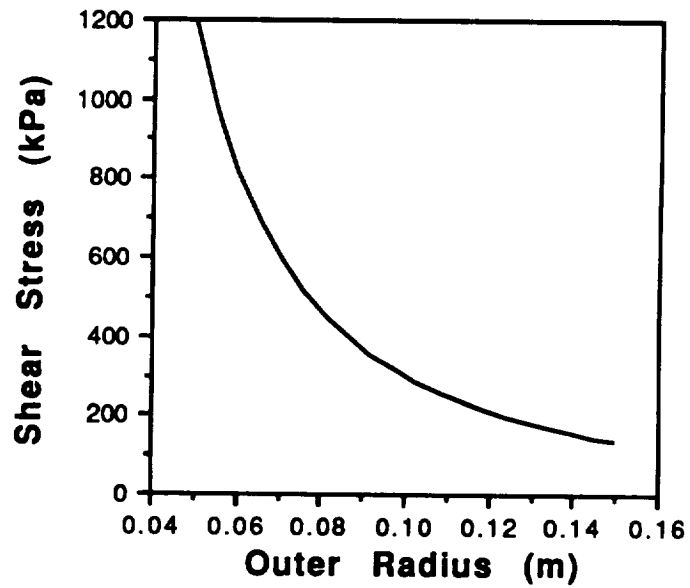
Figure I.7. Shear Stress as a Function of Outer Radius
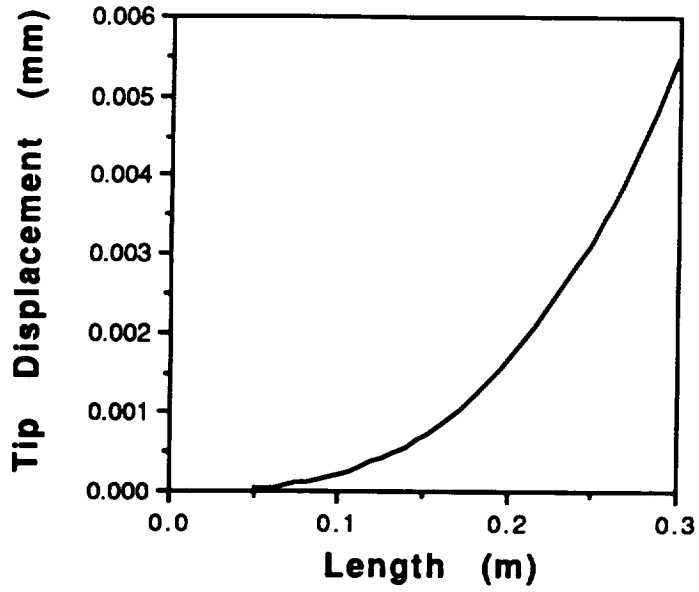
Figure I.8. Tip Displacement as a Function of Length
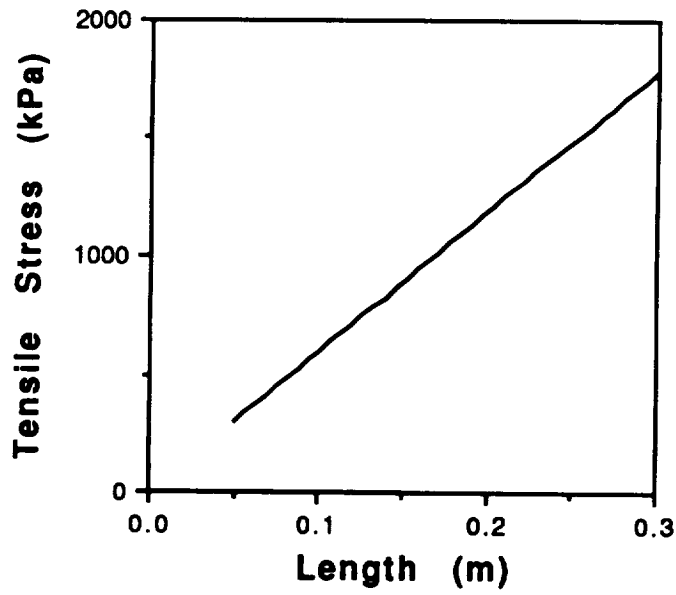

Figure I.9. Tensile Stress as a Function of Length
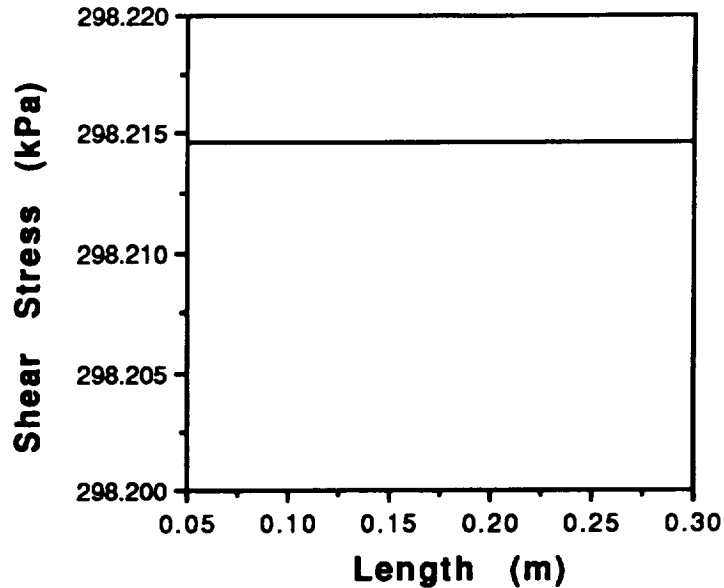
Figure I.10. Shear Stress as a Function of Length

From the TK results, the interface was sized with the following dimensions

R = 0.06 m
c = 0.1667
L = 0.04 m

Recommendations

Because the scope of the project did not allow time to analyze the interface dynamically, the sizing of the interface included a large safety factor. To reduce the safety factor and more reliably predict the behavior of the interface, FTS recommends that a dynamic analysis of the interface be done. This may result in the addition of some vibration isolation requirements for the chassis and the structural interface or a resizing of the interface itself.

References

I.1.   Gere, J.M. and S. Timoshenko, *Mechanics of Materials* , 2nd-Ed., PWS-Kent Publishing, Boston, 1984, p.736.

C - 3